



Quantitative Assessment of Navigational Safety in Storm Surge Barrier Design

A Systematic Maneuvering-Based Approach for Early Evaluation of Alternative Configurations

MSc Thesis

S.C. Konstapel

Delft University of Technology

Quantitative Assessment of Navigational Safety in Storm Surge Barrier Design

A Systematic Maneuvering-Based Approach for
Early Evaluation of Alternative Configurations

by

S.C. Konstapel

in partial fulfillment of the requirements for the degree of
Master of Science in Civil Engineering
at the Delft University of Technology

Student ID	4472519
Assessment Committee	Prof. dr. ir. M. van Koningsveld (Chair) Prof. dr. ir. S.N. Jonkman
Daily Supervisors	D. Gordon, PrEng MBA, Haskoning Ir. D. Popov, Haskoning N. Pourmohammad-Zia, PhD, TU Delft F. Baart, PhD, Rijkswaterstaat
Project Duration	September, 2024 - January, 2026
Faculty	Civil Engineering & Geosciences

An electronic version of this thesis is available at <http://repository.tudelft.nl/>.

AI-based language assistance was used to improve clarity, grammar, and overall writing style; all scientific content, interpretations, and conclusions are the author's own.

Cover: Greater Houston Port Region (photo by European Space Agency)

Preface

The completion of this thesis marks the final stage of a challenging yet rewarding academic journey. Along the way, various obstacles were encountered that at times complicated progress and demanded persistence, adaptability, and patience to overcome. While the path to the finish line was not always straightforward, these detours proved to be a necessary part of the learning process, as taking them contributed significantly to both my academic development and personal growth.

Mr. Jonkman, thank you for introducing me to the topic of this thesis and for sparking my interest in the subject that ultimately shaped this research. Nadia and Fedor, thank you for your critical feedback and for challenging me to look at my work from new perspectives. Your insights were particularly valuable during moments when progress felt stalled and helped sharpen both the analysis and the overall direction of this thesis.

David and Daniil, I would like to thank you for taking me under your wings during my time at Haskoning. Your willingness to share your extensive nautical knowledge, to patiently answer my many questions, and to provide continuous guidance was invaluable to this research. I am especially grateful for your moral support, which helped me navigate moments of uncertainty with confidence. To all the other colleagues I had the pleasure of meeting at Haskoning, thank you for creating a welcoming and supportive working environment. Your openness, kindness, and readiness to offer help made my time there both enjoyable and enriching.

Mr. Van Koningsveld, thank you for stepping in when the project risked going port (left). Your guidance, thoughtful feedback, and willingness to take the time to steer this research back on course were instrumental in bringing this journey to a successful conclusion.

Finally, to my friends and my mother, thank you for your unwavering encouragement throughout this entire process. Your patience, and belief in me provided a constant source of motivation, particularly during the more demanding phases of this work.

*S.C. Konstapel
Amsterdam, January 2026*

Abstract

Rising sea levels and increasing storm intensity are driving the implementation of large-scale storm surge barriers globally to protect coastal communities and critical infrastructure. As these structures are increasingly located within major maritime access routes, their design introduces new navigational challenges that directly affect nautical safety. While extensive experience exists in the hydraulic and structural design of storm surge barriers, the navigational implications of alternative barrier configurations have received comparatively limited quantitative attention. Existing studies often focus on single configurations or rely on qualitative assessments conducted late in the design process, leaving a gap in systematic, configuration-specific methods that support early-stage design decisions.

The objective of this thesis is to develop and apply a quantitative assessment framework that enables systematic evaluation of the nautical safety performance of alternative storm surge barrier configurations during early design stages. The framework is grounded in the premise that, at this stage of design, nautical safety performance is most directly reflected in vessel maneuverability under constrained geometric and environmental conditions. Rather than attempting to predict accident probabilities or prescribe absolute safety classifications, the method focuses on configuration-dependent maneuvering demand and available control margins as necessary preconditions for safe navigation.

A structured assessment framework is developed that integrates spatial schematization of the navigational environment, critical environmental forcing scenarios, representative design vessels, fast-time ship maneuvering simulation, and quantitative nautical safety assessment metrics. These metrics describe maneuvering performance in terms of spatial, temporal, and control margins, enabling reproducible and configuration-specific comparison. Fast-time simulation is employed to ensure computational efficiency and repeatability, making the framework suitable for iterative application during early design phases.

The practical applicability of the framework is demonstrated through a case study of the proposed Bolivar Roads storm surge barrier in Texas. Multiple alternative barrier configurations are evaluated using the fast-time simulation model SHIPMA. Simulations are conducted for a set of representative design vessels under selected flood and ebb tidal conditions, using consistent spatial schematization and environmental assumptions across configurations. Simulation outputs are post-processed to derive the values of the quantitative safety metrics for each configuration.

The results show that nautical safety performance is highly sensitive to barrier geometry. Configurations featuring wider gate openings and more favorable alignment and siting consistently exhibit larger spatial and temporal maneuvering margins, reduced control effort, and more stable vessel behavior. Conversely, configurations with constrained openings or unfavorable alignment impose increased maneuvering demand and reduced controllability. These findings demonstrate that geometric design choices can substantially influence navigational safety performance and that such effects can be captured quantitatively using the developed framework. While the absolute values of the assessment metrics are subject to modeling assumptions and simplifications, the relative differences between configurations provide meaningful insight for comparative evaluation. As such, the results are not intended to replace expert judgment but to serve as structured input for pilot and stakeholder discussions, supporting transparent and informed interpretation of navigational safety implications.

This research contributes a systematic, maneuvering-based framework that bridges the gap between hydraulic design and nautical safety assessment in storm surge barrier projects. By enabling early-stage, quantitative comparison of alternative configurations, the framework provides capabilities that were previously unavailable in design practice. The case study illustrates the framework's practical value and transferability to other navigation-constrained barrier locations. Future research should prioritize integration of configuration-specific hydrodynamic modeling, enhanced representation of human factors, and further refinement of assessment metrics to improve physical realism and decision relevance.

Contents

Preface	i
Abstract	ii
Nomenclature	vi
1 Introduction	1
1.1 Context	1
1.1.1 Global Emergence of Storm Surge Barriers	1
1.1.2 Storm Surge Barriers: Balancing Objectives	1
1.1.3 Hydraulic Structures and Nautical Risk	2
1.1.4 Problem in Practice: The Bolivar Roads Storm Surge Barrier	4
1.2 Problem Statement	5
1.3 Research Gap	5
1.4 Research Objective	6
1.5 Research Questions	6
1.5.1 Main Research Question	6
1.5.2 Sub Research Questions	6
1.6 Scope	6
1.7 Report Structure	7
2 Theoretical Background	8
2.1 Spatial Schematization	8
2.1.1 Origin-Destination Combinations	9
2.1.2 Geometric Domain Size	9
2.1.3 Nautical and Bathymetric Layout	9
2.1.4 Spatial Data	10
2.2 Environmental Forcing and Hydrodynamic Effects	11
2.2.1 Wind Effects	11
2.2.2 Current Effects	12
2.2.3 Wave Effects	12
2.2.4 Water Depth	13
2.2.5 Shallow Water Effects	14
2.2.6 Bank Suction	15
2.2.7 Other	15
2.2.8 Environmental Data	16
2.3 Design Vessels	16
2.3.1 Vessel Characteristics: Geometric Specifications	16
2.3.2 Vessel Characteristics: Control Mechanisms	17
2.3.3 Vessel Data	17
2.4 Physical Maneuvering Indicators	18
2.4.1 Heading	18
2.4.2 Course Over Ground (COG)	19
2.4.3 Drift Angle	19
2.4.4 Swept Path	20
2.5 Ship Maneuvering Simulation Models	21
2.5.1 Fast-Time Simulation	21
2.5.2 Real-Time Simulation	22
2.5.3 Other Modeling Approaches	23
2.6 Quantitative Nautical Safety Assessment Metrics	23

2.6.1	Metric Families	23
2.6.2	Extent of Navigational Risks in Barrier Environments	24
3	Methods and Materials	25
3.1	Method: Component Specification and Synthesis	25
3.1.1	Spatial Schematization	25
3.1.2	Environmental Forcing and Hydrodynamic Effects	27
3.1.3	Design Vessels	28
3.1.4	Physical Maneuvering Indicators	30
3.1.5	Ship Maneuvering Simulation Model	30
3.1.6	Nautical Safety Assessment Metrics: Framework and Definitions	31
3.1.7	Method Synthesis	40
3.2	Case Study: Bolivar Roads, “The Doorway to Galveston Bay”	41
3.2.1	Context and Significance of Bolivar Roads	41
3.2.2	The Need for a Storm Surge Barrier at Bolivar Roads	42
3.2.3	Bolivar Roads Gate System	42
3.2.4	Evaluation Study	43
4	Results	45
4.1	Spatial Schematization	45
4.1.1	Governing Origin-Destination Combinations	45
4.1.2	Geometric Domain Size	46
4.1.3	Nautical and Bathymetric Layout	47
4.2	Environmental Forcing and Hydrodynamic Effects	51
4.2.1	Environmental Data Sources and Dominant Forcing Mechanisms	51
4.2.2	Wind	52
4.2.3	Currents	52
4.2.4	Worst Navigable Conditions	54
4.2.5	SHIPMA-Specific Environmental Inputs	54
4.3	Design Vessels	55
4.3.1	Identification of Vessel Population	55
4.3.2	Representative Design Vessels	55
4.3.3	Vessel Models for Simulation	56
4.4	Physical Maneuvering Indicators	56
4.5	Ship Maneuvering Simulation: SHIPMA	56
4.5.1	SHIPMA-Specific Input Formats	56
4.5.2	Autopilots	58
4.5.3	Maneuvers	58
4.5.4	Initial Conditions	60
4.5.5	Simulation Cases	60
4.5.6	Simulation Outputs	62
4.6	Nautical Safety Assessment Metrics	62
4.6.1	Presentation of Nautical Safety Assessment Metrics	62
4.6.2	Descriptive Analysis of Assessment Metric Outcomes	65
5	Discussion	68
5.1	Limitations	68
5.1.1	Methodological Choices	68
5.1.2	Case Study Choices	70
5.2	Positioning of the Contribution	71
6	Conclusion	74
6.1	Answers to the Research Questions	74
6.1.1	Synthesis	76
6.2	Recommendations for Future Research	77
	References	79
A	Physical Maneuvering Indicators	84

B Bolivar Roads Nautical Chart	85
C Geometric Barrier Design Parameters	87
D Wind Data Bolivar Roads 2023	89
E Current Data Bolivar Roads 2023	94
F Design Vessels Bolivar Roads	99
G Supplemental SHIPMA Set-Up Figures	102
G.1 Current Fields	102
G.2 Bank Suction	104
G.3 Desired Tracks	107
H Assessment Metrics S.C. 1	114
List of Figures	120
List of Tables	121

Nomenclature

Abbreviations

Abbreviation	Definition
AASHTO	American Association of State Highway and Transportation Officials
AIS	Automatic Identification System
AtoN	Aids to Navigation
Beam Clr. I.B.	Beam Clearance In Barrier
BTS	Bureau of Transportation Statistics
COG	Course Over Ground
CRS	Coordinate Reference System
CSRM	Coastal Storm Risk Management
Dir.	Direction
Dist. A.B.	Distance After Barrier
Dist. B.E.	Distance Before Entry
ER	Ecosystem Restoration
FTS	Fast-Time Simulation
GAL	Galveston
GHPB	Greater Houston Port Bureau
GLO	General Land Office
HOU	Houston
IALA	International Association for Marine Aids to Navigation
IB	Inbound
LOA	Length Overall
MARIN	Maritime Research Institute Netherlands
Max. DA I.B.	Maximum Drift Angle In Barrier
MMSI	Maritime Mobile Service Identity
NOAA	National Oceanic and Atmospheric Administration
OB	Outbound
O-D	Origin-Destination
PIANC	Permanent International Association of Navigation Congresses
RoT	Rate of Turn
RPM	Revolutions Per Minute
RTS	Real-Time Simulation
Rudder Range I.B.	Rudder Range In Barrier
S.C.	Simulation Case
SG	Sector Gate
SLR	Sea Level Rise
SWEG	Shallow Water Environmental Gate
Time A.B.	Time After Barrier
Time B.E.	Time Before Entry
UKC	Under Keel Clearance
U.S.	United States
USACE	United States Army Corps of Engineers
VLG	Vertical Lift Gate

1

Introduction

1.1. Context

1.1.1. Global Emergence of Storm Surge Barriers

Rising sea levels, driven by global temperature increases, are accelerating the risk of coastal flooding, posing significant threats to infrastructure, livelihoods, and human life (Mooyaart et al., 2014). Currently, over 600 million people reside in coastal zones worldwide (Neumann et al., 2015), a figure projected to surpass 1 billion by 2060 due to population growth and a continuing trend in migration toward coastal regions (Merkens et al., 2016). These dynamics, combined with the increasing frequency of chronic flooding in low-lying areas, are expected to drive annual global flood losses to an estimated \$60 - 63 billion by 2050 (Hallegatte et al., 2013). A large percentage of these vulnerable populations inhabit estuaries and seaside cities, where the growing utilization of coastal zones amplifies exposure to the risks posed by storm surge (Trace-Kleeberg et al., 2023).

In recent decades, storm surge barriers have emerged as a technically and economically viable solution for coastal protection, particularly in estuaries with extensive coastlines and limited space for traditional defenses (Mooyaart & Jonkman, 2017). Following the devastating North Sea flood of 1953, the Netherlands pioneered the Delta Works, constructing six movable storm surge barriers over a span of 45 years (Walraven et al., 2022). These barriers, groundbreaking for their time, established engineering precedents that have since inspired similar infrastructure worldwide (Deltares, 2018). By 2017, 18 storm surge barriers had been constructed globally (Mooyaart & Jonkman, 2017), and between 2017 and 2023, this number surged to over 50 (Trace-Kleeberg et al., 2023). Several nations are currently exploring the feasibility of constructing new barriers or upgrading existing ones to mitigate increasing flood risks exacerbated by climate change (Deltares, 2018). In the U.S. alone, studies have recommended storm surge barriers for at least 11 estuaries (Orton et al., 2023).

Storm surge barriers are at present recognized as critical for the socioeconomic resilience of many coastal regions. By operating during extreme weather events, they prevent catastrophic flooding while preserving the continuity of urban, industrial, and ecological systems when environmental conditions are not extreme and the barriers are open. Their importance continues to grow as flood disasters increase in frequency and magnitude due to urban expansion and economic development in coastal areas. However, despite their demonstrated effectiveness in reducing flood risks, these barriers are not without challenges. The following subsections elucidate some of these challenges.

1.1.2. Storm Surge Barriers: Balancing Objectives

The design and operation of hydraulic structures often require balancing multiple, and sometimes competing, objectives, including flood protection, environmental preservation, navigational safety, economic feasibility (at structure as well as system level) and long-term operational reliability. Storm surge barriers exemplify this complexity: they must provide highly reliable flood protection during extreme events, while ensuring that other functions of the estuarine or port system remain intact under normal operating conditions (Jonkman et al., 2014). As a result, barrier design inherently involves trade-offs

across several domains, many of which have been extensively examined in the literature, including economic feasibility, environmental and hydrodynamic impacts, and long-term structural performance.

From an economic perspective, Kind (2024) quantified the financial implications of barrier closures for ports and shipping, shedding light on the stakes associated with operational decision-making. Mooyaart et al. (2023) similarly developed an optimization framework for coastal flood defense systems that balances investments in dike reinforcement and barrier closure reliability, illustrating how economic and hydraulic objectives interact under distinct sea level rise (SLR) scenarios.

From an environmental and hydrodynamic perspective, researchers have shown that storm surge barriers can significantly alter estuarine systems. Orton et al. (2023) identified the need for coordinated long-term studies on how storm surge barriers affect hydrodynamics, sediment transport, and ecosystem connectivity, and Feizabadi et al. (2025) demonstrated through hydrodynamic modeling that barrier placement and geometry strongly influence salinity distribution, stratification, and tidal exchange. Similarly, Cozzoli et al. (2017) compared the long-term benthic habitat responses of two Dutch estuaries, one modified by channel deepening for navigation and the other by a storm surge barrier for flood safety, showing how distinct management strategies can lead to contrasting ecological outcomes. Collectively, these studies highlight the environmental sensitivities and system wide consequences associated with barrier implementation.

A further body of work examines barrier reliability, maintenance, and long-term performance. Bakker et al. (2025) researched the cumulative effects of clustered storm events on the operational reliability of the Maeslant Barrier, while Trace-Kleeberg et al. (2023) demonstrated that rising mean sea levels will progressively constrain maintenance windows, demanding adaptive management to ensure barrier reliability in the long run. Complementary to these findings, Vader et al. (2023) developed a framework for assessing the remaining life of storm surge barriers by evaluating how external drivers such as sea level rise, climate change, and socio-economic developments affect both their technical and functional performance. Together, these studies underscore that long-term functionality depends not only on structural integrity but also on operational adaptability.

Finally, research has also advanced on barrier concept design and selection methods. Dircke et al. (2011) provided a global comparative overview of navigable storm surge barriers, outlining structural and hydraulic characteristics of major gate types and proposing criteria for selecting appropriate concepts under varying site and design conditions.

Taken together, this body of research illustrates that storm surge barriers must satisfy a diverse set of objectives that often impose competing demands, requiring designers to manage trade-offs across economic, hydraulic, environmental, and operational domains. One of the most challenging trade-offs arises in relation to navigational safety, which, in the case barriers are integrated into busy navigation channels such as port approaches, must be maintained despite geometric constraints and altered flow conditions created by the barrier. These navigational implications and associated risks are examined in detail in the following section.

1.1.3. Hydraulic Structures and Nautical Risk

Hydraulic structures, such as navigation locks, movable gates, bridges over water, and storm surge barriers, are becoming essential components of modern water management, waterborne transport, and coastal protection systems. When positioned within navigable waterways, however, these structures can introduce significant operational and safety challenges (Zagonjoli et al., 2024). Several factors contribute to these risks:

- **Constrained geometry:** reduced channel width or overhead clearance limits the maneuvering space available to vessels (Knott & Winters, 2018).
- **Hydrodynamic effects:** the introduction of a hydraulic structure alters local hydrodynamics, potentially amplifying tidal currents through the navigable openings and creating zones of turbulence or eddies near piers and abutments (Orton et al., 2023). These altered currents can cause unexpected vessel drift or yaw, compromising vessel controllability (Daniel & Paulus, 2019).
- **Human factors:** pilot error, often exacerbated by poor visibility, high traffic density, or complex approach geometry, can increase accident probability (Knott & Winters, 2018).

- Design-induced limitations: introduction of hydraulic structures can create complex maneuvering environments. Misalignment between approach channels and passage openings may force severe course corrections and approaches at an angle, reducing the margin for error and increasing maneuvering difficulty (GHPB, 2023a).
- Increasing vessel sizes: over recent decades, the growing demand for maritime transport has led to a significant increase in vessel traffic and sizes (Marino et al., 2023).

The factors above substantially increase the potential for vessel-structure incidents, and operational delays. The consequences of such vessel-structure incidents can be severe, extending beyond infrastructure damage to include loss of life, environmental pollution, and prolonged economic disruption. These risks are not hypothetical, historical accident records demonstrate their persistence and global relevance: between 1960 and 2015, 35 major bridge collapses worldwide were caused by ship or barge collisions, resulting in 342 fatalities (Knott & Winters, 2018). In the United States alone, the U.S. Coast Guard recorded 2,692 vessel collisions with bridges over a ten-year period (Knott & Winters, 2018).

Recent events underscore this vulnerability. In March 2024, the Francis Scott Key Bridge in Baltimore collapsed following a container ship collision, killing six maintenance workers and halting Port of Baltimore operations for 11 weeks due to the consequential closure of the waterway. The incident affected more than 8,000 jobs and the economic impact was estimated at \$15 million per day, excluding the replacement cost which will amount to between \$1.7-1.9 billion (Hassan, 2024). Europe has also witnessed significant incidents. In December 2024, a ship collision with a lock gate on the Mosel River in Germany blocked a vital shipping route for raw materials, stranding over 70 vessels. Repairs are expected to last until spring 2025, causing severe disruptions to supply chains as the river will be closed to cargo shipping during this period (Reuters, 2024). Similarly, in October 2024, two severe collisions on Dutch waterways highlighted the sensitivities of hydraulic structures to nautical traffic. A gravel-laden cargo ship collided with a railway bridge, while another ship struck a weir, resulting in significant infrastructure damage and disruptions to transport networks (Deltares, 2024). These examples demonstrate that the impacts of vessel-structure incidents extend beyond the immediate site, often triggering regional or even national economic repercussions due to the central role that ports and waterways play in global supply chains, emphasizing the need for proactive risk assessment and management.

Although the navigational implications of storm surge barriers have been acknowledged in both engineering and policy literature, existing studies approach the subject fragmentarily, focusing on local cases, empirical design guidance, or qualitative assessments rather than on systematic, quantitative evaluation frameworks. Design guidelines such as PIANC (2005), PIANC (2014), and AASHTO (2020) establish navigation as a core functional requirement for storm surge barriers and their approach channels, prescribing baseline geometric allowances and clearance margins to ensure safe vessel passage. However, these standards are necessarily generic, relying largely on expert judgment or empirical formulae, and offer no reproducible criteria for quantifying navigational risk in complex hydraulic settings.

Several overview studies similarly recognize navigation as a central design driver but continue to treat it qualitatively. Mooyaart et al. (2014) and Mooyaart and Jonkman (2017) identified navigation requirements, together with tidal exchange and water quality, as key functional determinants of barrier layout, gate type, and span, yet noted the absence of standardized evaluation methods for maneuvering safety. Dircke et al. (2011), in their review of global navigable barriers, similarly concluded that while navigability is routinely considered in concept selection, explicit analysis of navigability implications is seldom undertaken. More recent work by Kluijver et al. (2019) on the New York metropolitan area reiterated this limitation, showing that navigability continues to be addressed through qualitative criteria rather than quantitative, risk-based assessment.

Case-specific design studies have repeatedly identified navigation as a critical feasibility constraint. Van Ledden et al. (2012), in their reconnaissance study for a Mississippi River barrier, described navigation as the key challenge to project viability, requiring careful consideration of location, gate geometry, and visibility. Similarly, Walraven et al. (2022) emphasized that collision risks, accessibility, and reliable operation must be incorporated early in barrier design. Despite such recognition, most practical evaluations of navigational risk remain descriptive, and findings are rarely transferable beyond the specific project context. These case-specific evaluations also tend to examine only the final or preferred configuration, without exploring the trade-offs between multiple feasible designs.

Beyond these physical, operational and design related challenges, nautical safety also contains an inherently subjective dimension. Pilots may differ in their assessment of whether a particular maneuver or operating condition is acceptable, depending on their experience, familiarity with local waterways, vessel characteristics, and personal risk tolerance. Under identical hydraulic and geometric conditions, one pilot may regard a passage as safely manageable while another may consider it marginal. This subjectivity is amplified near hydraulic structures, where constrained geometries and rapidly varying currents reduce the margin for error. While expert judgment remains indispensable, its variability highlights the need for complementary quantitative indicators that enable more structured, transparent, and reproducible evaluations of navigational safety.

The existing literature makes it clear that there is a growing need to reconcile two objectives that can be in tension: robust flood defense and safe, efficient navigation. Achieving this balance requires understanding how design choices, such as navigable gate width, alignment, and siting, influence vessel maneuverability and accident risk under realistic environmental conditions. Failure to adequately account for these considerations can result in new infrastructure that is structurally sound, but inadvertently compromises navigational safety, threatening the very economic and societal systems it is intended to protect. This is illustrated on the basis of a real-world example in the following section.

1.1.4. Problem in Practice: The Bolivar Roads Storm Surge Barrier

The Texas coast serves as a nationally significant economic and ecological corridor, hosting major ports, energy infrastructure, and diverse coastal habitats. It supports the state's role as a leader in energy production and international trade while providing natural defenses and ecosystem services (USACE, 2021c). The importance of the Texas coast is reflected by the numbers shown in Figure 1.1.

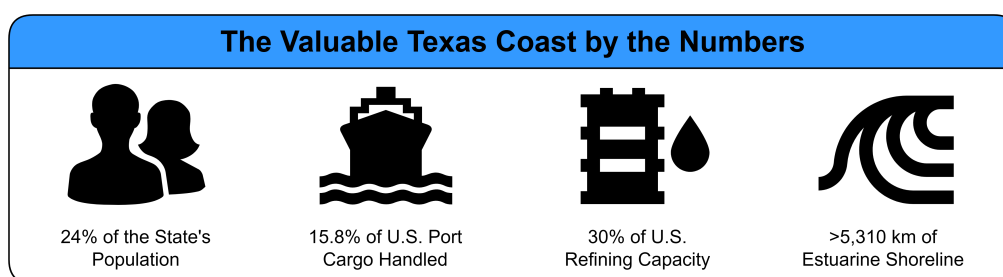


Figure 1.1: Numbers that highlight the value of the Texas coast (USACE, 2021c).

The Texas coast however, faces growing threats from coastal storms, rising sea levels, and erosion, which increasingly endanger residential, commercial, and industrial assets (USACE, 2021c). These factors pose risks not only to the region's social, economic, and environmental resources but also to the broader U.S. welfare. With climate change projected to increase the frequency and intensity of these events, a comprehensive strategy to protect Texas's coastal resources has become imperative. In response to the growing threats, the United States Army Corps of Engineers (USACE) and the Texas General Land Office (GLO) have collaborated to develop solutions that address these challenges. As such, a storm surge barrier has been proposed for Bolivar Roads (see Figure 1.2), a critical maritime gateway serving as the entrance to Galveston Bay and its adjacent key shipping channels such as the Houston and Galveston Ship Channels.

A simulation-based evaluation study of the proposed storm surge barrier design for Bolivar Roads has identified many of the same navigational risks described in Subsection 1.1.3. These risks include increased current velocities through narrow gates creating "a potential hazard for commercial ships attempting to line-up and adjust their speed to pass safely through the center of the gate system", barrier induced hydrodynamic effects which "affect the capability of the pilot to safely control the heading and speed of the ship when passing through the gate system", a challenging approach geometry that "requires severe angle turns", and constrained navigable widths requiring "perfect piloting" and "leaving no room for error" (Burkley et al., 2022; GHPB, 2023b). Some of these risks would "impact the spacing, timing, and navigation of ships for miles on either side of the gate complex" (Burkley et al., 2022).



Figure 1.2: Digital rendition of the proposed Bolivar Roads Gate System (USACE, 2021c).

The Bolivar Roads case demonstrates that the navigation challenges described in the preceding subsections are not merely theoretical. If these factors are not accounted for they could significantly increase the likelihood of vessel-structure incidents, thereby threatening both navigational safety and economic throughput (GHPB, 2023a). Addressing these issues in the early design phase is essential to ensure that the barrier meets its flood protection objectives without compromising one of the nation's busiest maritime gateways.

1.2. Problem Statement

Design decisions regarding the geometry and layout of navigable storm surge barrier configurations are typically taken during early project stages, when uncertainty is high but the freedom to influence system performance is greatest. Choices related to gate width, alignment, and siting made at this stage strongly constrain future navigational conditions and can have long-lasting implications for nautical safety and port accessibility, yet are difficult and costly to modify once implemented. As a result, limited insight into and inadequate consideration of the navigational implications of alternative barrier configurations during these early design stages may lead to an imbalance between the optimization of flood safety objectives and the assurance of nautical safety and long-term operational performance of critical ports and waterway systems.

1.3. Research Gap

Although storm surge barriers are increasingly being constructed within busy navigation routes and the associated risks are well recognized, no systematic and reproducible methodology currently exists for evaluating and comparing alternative barrier configurations with respect to nautical safety performance. In particular, existing assessment approaches provide limited support for early-stage design decisions.

Numerous studies have explored the multifaceted challenges associated with the design and operation of storm surge barriers, addressing topics ranging from economic feasibility to environmental impact and structural performance. However, openly available research focusing explicitly on nautical safety considerations, regarding the ability of vessels to safely and efficiently navigate in proximity to storm surge barriers, remains sparse and is often generic in nature. Where navigational aspects are considered, present assessments often rely on qualitative judgment or isolated case studies, providing limited insight into how alternative barrier configurations affect nautical safety.

The influence of specific barrier geometries, environmental conditions, and traffic characteristics on nautical safety outcomes has rarely been quantified using a structured, data-driven approach. Such insights are essential to support balanced design decisions that account for both flood protection and navigational safety objectives, and the current lack thereof restricts the ability to meaningfully and consistently assess navigational implications during early design stages. Addressing this methodological gap constitutes the central aim of this research.

1.4. Research Objective

The synthesis of the themes discussed in the previous sections provides the foundation for the research objective of this thesis:

to develop a systematic method for the quantitative evaluation and comparison of the navigational safety performance of various configurations of a storm surge barrier.

By systematically linking barrier design parameters, site-specific environmental conditions and traffic characteristics, and quantitative nautical safety performance metrics, the research aims to contribute to the currently limited pool of transparent, high-resolution, decision support studies for navigable storm surge barriers that relate storm surge barrier designs to navigational safety.

1.5. Research Questions

To achieve the research objective, the following research questions have been formulated.

1.5.1. Main Research Question

How can alternative storm surge barrier configurations be systematically evaluated in terms of their nautical safety performance during early-stage design?

1.5.2. Sub Research Questions

1. What are the key analytical and conceptual components required for a method that evaluates the nautical safety performance of storm surge barrier configurations at early design stages?
2. How can these components be integrated into a coherent and systematic framework for nautical safety assessment?
3. How can this framework be applied to a real-world case to evaluate its practical applicability and performance?
4. How can the results obtained from this framework be used to compare the nautical safety performance of multiple storm surge barrier configurations at early design stages?

1.6. Scope

This study focuses on the development and application of a systematic, quantitative method to evaluate and compare the navigational safety performance of different storm surge barrier configurations. The scope is limited to the early design and conceptual evaluation stages, where geometric layout, barrier siting, and navigable opening dimensions are still flexible and where objective assessment can meaningfully inform decision-making. The analysis evaluates how barrier design parameters, such as gate width, alignment, and siting, interact with representative environmental conditions and vessel characteristics to influence vessel maneuverability and nautical safety margins. The resulting safety indicators are intended to support relative, configuration-to-configuration comparisons under a consistent set of representative conditions, rather than to establish absolute or universally applicable navigational safety thresholds.

The study does not aim to provide a full operational or hydraulic design of a storm surge barrier, nor does it assess structural reliability, ecological impacts, economic optimization, sediment dynamics, or long-term maintenance strategies. These aspects, although critical to comprehensive barrier design, fall outside the methodological focus of this research and are addressed extensively in other literature. Similarly, the study does not attempt to capture the full range of subjective pilot judgments, instead, it complements expert opinion with reproducible, quantitative indicators that can support consistent

comparison across multiple design alternatives. The assessment is further restricted to the maneuvering behavior of individual vessels, and does not include traffic-level or encounter-based collision risk analysis, which would require separate probabilistic modeling approaches. As such, the framework is intended to function as a structured decision-support tool for early-stage design evaluation and expert discussion, rather than as a basis for definitive navigational safety approval or operational decision-making.

To demonstrate applicability, the proposed assessment framework is applied to the case of the Bolivar Roads storm surge barrier introduced in Subsection 1.1.4. The case serves solely as a testbed for evaluating the method's performance and does not seek to recommend an optimal design or provide a definitive navigational safety assessment for the specific project. Conclusions therefore pertain to the performance and applicability of the methodology rather than to the suitability of any particular barrier configuration in practice. It should be noted that throughout this report the terms nautical safety and navigational safety are used interchangeably to refer to the safe and efficient conduct of vessel navigation.

1.7. Report Structure

Chapter 1 introduces the research context and motivation, formulates the problem statement, research gap, objectives, and research questions, and defines the scope of the study. Chapter 2 provides the theoretical background required to evaluate navigational safety near storm surge barriers, identifying the key analytical and conceptual components that underpin the proposed assessment method. Chapter 3 translates these components into a coherent and systematic methodology, specifying the spatial schematization, simulation approach, and quantitative nautical safety assessment metrics, and introduces the Bolivar Roads case study to which the method is applied. Chapter 4 presents the results of the simulation-based assessments for the case study, focusing on the comparative nautical safety performance of alternative storm surge barrier configurations under representative conditions. Chapter 5 discusses these results in light of the methodological assumptions and limitations, positions the developed framework within the broader landscape of nautical safety assessment approaches, and reflects on its practical applicability and contribution. Finally, Chapter 6 synthesizes the findings to answer the research questions and provides conclusions and recommendations for future research. The report structure is summarized in Figure 1.3, which indicates the chapters in which each research question is addressed and illustrates the relationships between the main components of the study.

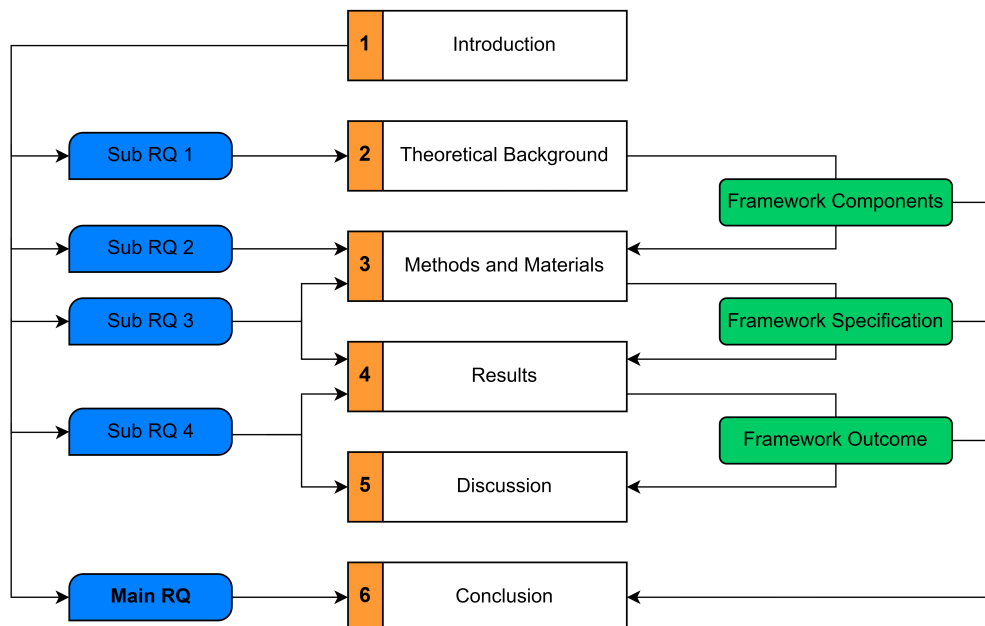


Figure 1.3: Overview of report structure, indicating where the research questions are addressed and how chapters are related.

2

Theoretical Background

To develop a systematic method for the quantitative evaluation and comparison of the navigational safety performance of storm surge barrier configurations, it is first necessary to establish a clear understanding of the analytical and conceptual components on which such a method must be built. This chapter therefore reviews and synthesizes existing methodological and research literature to identify the essential building blocks required for a reproducible assessment of nautical safety. These components are considered essential because a quantitative assessment of navigational safety near storm surge barriers inherently requires the explicit representation of geometric constraints, environmental forcing, vessel maneuverability, and objective performance measures, each of which addresses a distinct and non-substitutable aspect of the safety problem. Rather than presenting a prescriptive procedure, the chapter delineates the key components that govern how barrier geometry, environmental forcing, vessel characteristics, simulation approaches, and safety indicators can be coherently combined in the evaluation of maneuvering safety. The identified components are organized according to their functional role within the assessment process, distinguishing between method inputs (including spatial schematization, environmental forcing, and design vessels), modeling and simulation components (such as physical maneuvering indicators and ship maneuvering simulation models), and method outputs in the form of quantitative nautical safety assessment metrics. This functional structuring explains why these components directly inform the structure and sequencing of the assessment method developed in Chapter 3. By articulating what is already known, what can be adopted, and how these elements logically relate to one another, this chapter establishes the framework within which the proposed method is subsequently specified and applied.

2.1. Spatial Schematization

The physical space in which vessels maneuver is one of the most decisive factors influencing navigational safety, as it dictates the vessel's ability to maintain safe control, avoid collisions, and transit efficiently under the influence of environmental forcing such as winds and currents (Burmeister, 2020). For storm surge barriers specifically, the spatial characteristics of the barrier directly influence the heading adjustments, alignment behavior, and clearance margins that govern safe vessel passage (Burkley et al., 2022).

Spatial schematization refers to the structured representation of the navigational environment in geometric terms, encompassing the physical layout of the waterway, surrounding infrastructure, and storm surge barrier configurations under consideration. In the context of nautical safety assessments, spatial schematization is a foundational analytical component because it determines the geometric boundary conditions within which vessels must maneuver (PIANC, 2005).

For an assessment method aimed at evaluating the navigational safety performance of storm surge barrier configurations, spatial schematization is therefore indispensable. It formalizes the physical setting in which ships operate and ensures that all geometric constraints and relevant navigational features are explicitly defined, thereby allowing subsequent analyses of vessel motion, environmental influences,

and maneuvering behavior to reflect real-world conditions as accurately as possible. The following subsections discuss the three essential aspects of spatial schematization: the governing origin-destination combinations, the geometric domain size, and the representation of the nautical and bathymetric layout.

2.1.1. Origin-Destination Combinations

The spatial context relevant to a storm surge barrier depends on the vessel routes that intersect or approach its navigable opening (USACE, 2021c). Identifying the governing origin-destination (O-D) combinations is essential, as these routes determine the directions from which vessels approach and depart the structure. Not all possible routes require consideration: depending on the barrier's location relative to the port layout, some traffic flows may become operationally insignificant or geometrically infeasible, whereas others may become critical due to traffic density, vessel size, or challenging alignment requirements (Burkley et al., 2022).

The selection of governing O-D combinations directly influences the spatial schematization in two principal ways. First, it determines which segments of the waterway must be included in the modeled domain; specific bends, approach channels, or harbour basins may only be relevant for certain approach directions. Second, the chosen O-D combinations define the approach geometry at the barrier opening itself, shaping the required alignment distance, the potential for drift angle development, and the overall maneuvering complexity experienced by transiting vessels. Establishing the governing O-D pairs is thus a prerequisite for determining the spatial extent and orientation of the navigational domain used in the assessment of navigational safety in storm surge barrier design.

2.1.2. Geometric Domain Size

The selection of an appropriate domain size is a critical aspect of spatial schematization. The geometric domain must be sufficiently large to capture not only the barrier passage itself but also all relevant navigational processes that occur upstream and downstream of the storm surge barrier (Burkley et al., 2022). This includes the regions in which vessels initiate alignment, execute necessary course adjustments before or after barrier crossing, respond to environmental forces, develop drift, and stabilize their trajectory following passage through the barrier.

Upstream and downstream extents must therefore allow vessels to establish a steady-state approach, undertake course adjustments smoothly, and complete post-transit recovery without encountering artificial limits imposed by the modeled boundaries (PIANC, 2014). Likewise, the lateral extent of the domain must incorporate all physical constraints, such as shorelines, levees, jetties, harbour basins, and other infrastructure that defines or restricts the navigable corridor (PIANC, 2005). The extent and fidelity of the spatial schematization determine whether governing route geometries, approach maneuvers, and potential collision interfaces are adequately captured. An inadequately sized or overly simplified domain risks truncating vessel trajectories or omitting physical features that significantly influence vessel maneuverability.

The required domain size is ultimately governed by the selected origin-destination combinations and the spatial influence of the barrier configuration. Ensuring that the modeled domain is sufficiently extensive and detailed is essential for obtaining representative and reliable insights into vessel behavior near the storm surge barrier.

2.1.3. Nautical and Bathymetric Layout

A complete spatial schematization requires the representation of all nautical and bathymetric features that influence vessel maneuverability near the barrier and fall within the determined geometric domain (Eloot et al., 2007). This includes both the fixed elements of the harbour layout and the variable geometries associated with alternative barrier designs.

The nautical layout must incorporate all structures that shape the navigational corridor, including landmasses, shorelines, anchorage areas, jetties, piers, and other infrastructure relevant to vessel movement (Gong et al., 2007). These features define the lateral and longitudinal limits of the waterway and establish the collision interfaces and clearance margins central to safety assessments. Bathymetric schematization is equally important. Accurate depth information is required to capture shallow-water effects, variations in under keel clearance (UKC), and potential grounding hazards (Eloot et al., 2007).

Finally, all alternative barrier configurations must be represented consistently within the spatial schematization. Variations in navigable opening width, alignment relative to the channel, sill elevation, and structural footprint each impose distinct geometric constraints on vessel movement. Explicitly incorporating these alternatives ensures that the assessment method can robustly compare the nautical safety performance of competing barrier designs.

2.1.4. Spatial Data

Accurate spatial data are a prerequisite for the spatial schematization described in this section. Examples include: nautical charts, bathymetric datasets, and georeferenced representations of the barrier structures. These data help to provide the geometric basis for defining the navigable domain in which vessels operate and ensure that the modeled environment reflects the actual spatial constraints encountered during barrier approach, transit, and departure. The quality and resolution of the spatial data directly influence the reliability of the schematization and, consequently, the validity of subsequent maneuvering simulations and safety assessments. Consistent and well-referenced spatial datasets are therefore essential inputs to the developed assessment method.

Intermezzo: Ship Motion

Prior to covering the other analytical and conceptual components of the assessment method, it is important to understand basic ship motion terminology. There are six degrees of freedom that a ship can experience (see Figure 2.1). Namely, one translation and one rotation about each of its three reference axes, all of which originate in the vessel's center of mass: the longitudinal (x) axis, the transverse (y) axis, and the vertical (z) axis (De Winter, 2018).

Translatory Motions

- Surge: refers to the linear longitudinal motion of a vessel along its bow-stern axis.
- Sway: denotes the linear transverse motion of a vessel along its port-starboard axis.
- Heave: describes the linear vertical motion of a vessel along its up-down axis.

Rotary Motions

- Roll: refers to the angular motion of a vessel about its longitudinal (x) axis, resulting in tilting or oscillatory rotation from side to side.
- Pitch: denotes the angular motion of a vessel about its transverse (y) axis, corresponding to the alternating rise and fall of the bow and stern.
- Yaw: represents the angular motion of a vessel about its vertical (z) axis, corresponding to the turning or rotational movement that alters the vessel's heading.

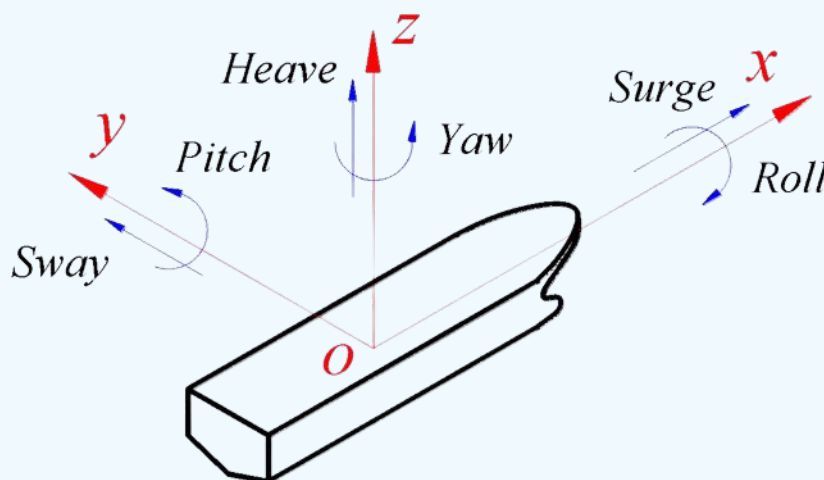


Figure 2.1: Translatory and rotary ship motions (De Winter, 2018).

2.2. Environmental Forcing and Hydrodynamic Effects

Vessel maneuverability in the vicinity of a storm surge barrier is shaped not only by the geometric constraints of the navigable opening, but also by the environmental forcing acting on the vessel as it approaches, transits, and departs the structure (Eloot et al., 2007). Wind, currents, waves, and water depth define the external forcing and boundary conditions under which a vessel must be controlled, while hydrodynamic interaction phenomena, such as shallow-water effects and bank suction, further influence the vessel's heading response, drift development, turning capability, and required control effort (Quy, 2008). Through their interaction with the fixed geometry of the barrier and its approaches, these forcing mechanisms and hydrodynamic effects can substantially influence vessel motion and thereby alter both the difficulty and the safety of the transit.

For a method intended to evaluate the nautical safety performance of alternative storm surge barrier configurations, identifying and characterizing the relevant environmental forcing and hydrodynamic effects is therefore essential (Gong et al., 2007). This section introduces the key external forcing mechanisms and interaction effects that must be considered in such assessments, explains their influence on vessel maneuvering behavior, and establishes their role as fundamental boundary conditions in the developed method.

2.2.1. Wind Effects

Wind effects refer to the influence of atmospheric forces acting on a vessel due to wind pressure exerted on its exposed surfaces above the waterline, including the superstructure, hull sides, deck equipment, and any cargo projecting into the airflow. These forces generate lateral sway and yawing moments that can alter a vessel's trajectory, induce drift, and impair heading control, particularly during low-speed maneuvers or operations in confined waterways (Fossen, 2011).

In the context of storm surge barriers, wind constitutes a critical environmental factor because it can significantly reduce a vessel's ability to maintain its intended path in regions where spatial tolerances are inherently limited (Burkley et al., 2022). Even moderate crosswinds can increase drift angles, delay alignment with the navigable opening, and lead to larger rudder or thruster inputs (Shigunov, 2020). Such deviations elevate the risk of structural allisions with the barrier, as well as the risk of unintended encroachment toward channel boundaries while maneuvering.

The magnitude and operational impact of wind forces depend strongly on the relative angle between the wind vector and the vessel's heading (Sutulo & Guedes Soares, 2021). Headwinds and following winds primarily influence vessel speed through added resistance or added propulsion but tend to have limited effect on lateral motion. Crosswinds, by contrast, impose a lateral aerodynamic force that displaces the vessel sideways, increasing the likelihood of drift-induced misalignment with the barrier opening or adjacent navigation channels. In addition to mean wind conditions, short-term wind gusts can introduce transient increases in aerodynamic loads and yaw moments, potentially amplifying drift and control demands during critical maneuvering phases.

Wind effects are influenced by several key factors (Fossen, 2011):

- **Wind Speed and Direction:** Higher wind velocities result in greater aerodynamic loads on the vessel. Crosswinds are the most critical because they generate the largest sway forces and yaw moments.
- **Windage Area and Geometry:** The magnitude of the wind force is proportional to the vessel's exposed surface area. Vessels with large superstructures, such as container ships, ro-ro vessels, or cruise vessels, are particularly susceptible to wind-induced drift and yaw. Not only the area, but also the shape and arrangement of wind-exposed surfaces affect how wind forces are distributed.
- **Vessel Loading Condition:** Lightly loaded vessels sit higher in the water, exposing more surface area to wind and reducing underwater resistance, thereby increasing sensitivity to wind forcing.
- **Maneuvering Speed:** At low speeds, hydrodynamic forces generated by the hull, rudder, and propulsion system are weaker, making the vessel more vulnerable to external forces such as wind. This is especially relevant during alignment, approach, and transit through narrow barrier openings.

2.2.2. Current Effects

Current effects refer to the hydrodynamic forces exerted on a vessel by water movement, typically arising from tidal flow, river discharge, or local circulation patterns. These forces act primarily on the submerged portion of the hull and appendages and can significantly influence the vessel's trajectory, drift angle, turning behavior, and speed over ground (Fossen, 2011). Currents modify the vessel's motion relative to the seabed and can produce substantial deviations from the intended path if not properly compensated for (Elloot et al., 2007).

In the context of storm surge barriers, currents are a critical environmental factor because the interaction between the flow field and the fixed geometry of the barrier can create additional hydrodynamic complexities (Orton et al., 2019). Flow acceleration through narrow openings, eddy formation downstream of barrier piers, or changes in current direction relative to the approach channel can increase drift, delay alignment, or induce unexpected yaw (Daniel & Paulus, 2019). These effects reduce available maneuvering margins and can elevate the risk of structural allisions or grounding during barrier approach and transit.

Current effects are commonly classified by their direction relative to the vessel's heading (Gokarn, 2024). Head currents oppose a vessel's forward motion, reducing speed over ground and potentially limiting the vessel's ability to maintain directional control through steering inputs or complete heading changes in time-sensitive maneuvers. Following currents increase speed over ground but reduce a vessel's controllability, increasing stopping distances and decreasing the time available for corrective actions. Cross currents exert lateral forces that displace the vessel sideways. These are typically the most hazardous near storm surge barriers, as they can induce drift angles that compromise alignment with the navigable opening or cause encroachment toward structural elements.

The magnitude and operational impact of current effects are influenced by several key factors (Fossen, 2011):

- **Current Velocity and Direction:** Stronger currents impose larger hydrodynamic forces on the hull. The angle between the current vector and the vessel's heading determines whether the current contributes to longitudinal drag, added propulsion, or lateral drift.
- **Vessel Speed:** At low speeds, hydrodynamic forces generated by the hull and rudder are comparatively weak, making the vessel more susceptible to current-induced drift and steering difficulty. Low-speed vulnerability is particularly relevant during alignment and transit through narrow barrier openings.
- **Hull Form and Draught:** Vessels with deeper draughts or broader underwater profiles experience greater current-induced loading. Flat-sided hulls are especially sensitive to lateral currents, which increase sway forces and yaw moments.
- **Under Keel Clearance and Channel Confinement:** Shallow or constricted waterways can accelerate flow due to reduced cross-sectional areas. Such confinement intensifies hydrodynamic forces on the hull and can produce uneven flow patterns that affect heading stability near the barrier.
- **Rudder and Propulsion Configuration:** Vessels equipped with advanced maneuvering systems, such as high-lift rudders, azimuth thrusters, or controllable pitch propellers, can counteract current effects more effectively than ships with conventional rudder-propeller arrangements.

2.2.3. Wave Effects

Wave effects refer to the forces and motions induced on a vessel by incident waves and swell. Unlike steady wind or current loading, waves generate oscillatory forces that can cause unsteady surge, sway, roll, pitch, and yaw motions (Gokarn, 2024). These motions may impair a vessel's ability to maintain a stable heading and consistent speed, particularly during low-speed maneuvers typical of barrier approach, alignment, and transit (Maljković et al., 2024).

In the context of storm surge barriers, wave effects are of particular relevance because barrier locations, often situated in estuaries, tidal inlets, or semi-exposed coastal waters, can experience wave conditions significantly more energetic than those found in sheltered harbour basins. Depending on the orientation of the navigable opening with respect to the wave direction, waves may induce yawing moments that

complicate alignment, increase drift, or require excessive rudder or thruster input (Shigunov, 2020). In more severe cases, waves can reduce speed through water or cause intermittent loss of propeller or rudder immersion, thereby reducing control authority at critical moments. Even moderate wave action can destabilize the vessel's approach trajectory or increase the likelihood of encroachment toward structural elements.

Wave effects are commonly distinguished by their direction relative to the vessel's heading (Gokarn, 2024). Head waves primarily act in the longitudinal direction, causing pitching and speed loss due to added resistance. This may impair the vessel's ability to maintain steering control or complete heading corrections in a timely manner during approach and transit. Following waves can increase vessel speed unintentionally, posing risks related to increased stopping distance, surf-riding, or broaching, especially for vessels with fine hull forms or small under keel clearance. Beam and quartering waves generate significant sway forces and yawing moments, which can alter the vessel's alignment, increase drift angles, and reduce directional stability. These conditions are typically the most hazardous when approaching narrow navigable openings.

The magnitude and operational relevance of wave effects depend on several key factors (Fossen, 2011):

- **Wave Height, Period, and Direction:** Higher and longer-period waves carry more energy and induce greater vessel motions. The alignment between the wave direction and the vessel's heading determines whether yaw, drift, roll, or speed variation dominates the vessel's response.
- **Vessel Size, Hull Form, and Loading Condition:** Larger vessels generally experience smaller angular motions but may still encounter substantial drift or yaw under beam waves. Lightly loaded vessels have higher freeboard, making them more susceptible to combined wind-wave effects and increasing the likelihood of pronounced roll or heave.
- **Maneuvering Speed:** At low speeds, typical during barrier approach, the vessel's hydrodynamic damping is reduced, increasing susceptibility to wave-induced yaw and drift. Lower speeds may also diminish rudder effectiveness when counteracting wave loads.
- **Nearshore and Channel Effects:** Waves can transform significantly in shallow or confined waters. Shoaling, refraction, and wave-current interaction near barrier sills or channel margins can alter wave height or direction, amplifying yawing moments or speed variations at precisely the points where navigational precision is most critical.

2.2.4. Water Depth

Water depth refers to the instantaneous vertical distance between the water surface and the seabed along the vessel's navigational path. Unlike wind, waves, and currents, which impose dynamic external forces, water depth functions as an environmental geometric boundary condition that governs the available under keel clearance and the hydrodynamic regime in which a vessel operates. Variations in water depth affect the vessel's ability to maneuver effectively, influence resistance and propulsion characteristics, and determine the safety margins required to avoid grounding (Hutchison et al., 2003).

In the context of storm surge barriers, water depth is a critical consideration because barrier construction, sill elevation, and associated dredging works can alter the depth profile of approach channels and navigable openings. Changes in depth influence the vessel's vertical clearance over the barrier sill, affect the likelihood and severity of squat, and modify steering and alignment behavior during low-speed maneuvers. Insufficient water depth or large spatial gradients can constrain maneuvering options, reduce control authority, and increase the risk of grounding or loss of steering capability during approach and transit.

The operational significance of water depth is influenced by several key factors (Vantorre et al., 2017; Gokarn, 2024):

- **Tidal Level:** Water depth varies with the tidal cycle, directly affecting under keel clearance and the hydrodynamic regime experienced by the vessel. Low-tide conditions can reduce maneuverability and increase grounding risk, while high-tide conditions may provide additional clearance but modify current strength.

- **Bathymetric Configuration:** Spatial variations in seabed morphology, including dredged channels, natural shoals, and depth transitions near barrier sills, determine where shallow-water conditions may occur and influence the vessel's ability to maintain safe clearance throughout the transit.
- **Vessel Draught and Loading Condition:** A deeper-draught vessel, or a vessel with increased trim, operates with reduced vertical clearance and is more susceptible to depth-related maneuvering constraints, including enhanced resistance, altered flow around the hull, and increased squat.
- **Vessel Speed:** Water depth interacts with vessel speed to determine the severity of squat and the associated changes in hydrodynamic forces acting on the hull. Higher speeds in shallow water reduce under keel clearance and can significantly alter maneuvering behavior.

2.2.5. Shallow Water Effects

Shallow water effects refer to the hydrodynamic phenomena that arise when a vessel operates in water of limited depth relative to its draught. In such conditions, the flow field around the hull is vertically constrained, altering pressure distributions, increasing hydrodynamic resistance, and modifying the vessel's response to steering and propulsion inputs (Gokarn, 2024). These effects do not originate from an external environmental force but instead emerge from the interaction between the vessel and the restricted hydrodynamic domain. As a result, shallow water conditions can significantly reduce maneuverability and induce changes in trim and squat, particularly during low-speed operations where hydrodynamic control forces are already diminished (Liu et al., 2015).

In the context of storm surge barriers, shallow water effects are of particular importance because depth-limited regions may occur near barrier sills, within dredged approach channels, or at transitions between deep and shallow sections. Even when the overall navigation channel provides adequate depth, localized reductions in under keel clearance, whether due to sill elevation, sedimentation, or tidal variability, can intensify shallow-water effects and increase the likelihood of contact with the channel bottom at precisely the points where accurate alignment and heading control are essential. These conditions may increase drift angles, reduce directional stability, and limit a vessel's ability to complete timely course adjustments during approach and transit (Vantorre et al., 2017).

The magnitude and operational relevance of shallow water effects depend on several key factors (Burmeister, 2020; Gokarn, 2024; Maljković et al., 2024):

- **Under Keel Clearance and Water Depth to Draught Ratio:** UKC, the vertical distance between the lowermost point of the vessel's hull and the seabed, is the primary determinant of shallow water influence. Reduced UKC amplifies shallow water effects, including increased hydrodynamic resistance, diminished propeller and rudder efficiency, and squat, a speed-dependent reduction in UKC caused by pressure decrease beneath the moving hull. The relative degree of depth limitation is commonly expressed through the water depth (h) to draught (T) ratio, h/T , with lower values indicating stronger shallow water effects and greater susceptibility to increased resistance, trim changes, and reduced directional stability.
- **Vessel Speed:** Shallow water effects scale nonlinearly with vessel speed. Higher speeds increase the dynamic pressure deficit beneath the hull, intensifying squat and elevating resistance. At very low speeds, the reduced hydrodynamic damping that already occurs in shallow water further diminishes steering effectiveness.
- **Hull Form and Displacement:** Full bodied vessels and those with large underwater profiles displace more water, increasing flow restrictions in shallow regions and resulting in greater resistance, larger squat, and reduced maneuvering responsiveness.
- **Propeller and Rudder Immersion:** Limited depth alters wake flow and can reduce the inflow to propulsion and steering devices. Loss of propeller or rudder immersion, or adverse flow conditions caused by shallow depths, reduce steering authority and complicate heading corrections.

- **Channel Confinement:** Shallow water effects are magnified when combined with lateral confinement, as the restricted cross-sectional area intensifies flow acceleration around the hull. This can increase resistance, degrade turning ability, and further reduce maneuverability near barrier structures or within dredged approach channels.

2.2.6. Bank Suction

Bank suction is a hydrodynamic interaction phenomenon that occurs when a vessel navigates in close proximity to the lateral boundary of a channel, particularly alongside steep or vertical banks (Hutchison et al., 2003). As the vessel moves forward, it displaces water along the hull. When this flow is restricted by the nearby bank, the water accelerates through the narrowing gap, leading to a localized pressure reduction on the bank side of the hull. The resulting pressure differential generates a lateral suction force that pulls the vessel toward the bank, typically causing the stern to be drawn inward while the bow swings outward, producing a characteristic yawing motion (Gokarn, 2024).

In the context of storm surge barriers, bank suction is a critical navigational consideration because the navigable barrier openings and adjacent channels are often narrow, dredged, or laterally constrained by structural elements. In such settings, even moderate proximity to a bank can produce substantial suction forces that reduce maneuverability and increase the risk of unintended lateral movement toward critical infrastructure. Bank suction is especially problematic during low-speed operations common near barrier openings, where rudder effectiveness and hydrodynamic damping are diminished, making the vessel more sensitive to asymmetric flow and pressure conditions (Eloot et al., 2007).

The strength and operational relevance of bank suction are influenced by several key factors (Eloot et al., 2007; Vantorre et al., 2017):

- **Beam Clearance:** The smaller the lateral distance between the vessel and the bank, the greater the flow constriction and associated pressure reduction. Reduced beam clearance therefore increases the magnitude of the suction force.
- **Vessel Speed:** Higher forward speeds increase the volume of water displaced and the flow velocity along the hull, amplifying pressure differentials and strengthening suction effects.
- **Channel Geometry and Depth:** Narrow or shallow channels confine the flow field, increasing the acceleration of water between the hull and the bank and heightening the vessel's susceptibility to suction-induced yaw.
- **Vessel Size and Hull Form:** Vessels with broad beams, large underwater profiles, or full bodied hull forms displace more water, producing stronger asymmetric flow patterns and more pronounced suction forces when operating near a bank.
- **Bank Slope and Roughness:** Steep or vertical banks generate more pronounced suction forces than gently sloping banks, which allow water to disperse more easily and thereby reduce the severity of flow acceleration and pressure reduction.

2.2.7. Other

While wind, waves, currents, water depth, and shallow-water or bank-induced effects directly interact with the vessel by applying forces and moments that influence its dynamic response, other environmental factors affect navigational safety through different mechanisms. Reduced visibility due to fog, precipitation, or nighttime conditions does not exert physical forcing on the vessel, but instead influences pilot perception, situational awareness, and the ability to perceive aids to navigation (AtoN), channel boundaries, and barrier structures. Such conditions can increase cognitive workload and reliance on electronic navigation systems during approach and alignment, thereby affecting the practical difficulty of a transit without altering the underlying vessel dynamics. Although these perception-related factors are widely recognized as relevant to navigational safety, they influence vessel transits through human interpretation and decision-making rather than through direct physical interaction with the vessel, and therefore represent a fundamentally different class of effects than the environmental forcing components discussed in the preceding sections.

2.2.8. Environmental Data

Accurate and representative environmental data are essential for properly accounting for the environmental forcing and hydrodynamic effects described in the preceding subsections. Consistent with the geometric domain definition described in Subsection 2.1.2, environmental forcing data are required across the entire simulation domain, encompassing vessel approach, passage through the barrier area, and downstream navigation. This ensures that the influence of environmental conditions on vessel maneuvering behavior is represented continuously throughout all phases of the simulated transit. The magnitude, temporal and spatial variability, and operational relevance of wind, current, waves, and water depth depend directly on the prevailing environmental conditions at the barrier location. Shallow-water effects and bank-induced forces, while influenced by environmental forcing, are further governed by the nautical and bathymetric layout and vessel-specific characteristics. Nevertheless, reliable and well-characterized data are a prerequisite for constructing realistic environmental scenarios and for ensuring that the resulting navigational safety assessment reflects operational reality.

2.3. Design Vessels

Design vessels constitute another fundamental component of a method intended to assess the nautical safety performance of storm surge barrier configurations, as they determine the vessel-specific maneuvering characteristics, spatial margins relevant for safe passage, and hydrodynamic responses that must be considered in the evaluation (PIANC, 2014). A design vessel is a vessel whose characteristics are representative of, or operationally critical to, the traffic expected to transit the barrier. By formally specifying these vessels, the assessment defines the physical and maneuvering constraints that form the basis for evaluating safe vessel passage.

Within the context of a simulation-based assessment method, design vessels serve as the primary operational inputs that define vessel behavior in relation to the spatial schematization and environmental forcing described in Section 2.1 and Section 2.2, respectively. They provide the geometric properties (such as length, beam, and draught), hydrodynamic attributes (including mass distribution and hull form), and control mechanisms (such as rudder, propeller, and thruster configurations) required to analyze alignment behavior, drift development, control demands, and clearance margins. The suitability, from a nautical standpoint, of a barrier configuration therefore depends on how well it accommodates the maneuvering envelopes and operational limitations associated with the selected design vessels.

2.3.1. Vessel Characteristics: Geometric Specifications

A vessel's geometric specifications define its physical footprint in the navigable domain and dictate the spatial margins required for safe passage (PIANC, 2014). These characteristics influence the vessel's swept path, required approach and alignment space, and the clearance margins necessary to avoid contact with structural elements. In addition, these dimensions strongly affect how the vessel responds to environmental forcing (see Section 2.2). As such, the geometric specifications of design vessels form a foundational input for an assessment method aimed at evaluating the navigational safety performance of storm surge barrier configurations, shaping both the maneuvering space required and the vessel's susceptibility to environmental effects when transiting a barrier.

The principal geometric parameters relevant for design vessel definition are (PIANC, 2022):

- **Length Overall (LOA):** The length overall denotes the maximum longitudinal extent of a vessel, measured from the foremost point of the bow to the aftmost point of the stern. This dimension directly influences the vessel's swept path and is critical for evaluating clearance margins, turning radii, and maneuvering capabilities in constrained environments.
- **Beam:** The beam represents the widest transverse measurement of the vessel, typically taken at the midship section. This dimension strongly affects lateral clearance margins, particularly in confined navigation channels. A wider beam generally enhances transverse stability but may also increase hydrodynamic resistance and intensify bank interaction effects in narrow waterways.
- **Draught:** Draught, the vertical distance between the waterline and the bottommost point of the vessel's hull, determines the minimum water depth required for safe navigation and is fundamental for calculating under keel clearance. Vessels with greater draught exhibit reduced maneuverability in shallow water, increasing their susceptibility to depth-related hydrodynamic phenomena.

2.3.2. Vessel Characteristics: Control Mechanisms

A vessel's control mechanisms govern its ability to generate the forces and moments required to adjust heading, maintain course, counteract environmental disturbances, and execute maneuvers with sufficient precision (Gokarn, 2024). Knowledge of these systems is fundamental to understanding ship maneuvering behavior, as they determine the vessel's control authority and thereby define the maneuvering capabilities that can be relied upon during transit of a storm surge barrier (Lataire et al., 2018). Within the assessment method, the characteristics of these control devices, namely the rudder, propeller, and thrusters, provide the essential inputs for evaluating a vessel's responsiveness, its capacity to execute alignment and turning maneuvers, and its ability to maintain safe clearance margins under varying environmental conditions.

A vessel's principal control mechanisms consist of the following (Lataire et al., 2018; Gokarn, 2024):

- **Rudder:** The rudder is a hydrodynamic control surface located aft of the propeller that enables a vessel to change its heading by generating a lateral force when deflected from the centerline (0° position). When water flows across the rudder surface, the deflection angle creates an asymmetric pressure distribution that induces a yawing moment, turning the vessel in the intended direction. The rudder is the primary steering device on most conventionally propelled ships and is most effective when sufficient inflow, generated by forward motion or propeller wash, passes over its surface. Rudder responsiveness is therefore highly dependent on vessel speed and propeller activity.

From a nautical safety perspective, rudder performance governs a vessel's ability to maintain course, execute controlled turns, and recover from deviations caused by environmental forces such as wind or currents. Consequently, rudder effectiveness is directly related to a vessel's ability to remain within navigable boundaries and avoid collisions during critical maneuvers. The maximum rudder angle, typically around 35° , defines the operational steering limit, beyond this, flow separation reduces lift and increases drag, diminishing control authority.

- **Propeller:** The propeller converts mechanical energy from the ship's main engine into thrust acting along the longitudinal axis, driving the vessel ahead or astern depending on the direction of rotation. In addition to providing propulsion, the propeller plays an important role in maneuvering by increasing flow velocities past the rudder, thereby enhancing steering response, especially at low speeds when natural inflow is limited.

In the context of nautical safety, propeller performance affects the vessel's ability to accelerate, decelerate, and maintain control under dynamic environmental conditions. The maximum revolutions per minute (RPM) of the propeller define the upper limit of available thrust and therefore shape the vessel's stopping distance, response time during evasive actions, and capacity to counteract drift or yaw induced by external forces.

- **Thruster:** Thrusters are auxiliary propulsion units designed to generate lateral forces for enhanced maneuvering control, particularly at low speeds or when the vessel is nearly stationary. Typically installed at the bow or stern, thrusters direct a jet of water perpendicular to the vessel's longitudinal axis, enabling lateral translation or heading corrections without relying on forward motion. Not all vessels are equipped with thrusters.

From a nautical safety perspective, thrusters provide additional sway and yaw control when rudder effectiveness is reduced due to low inflow velocity. They are essential for maintaining positional accuracy and to correct for environmental disturbances in situations where fine control is essential, such as when navigating near hydraulic structures or within restricted waterways. The maximum thrust force available defines the operational limit of these systems and varies depending on the thruster type, size, and installed power.

2.3.3. Vessel Data

The identification of appropriate design vessels requires careful consideration of both present and future traffic compositions, including the range of vessel sizes, types, and operational profiles likely to transit the barrier during its design lifetime. This process typically relies on the analysis of vessel traffic data, such as Automatic Identification System (AIS) records, to ensure that the selected design vessels reflect real-world operational patterns and represent the vessels that exert the most critical demands

on navigability. Such vessels may be critical due to their dimensions, limited maneuverability, hydrodynamic sensitivity, loading condition, or operational frequency. As a result, multiple design vessels may be required to capture the governing navigational challenges.

The design vessels used in the assessment thus serve as structured, representative abstractions of actual traffic, enabling a systematic evaluation of nautical safety performance across the barrier's intended operating spectrum. Accurate representation of vessel characteristics through careful design vessel selection is therefore a prerequisite for credible simulation-based assessments of nautical safety for storm surge barrier configurations.

2.4. Physical Maneuvering Indicators

A vessel's maneuvering behavior is the result of the combined influence of the spatial environment in which it operates (Section 2.1), the environmental forcing acting upon it (Section 2.2), and the vessel's geometric and control characteristics (Section 2.3). These interacting factors determine how a vessel turns, aligns, drifts, and occupies space while navigating through a waterway, and thereby, they have large implications for nautical safety (Gray et al., 2003; Du et al., 2018; Gucma et al., 2022). The resulting ship motion can be described using a set of key physical maneuvering indicators, namely: heading, course over ground, drift angle, and swept path. Illustrations of each of these maneuvering indicators are provided in Appendix A.

These indicators provide a quantitative representation of a vessel's dynamic behavior and are essential for interpreting how safely and effectively a vessel can transit a storm surge barrier. They link the physical motion of the ship to the operational constraints of the navigational domain and form a foundational input to the assessment method. Understanding and monitoring these indicators is therefore vital for evaluating alignment performance, drift development, clearance margins, and overall navigational safety in the vicinity of a barrier structure.

2.4.1. Heading

Heading is defined as the instantaneous direction in which a vessel's bow is pointed, expressed in degrees relative to true north (Gokarn, 2024). It represents the vessel's orientation independent of its actual motion over the ground or through the water. In contrast to the course over ground (see Subsection 2.4.2), which reflects the resultant trajectory of the vessel, heading is determined solely by steering inputs and the vessel's rotational response (Gokarn, 2024).

Heading is a critical parameter in nautical safety assessments because it serves as the primary reference for navigational alignment, particularly in confined waterways or in the vicinity of hydraulic structures such as storm surge barriers. A discrepancy between a vessel's heading and its actual path of motion can indicate the presence of drift or yaw instability, both of which increase the risk of structural allision or navigation channel departure (Vantorre et al., 2017). This discrepancy is especially consequential during low-speed operations, where hydrodynamic control forces are reduced and corrective maneuvers become less effective (Gokarn, 2024).

Accurate heading control is essential during approach, alignment, and passage maneuvers. For example, a vessel approaching a narrow navigable opening must achieve and maintain the appropriate heading well in advance to ensure safe transit. Deviations from the desired heading may require large rudder corrections, increase lateral drift, or induce yaw instability, all of which elevate the risk of structural allision.

Several interrelated factors influence a vessel's heading (Fossen, 2011; Gokarn, 2024):

- **Rudder Input:** The rudder is the primary mechanism for changing a vessel's heading. Its effectiveness depends on vessel speed, rudder angle, and hydrodynamic inflow generated by forward motion or propeller wash.
- **Propulsion Configuration:** Thrusters or advanced propulsion systems (e.g., azimuthing propellers) enhance heading control, particularly at low speeds when rudder-induced turning capability is reduced.

- **Environmental Forces:** Crosswinds, lateral currents, and wave-induced yawing moments can rotate the vessel away from its intended heading. These effects are most pronounced during low-speed maneuvers, or when the vessel has a large windage area or deep draught.
- **Hull Geometry and Loading Condition:** A vessel's mass distribution, hull form, and loading condition influence its yaw moment of inertia and hydrodynamic turning characteristics, affecting responsiveness to steering commands.

2.4.2. Course Over Ground (COG)

Course over ground (COG) refers to the actual trajectory that a vessel follows over the Earth's surface, expressed in degrees relative to true north (Gokarn, 2024). Unlike heading, which defines the direction in which the vessel is pointed, COG represents the resultant direction of motion arising from the combined effect of propulsion, steering inputs, and external forces such as wind and currents (Gokarn, 2024).

In nautical safety assessments near storm surge barriers, COG is a fundamental parameter because it indicates the vessel's real-time path through the navigable domain (Liu, 2020). It is used to evaluate whether the vessel is maintaining its intended track or deviating toward structural elements or channel boundaries (Xiao et al., 2014). Accurate control and prediction of COG are therefore essential for safe transit in constrained or high-risk waterways, where even small deviations may lead to hazardous encroachments.

A key aspect of COG is that it may differ substantially from the vessel's heading, particularly under the influence of lateral environmental forces (Gokarn, 2024). This difference is captured by the drift angle (see Subsection 2.4.3). If not properly managed, such discrepancies can lead to misalignment with channel axes or barrier openings, increasing the probability of structural allision or grounding.

A vessel's COG is influenced by several interrelated factors (Fossen, 2011; Gokarn, 2024):

- **Environmental Forces:** Currents can displace a vessel laterally, shifting its COG away from its heading direction. Winds, especially when acting on vessels with large exposed lateral surfaces, can similarly induce off-track motion.
- **Vessel Speed and Momentum:** At low speeds, vessels are more susceptible to COG deviations due to reduced hydrodynamic stability, diminished rudder effectiveness, and lower resistance to lateral environmental forcing.
- **Hull Geometry and Loading Condition:** Draught, hull shape, and windage area affect how a vessel responds to wind and currents (see Subsection 2.2.1 and Subsection 2.2.2). Deeper draught vessels or those with large side profiles exhibit stronger drift tendencies.
- **Propulsion and Steering Configuration:** Ships equipped with advanced maneuvering systems, such as azimuthing propellers or dynamic positioning systems, can counteract COG deviations more effectively than conventionally powered vessels, particularly at low speeds.

2.4.3. Drift Angle

Drift angle is defined as the angular difference between a vessel's heading and its course over ground (Fossen, 2011). It quantifies the extent to which a vessel is moving sideways relative to the direction it is pointed. A non-zero drift angle indicates the presence of lateral forces acting on the vessel, causing displacement from its intended trajectory (Gokarn, 2024).

In the context of nautical safety assessments near storm surge barriers, drift angle is a critical parameter because it directly influences the vessel's lateral position, alignment stability, and navigational predictability during approach and transit (Gong et al., 2007). Excessive drift can result in encroachment toward channel boundaries, adjacent traffic lanes, or structural elements, thereby increasing the likelihood of grounding, bank contact, or allision with barrier components. Drift angle also serves as an indicator of control difficulty: larger drift angles typically correspond to increased corrective steering demand, reduced directional stability, and diminished navigational safety margins (Gong et al., 2007).

A vessel's drift angle is influenced by several key factors (Fossen, 2011; Gokarn, 2024):

- **Crosscurrents:** Crosscurrents exert lateral forces on the underwater hull, displacing the vessel sideways and shifting its COG away from the heading direction, thereby increasing the drift angle.
- **Crosswinds:** Crosswinds acting on the vessel's exposed superstructure can induce yawing moments, particularly for ships with large windage areas such as container vessels or car carriers.
- **Vessel Speed:** At low speeds, hydrodynamic lift and rudder effectiveness decrease, reducing the vessel's ability to counteract lateral forces and resulting in greater drift angles.
- **Hull Form and Draught:** Full bodied or deeply laden vessels experience stronger lateral hydrodynamic forces and slower corrective response, making them more prone to drift under wind or current loading.
- **Steering Characteristics:** Vessels equipped with thrusters or advanced maneuvering systems, such as azimuthing propellers, can counteract drift more effectively, whereas conventionally powered single-screw vessels have more limited ability to correct lateral displacement.

2.4.4. Swept Path

Swept path refers to the total area occupied by a vessel and its extremities as it moves along a trajectory, particularly during maneuvers such as turning, aligning, or transiting constrained waterways (Liu, 2020). It represents the vessel's dynamic footprint, capturing the outermost positions of the bow, stern, and sides as influenced by yaw, drift, turning radius, and other aspects of maneuvering behavior. Swept path is therefore not a static geometric outline, it is a dynamic spatial envelope shaped by the combined effects of a vessel's handling characteristics and external environmental conditions (Liu, 2020).

In nautical safety assessments near storm surge barriers, swept path is a fundamental concept because it defines the minimum navigational space required for safe transit (Quy, 2008). It provides the basis for evaluating whether a vessel can move through a barrier opening or adjacent channel without encroaching on structural elements, channel boundaries, or shallow-water regions. Accurate estimation of a vessel's swept path is therefore essential for determining whether the available navigational space is sufficient to accommodate vessel motion under the governing, environmentally influenced, maneuvering conditions.

A vessel's swept path is influenced by several interrelated factors (PIANC, 2014; Buckers, 2017; Verdugo et al., 2018):

- **Drift Angle:** A larger drift angle increases the lateral offset between the vessel's heading and its actual trajectory, broadening the swept path.
- **Turning Radius:** When navigating along curved trajectories, the vessel pivots around its center of rotation, with the stern typically swinging outward. Larger turning radii and greater stern swing contribute substantially to swept path width.
- **Vessel Dimensions:** Length and beam directly affect the spatial envelope a vessel occupies. Larger vessels not only occupy more space but often also exhibit slower turning responses and greater stern swing, both of which increase the width of their swept paths.
- **Speed and Rudder Activity:** At low speeds, reduced hydrodynamic forces lead to slower heading changes and wider turns. At higher speeds, understeer or oversteer may occur depending on hull form, rudder angle, and flow dynamics, influencing the shape and width of the swept path.
- **Environmental Conditions:** Crosscurrents and crosswinds can displace the vessel laterally or alter its turning behavior, enlarging the swept path as the vessel counteracts these forces.

2.5. Ship Maneuvering Simulation Models

The navigational safety performance of storm surge barrier configurations cannot be evaluated through conceptual analysis alone, it requires a modeling framework capable of integrating the spatial schematization (Section 2.1), environmental forcing and hydrodynamic effects (Section 2.2), design vessel characteristics (Section 2.3), and the resulting physical maneuvering indicators (Section 2.4). Ship maneuvering simulation models provide this framework. They generate time-dependent vessel trajectories by numerically solving the ship's equations of motion under specified environmental and geometric conditions, and operational inputs, thereby allowing vessel-environment-geometry interactions to be assessed in a systematic and reproducible manner (Hutchison et al., 2003; Eloot et al., 2007).

Several categories of maneuvering simulation models exist, each differing in their level of fidelity, computational complexity, degree of human involvement, and typical application. The two principal classes are fast-time simulations and real-time simulations, which have become the dominant tools in contemporary waterway and navigational safety studies (PIANC, 2014; IALA, 2022). Fast-time simulations (FTS) compute vessel trajectories autonomously based on mathematical maneuvering models and control algorithms, enabling efficient exploration of large scenario sets. Real-time simulations (RTS), by contrast, incorporate human pilots or mariners operating within a simulator environment, and are typically used for validation, training, and stakeholder engagement.

In addition to these established approaches, other modeling paradigms have emerged in recent research and practice, including reinforcement-learning-based ship handling models, and maneuvering models rooted in control theory. While these methods are less commonly applied in the context of hydraulic structure navigability, they illustrate the broader spectrum of tools available for representing ship maneuvering behavior.

The purpose of this section is not to select a specific simulation approach, but to outline the modeling options available and to clarify their respective roles within a navigational safety assessment. The subsequent chapter (Chapter 3) builds on this foundation by justifying the choice of simulation model used in the developed assessment method.

2.5.1. Fast-Time Simulation

Fast-time simulation models are computational tools that predict ship trajectories based on mathematical formulations of ship dynamics. Vessel motion is typically governed by equations of motion in surge, sway, and yaw, with hydrodynamic coefficients derived from empirical data, model tests, or numerical maneuvering models (Quy, 2008; PIANC, 2014). Control inputs, such as rudder angle, propeller revolutions, and thruster activity, are generated by an autopilot algorithm that functions as a virtual navigator maintaining the vessel on a predefined track (Eloot et al., 2007). As all control decisions are automated, simulations run much faster than real time, making it possible to evaluate large numbers of scenarios efficiently.

Fast-time simulation is particularly suited to the early design and concept development phases of navigable hydraulic infrastructure projects. It is widely used to evaluate preliminary channel or port approach layouts, test alignment geometries, identify potential navigational bottlenecks, and verify the adequacy of spatial margins (PIANC, 2014; Lataire et al., 2018; Formela, 2020). For example, FTS can be applied to assess channel width, turning basin dimensions, and under-keel clearance requirements under varying environmental conditions (Quy, 2008). This type of simulation model further enables the evaluation of multiple vessel types and sizes, supporting the identification of governing design vessels in the context of waterway planning (PIANC, 2014).

The primary advantages of fast-time simulation are efficiency, objectivity, and repeatability. Because the simulation process is fully automated, identical input conditions yield identical results, eliminating variability associated with human operators (IALA, 2022). This consistency allows for systematic parametric analyses in which the influence of wind, currents, water depth, or channel geometry on vessel performance can be quantified (Eloot et al., 2007; Lataire et al., 2018). FTS is also computationally inexpensive, making it well suited for exploring broad scenario matrices across multiple design alternatives (Quy, 2008). Its deterministic structure facilitates the extraction of quantitative safety indicators, such as swept path envelopes, drift angles, or minimum under keel clearance, that may subsequently support evaluations of nautical safety aspects (IALA, 2022).

Despite these advantages, fast-time simulation has inherent limitations. Because control actions are generated by pre-programmed algorithms, FTS cannot reproduce human decision-making processes, perceptual limitations, or situational awareness (IALA, 2022). Autopilot behavior assumes perfect knowledge of environmental and vessel states, which differs from real-world navigation where uncertainty, judgment, and experience shape maneuvering choices. As a result, the outcomes of fast-time simulations may be optimistic compared to actual ship handling. In addition, FTS requires predefined tracks or control strategies, meaning that alternative maneuvers or evasive actions cannot be explored unless explicitly scripted (Quy, 2008). Model validity further depends on the accuracy of hydrodynamic coefficients and environmental inputs. Inaccurate calibration can lead to misleading results, particularly in shallow or restricted waters where ship-bank and ship-bottom interactions dominate (Eloot et al., 2007). Consequently, PIANC (2014) and IALA (2022) recommend using fast-time simulation primarily for comparative evaluation and early-stage design optimization, rather than as a stand-alone validation tool for navigational safety.

2.5.2. Real-Time Simulation

Real-time simulation represents a human-in-the-loop approach in which professional mariners operate a virtual ship model within a simulator environment that runs at actual time scale. The simulator reproduces the full bridge setting, including visual scenes, radar, electronic chart displays, and navigational instruments, allowing participants to perceive and react to realistic sensory inputs (Verdugo et al., 2018; IALA, 2022). The underlying mathematical ship models are typically similar to those used in fast-time simulation, but in RTS they are linked to interactive control interfaces. Because the simulation operates in real time, the human operator's perception, reaction, and decision-making processes unfold naturally, replicating the cognitive complexity of real-world navigation (PIANC, 2014).

Real-time simulations are primarily used in detailed design and validation studies. Once a feasible waterway or barrier layout has been identified, pilots and other stakeholders participate in simulation sessions to verify that the design is operationally safe, practical, and consistent with real navigational behavior (PIANC, 2014; Verdugo et al., 2018). These sessions typically evaluate approach and departure maneuvers, tug operations, and vessel interactions under varying environmental conditions. As noted by Lataire et al. (2018), real-time simulation is indispensable for confirming that human-operated vessels can navigate proposed layouts within acceptable safety margins. It also supports training, procedure development, and familiarization with new or modified navigation areas prior to construction (Verdugo et al., 2018).

The main strength of real-time simulation lies in its realism and the explicit inclusion of human factors. RTS incorporates human expertise, perception, and decision-making aspects of navigation, that computational models alone cannot reproduce (Hutchison et al., 2003; Eloot et al., 2007). It also facilitates the testing of dynamic or interactive scenarios, such as vessel encounters, tug assistance, and emergency responses, in a controlled but operationally realistic environment (IALA, 2022). The qualitative insights provided by experienced pilots enhance the credibility of the assessment, reveal operational nuances not captured by mathematical models, and help refine navigational procedures and design details (Verdugo et al., 2018). For these reasons, PIANC (2014) identifies real-time simulation as the preferred tool for final design verification of approach channels and maneuvering areas.

However, real-time simulation is resource-intensive. It requires specialized facilities, trained personnel, and the involvement of qualified mariners, making the method costly and time-consuming (IALA, 2022). Because the simulation runs at a one-to-one time ratio, the number of scenarios that can be explored is limited compared to fast-time simulation. Results may also vary due to differences in pilot experience, skill, and judgment (Eloot et al., 2007). Moreover, although RTS offers high realism, it still cannot perfectly reproduce real-world factors such as stress, fatigue, or the unpredictable interactions associated with dense or multi-vessel traffic environments (Verdugo et al., 2018). Consequently, real-time simulation is generally reserved for critical or final project stages, complementing and validating the broader scenario exploration enabled by fast-time methods.

2.5.3. Other Modeling Approaches

Although fast-time and real-time simulation are the principal tools used in navigational safety studies, several other ship maneuvering modeling approaches have been explored in (recent) research. These methods are not commonly applied in the design or assessment of port layouts or storm surge barrier configurations, but they are a testament to the expanding landscape of ship maneuvering prediction tools and illustrate that alternatives to conventional simulation frameworks exist.

One group of emerging methods is machine learning based models, which use neural networks or deep learning to predict vessel motion directly from operational data (Luo & Zhang, 2016; Wakita et al., 2022; Wang et al., 2023; Zhang et al., 2023). Related studies apply these techniques specifically to trajectory prediction in real operational conditions or low-speed environments (Jiang et al., 2022). A further development is hybrid modeling, where machine learning components are combined with traditional maneuvering models to improve predictive performance (Tian et al., 2025). Other research applies reinforcement learning, in which an artificial agent learns maneuvering strategies through interaction with a simulated environment (Amendola et al., 2020). Finally, some studies have explored optimal-control formulations, which compute theoretically optimal maneuvers rather than simulating operational behavior (Thomas & Sclavounos, 2007).

While these alternative approaches demonstrate promising possibilities for future maneuvering prediction, they remain primarily research-oriented and are not yet established tools for systematic navigational safety assessments. Their relevance here is to highlight the breadth of available modeling techniques, complementing the fast-time and real-time simulation models discussed in Subsection 2.5.1 and Subsection 2.5.2, respectively.

2.6. Quantitative Nautical Safety Assessment Metrics

In order to evaluate the outputs of the ship maneuvering simulation models introduced in Section 2.5, quantitative nautical safety assessment metrics are essential. These metrics are linked to the theoretical concepts introduced in Section 2.1, Section 2.2, Section 2.3, and Section 2.4 through the ship maneuvering simulation models. Numerous research papers, standards, and operational approaches propose quantifiable indicators that translate vessel motions into objective measures of navigational safety, ranging from distance-based clearance measures and maneuverability parameters to control-effort or encounter-based indices. This section reviews these established quantitative approaches, identifying the extent to which they offer suitable, physically meaningful, and reproducible elements for evaluating the nautical safety performance of storm surge barrier configurations. In addition, the section considers study findings showing that navigational risks near storm surge barriers may extend well upstream and downstream of the structure, underscoring the need to examine vessel behavior beyond the moment of barrier passage. By surveying the current state of the art, the section clarifies which underlying concepts and metric families can serve as elements for the assessment metrics framework developed in Chapter 3, and highlights where existing methods fall short for the specific context of storm surge barrier evaluation.

2.6.1. Metric Families

A wide range of quantitative indicators is used in the existing literature to assess navigational safety and ship maneuverability. Many of these indicators measure a vessel's spatial relationship to its surroundings, including other vessels. Distance-based indicators include the *ship domain*, which describes the minimum safety area surrounding a vessel such that any intrusion into this area constitutes a potentially unsafe encounter (Montewka et al., 2009). Montewka et al. (2009) used this concept to empirically derive minimum passing distances between two vessels, that vary with relative bearing, vessel type, and operating conditions. Distance-based measures also appear in assessments of shiphandling difficulty, where the minimum distance to obstacles encountered during a transit is explicitly quantified as a *proximity index* (Gong et al., 2007). Classical maneuverability standards, such as the IMO¹ and CCNR² criteria that define quantitative performance requirements for turning, zigzag, and stopping tests, similarly incorporate spatial measures such as *advance*, *transfer*, *tactical diameter*, and *track reach* (Liu et al., 2015). These parameters describe the lateral and longitudinal space a vessel requires during

¹International Maritime Organization

²Central Commission for the Navigation of the Rhine

course alterations or stopping maneuvers, thereby serving as geometric indicators of its spatial maneuvering demand (Liu et al., 2015). In collision risk models, designed to estimate long-term frequencies of collisions, geometric encounter concepts such as the *collision candidates*, *collision diameters*, *ship separation distances*, and the *closest point of approach* also reflect spatial safety margins, even though they are used probabilistically at the traffic-system scale (Friis-Hansen, 2008; Li et al., 2012). Taken together, these works demonstrate that a large portion of existing quantitative safety indicators are fundamentally spatial in nature.

A second group of indicators in the literature captures temporal aspects of vessel maneuverability and risk. In probabilistic collision risk modeling, the likelihood of collision depends partly on time-related indicators such as *time-to-encounter*, *time exposed to collision-candidate situations*, and the *time to closest point of approach* (Friis-Hansen, 2008; Li et al., 2012). Maneuverability standards also incorporate temporal performance criteria, for example by constraining the time required to achieve prescribed heading changes or come to a stop (Liu et al., 2015). Assessments of shiphandling difficulty similarly consider temporal allowance indirectly through indices that capture how quickly a vessel can realign itself in response to external forces (Gong et al., 2007). These indicators essentially quantify the amount of time available to complete a required maneuver before a hazardous situation materializes.

Finally, several studies emphasize indicators related to the vessel's available control authority, its ability to generate sufficient steering and propulsion forces to maintain safe navigation. Reviews of maneuverability criteria highlight measures such as *overshoot angles*, *yaw-checking ability*, *course-keeping indices*, and *turning-ability indices*, all of which reflect how effectively the vessel's control mechanisms can respond to dynamic disturbances or required course alterations (Liu et al., 2015). Control-effort measures are explicitly quantified in studies of shiphandling difficulty, where *rudder-usage indices*, *drift-angle indices*, and *reserved control-margin indices* translate the magnitude and intensity of control inputs into numerical indicators of maneuvering difficulty or navigational safety (Gong et al., 2007). Research on maneuverability in adverse conditions similarly defines safety through control-related thresholds, including *maximum allowable drift angles*, *required rudder forces*, and *power margins* needed to maintain heading or speed in challenging environmental conditions (Liu et al., 2015).

Across these diverse strands of literature, ranging from ship-domain theory and maneuverability standards to analyses of shiphandling difficulty and probabilistic collision risk modeling, quantitative navigational safety indicators consistently fall into these three recurring families. Spatial indicators capture clearance and proximity, temporal indicators capture the time available to complete maneuvers, and control-related indicators capture the vessel's steering and propulsion authority. Although the metrics are sometimes applied at the traffic system scale in the literature (which is outside the scope of this research that focuses on single vessel maneuverability), this pattern illustrates the extent to which existing research already conceptualizes nautical safety through measurable distance, time, and control allowances, providing a set of established building blocks from which Chapter 3 can synthesize a coherent and application-specific assessment metric structure for storm surge barrier evaluation.

2.6.2. Extent of Navigational Risks in Barrier Environments

The navigational implications of storm surge barriers are not confined to the moment of passage through the structure itself (Burkley et al., 2022; GHPB, 2023b). As discussed in Subsection 1.1.4, some of the risks identified during a simulation-based evaluation study of the proposed Bolivar Roads storm surge barrier would extend well beyond the barrier opening and “impact the spacing, timing, and navigation of ships for miles on either side of the gate complex” (Burkley et al., 2022). Vessel behavior upstream and downstream of the structure thus plays a critical role in determining overall navigational safety. These findings underscore that the assessment of nautical safety near storm surge barriers must not focus solely on the conditions within the barrier opening but must also account for the approach and departure phases of the transit, where alignment, stabilization, and recovery maneuvers occur. Insights which provide essential contextual foundations for the development of a coherent assessment metrics framework in Chapter 3.

3

Methods and Materials

Having identified and justified the analytical and conceptual building blocks required for a quantitative nautical safety assessment method for storm surge barriers in Chapter 2, this chapter synthesizes these components into a coherent and systematic assessment framework. The chapter specifies the methodological choices made with respect to each component and organizes them into a structured, stepwise assessment procedure, including the spatial schematization, environmental forcing representation, selection of design vessels, maneuvering indicators, ship maneuvering simulation approach, and quantitative safety assessment metrics. Together, these choices define a reproducible method for evaluating and comparing the navigational safety performance of alternative storm surge barrier configurations. Finally, the chapter introduces the Bolivar Roads storm surge barrier as the case study context for the subsequent application of the developed framework.

3.1. Method: Component Specification and Synthesis

This section translates the analytical and conceptual building blocks identified in Chapter 2 into a fully specified and reproducible assessment method. Each component is operationalized through explicit procedural steps, data requirements, and consistency constraints that together define how the assessment is to be implemented in practice. The section specifies how spatial schematization, environmental forcing, design vessels, physical maneuvering indicators, ship maneuvering simulation models, and quantitative safety assessment metrics are selected, parameterized, and applied in a consistent manner across alternative storm surge barrier configurations. Particular emphasis is placed on ensuring internal coherence and comparability, such that observed differences in assessment outcomes can be attributed to barrier configuration effects rather than methodological inconsistencies. The section concludes by synthesizing these elements into an integrated, stepwise framework that forms the basis for the case study application introduced thereafter.

3.1.1. Spatial Schematization

As discussed in Section 2.1, spatial schematization establishes the geometric representation of the navigational environment in which vessel trajectories are simulated. It defines the physical boundaries, approach routes, and bathymetric conditions that shape maneuvering behavior near a storm surge barrier. Because the assessment relies on simulated vessel motion, the spatial schematization must be constructed in a reproducible and systematic manner. This section specifies the procedure for identifying the governing origin-destination (O-D) combinations, defining the required geometric domain size, and assembling the nautical and bathymetric layout for use in the simulation model.

Determining Governing Origin-Destination Combinations

The first step in spatial schematization is to determine which vessel routes govern the navigational assessment. The method requires identifying all feasible transit routes that intersect the location of the proposed storm surge barrier. These routes are obtained from official nautical charts, port navigation guidelines, vessel traffic datasets, and consultation with experienced pilots or port authorities.

From this full set of routes, only the operationally relevant O-D combinations are retained. Routes that are rarely used, geometrically infeasible under barrier operation, or associated with small, low-risk vessel classes are excluded. The method then filters the remaining routes based on two criteria. First, O-D combinations that account for a substantial portion of deep-draft or maneuvering-critical vessel traffic must be included, as they strongly influence the spatial and operational constraints of barrier transit. Second, O-D combinations that require significant alignment, turning, or stabilization maneuvers near the barrier must be retained, because these routes are most sensitive to barrier geometry and environmental forcing.

The result is a minimal but representative set of governing O-D pairs that captures all critical approach directions. These governing O-D combinations form the basis for defining the simulation tracks and determining the spatial domain required to model realistic approach and departure behavior.

Determining the Geometric Domain Size

Once the governing O-D combinations are established, the geometric domain can be defined. The method requires a domain that is sufficiently large to capture the full set of maneuvers vessels perform during approach, barrier transit, and departure. Based on discussions with maritime experts it is decided that the longitudinal extent of the domain must therefore include at least one significant course change or bend upstream and downstream of the barrier along each governing O-D route. This requirement ensures that vessels can reach a steady-state approach trajectory prior to alignment with the barrier opening and complete their recovery and stabilization maneuvers after barrier transit.

The lateral extent of the domain must include all navigable channel boundaries, jetties, levees, breakwaters, harbour basins, and shoreline features that define or constrain maneuvering space. Lateral boundaries must be positioned sufficiently far from the vessel tracks to avoid imposing artificial constraints on drift development, heading corrections, or stern swing during simulations.

The vertical and hydrodynamic extent of the domain must incorporate all depth variations relevant to maneuverability, including dredged channel footprints, shoals, sills, or transitions between shallow and deep areas. Regions where under-keel clearance is limited, or where shallow-water or bank-interaction effects may arise, must be included explicitly.

To prevent numerical artifacts at the boundaries of the simulation environment, the domain must include a buffer zone beyond the minimum geometric requirements. This buffer ensures that hydrodynamic interactions and course-stabilization processes are not truncated prematurely at the model edges. The final domain must allow vessels to execute their full maneuvering envelope without encountering artificial spatial limitations.

Representing the Nautical and Bathymetric Layout

The final component of spatial schematization is the construction of the nautical and bathymetric layout within the defined domain. The method requires assembling a georeferenced representation of all fixed nautical features that influence vessel movement. These include coastlines, jetties, quay walls, breakwaters, navigation channel centerlines and edges, and any other infrastructure that constrains or guides vessel trajectories. In this way, it is guaranteed that vessels experience comparable boundary conditions across all configurations.

Bathymetric information must be incorporated with sufficient resolution to represent dredged channels, natural depth variations, and any depth-related constraints that shape maneuverability. Depth data can be obtained from hydrographic surveys, nautical charts, or port authority datasets.

To obtain meaningful insights into nautical safety, it is essential that the schematization reflects the nautical and bathymetric layout expected after barrier placement, as these may differ from the present-day situation. The introduction of a storm surge barrier may, for example, necessitate the widening or realignment of navigation channels through dredging, or the relocation of harbour elements to accommodate the structure.

For each alternative storm surge barrier configuration, the structural footprint, navigable openings, alignment, and other geometric elements must be added consistently and with identical spatial resolution. This ensures that the simulated vessel trajectories and hydrodynamic interactions accurately reflect the physical conditions corresponding to each alternative barrier configuration.

The spatial schematization can be developed in various geographic information system (GIS) or drafting software environments, such as QGIS, ArcGIS, Google Earth Pro, Maptitude, or AutoCAD, provided that the resulting georeferenced geometry can be exported in a format suitable for use in the chosen ship maneuvering simulation model.

3.1.2. Environmental Forcing and Hydrodynamic Effects

As discussed in Section 2.2, environmental forcing plays a central role in determining vessel maneuverability and must therefore be defined systematically within the assessment method. The purpose of this section is to specify how the method identifies which environmental forcing mechanisms are relevant, how the governing magnitudes of these forcings are selected to define “worst navigable scenarios”, and how these scenarios are subsequently prepared for use in the ship maneuvering simulation model.

Identifying Relevant Environmental Forcing Mechanisms

A critical methodological distinction must be made between two categories. Wind, currents, waves, and water depths are measurable external environmental forcings with definable magnitudes (and directions). These require explicit definition of operationally governing conditions. Shallow-water effects and bank suction, however, are not external forcings but hydrodynamic interaction phenomena. They do not have magnitudes that can be prescribed directly. Instead, they arise when vessel geometry, bathymetry, water depth, and proximity to boundaries produce the required flow conditions. Their inclusion in the assessment is therefore achieved indirectly, through accurate nautical and bathymetric schematization (Subsection 3.1.1) and through the use of a simulation model that incorporates mathematical formulations for these effects (Subsection 3.1.5). The method therefore does not define “worst navigable” values for these interaction effects, it rather ensures their correct representation through modeling fidelity.

The first step is to establish which environmental forcing mechanisms significantly influence vessel behavior across the simulation domain. The method begins with the full set of forcing mechanisms introduced in Section 2.2; wind, currents, waves and water depth, and then determines their local relevance using authoritative data sources. These include long-term measurement stations located near the barrier site, hydro-meteorological databases maintained by national or regional authorities, port authority guidelines, navigation manuals, and numerical models that provide spatially resolved information on currents, water levels, wind fields, and wave climates. Environmental datasets must undergo quality control and validation to ensure reliability, including checking for gaps or inconsistencies in measurement records and comparing observational datasets with model outputs where available.

Not all mechanisms described in Section 2.2 necessarily influence vessel maneuvering at every barrier site. Therefore, for each environmental forcing mechanism, the method evaluates whether it can materially influence alignment, drift, controllability, or clearance during barrier approach and transit. Mechanisms that are operationally negligible in the local context, such as waves in fully sheltered estuarine environments, must be excluded. The remaining mechanisms constitute the set of environmental drivers that must be accounted for in the assessment.

Ideal Environmental Modeling and Practical Constraints

In the ideal methodological setting, configuration-specific hydrodynamic modeling would be used to quantify how each barrier layout alters current patterns, flow acceleration, turbulence, and wave conditions in its vicinity. Such modeling would provide spatially resolved, configuration-dependent input fields, enabling highly accurate representation of maneuvering conditions in the simulations. However, full hydrodynamic modeling is resource-intensive and may be infeasible during early-stage design. The method therefore allows the use of representative current conditions, for which the flow fields around barrier elements are derived based on historical data, pilot and expert experience, and operational limits. Applying these conditions consistently across all configurations, this enables a systematic and comparable assessment even when configuration-specific hydrodynamic fields are unavailable. Depending on the availability and spatial coverage of measurements, numerical models may also be used to supplement or interpolate observed data, particularly in complex estuarine settings or where measurements are sparse.

Within the context of the present early design stage assessment method, wind gust effects are acknowledged conceptually but are not resolved explicitly, as doing so would require high-resolution temporal

modeling that is that is beyond the level of abstraction adopted in this study. Instead, their influence is implicitly accounted for through the selection of representative wind forcing conditions.

Defining Worst Navigable Conditions

For all measurable external forcing mechanisms deemed relevant, the method defines the worst navigable conditions: the most adverse combination of wind, current, waves, and water depths under which vessels are still permitted or expected to sail. These conditions represent adverse but realistic environmental states tailored to the site-specific physical setting, excluding extreme storm conditions during which navigation would be suspended. This ensures that the assessment reflects realistic operational boundaries rather than hypothetical extremes.

Worst navigable conditions must reflect the fact that environmental forcing is direction-dependent. Wind and current effects vary significantly between inbound and outbound transits, and the maneuvering challenges associated with alignment, drift development, and recovery are not symmetrical. For this reason, the method requires establishing separate worst navigable conditions for inbound and outbound traffic.

In addition, because each governing origin-destination (O-D) combination may expose vessels to different approach geometries, cross-current components, or turning requirements, worst navigable conditions must also be defined on a per-O-D combination basis. This ensures that each simulated transit is evaluated under the most adverse, but still operationally permissible, environmental conditions relevant to that specific direction of travel.

The method determines worst navigable conditions for each O-D and inbound/outbound case using three inputs:

1. Operational limits and navigational guidelines, obtained from pilot organizations, port authorities, and other regulatory sources such as shipping companies.
2. Historical hydro-meteorological data, used to identify upper-end values representative of challenging but navigable conditions. It is advised to do this in collaboration with maritime experts.
3. Expert judgment, used to select combinations of wind, current, waves (depending on which of these were identified as relevant for the specific barrier location), and water depth that are hydrodynamically and meteorologically plausible, and operationally governing for each transit direction.

These worst navigable conditions form the environmental basis for the simulation scenarios and must be applied consistently and uniformly across all alternative barrier configurations. The combination of defined environmental forcing mechanisms collectively provide the dynamic boundary conditions that govern the external loading on the vessel, linking the physical environment of the spatial schematization to the ship's hydrodynamic response.

Translating Worst Navigable Conditions into Simulation Inputs

Once the worst navigable conditions have been defined, the method requires that these conditions be translated into the input structure required by the selected ship maneuvering simulation model. Because environmental input formats differ between models, the method does not prescribe a universal parameterization. Instead, it requires that the defined environmental conditions be represented faithfully and consistently, preserving their magnitude, direction, and hydrodynamic coherence. All barrier configurations must be evaluated using identical environmental input sets to ensure comparability of results.

3.1.3. Design Vessels

As discussed in Section 2.3, the selection of design vessels is a central component of the assessment method, as vessel size, geometry, and maneuvering characteristics strongly influence alignment, drift development, controllability, and clearance during transit. The purpose of this section is to specify how the method identifies the relevant vessel population, selects representative design vessels for each origin-destination route, and ensures that these vessels are appropriately represented within the simulation model. The procedure is based on empirical vessel traffic data and expert validation, ensuring that the selected design vessels capture the governing maneuvering challenges associated with the local traffic mix.

Identifying the Relevant Vessel Population

The method begins by identifying the full population of vessels that routinely transit the O-D routes intersecting the proposed barrier. High-quality vessel traffic data, such as AIS records, port-call logs, or pilotage data, are obtained to capture essential attributes such as vessel identifiers (MMSI numbers), timestamps, movement patterns, loading conditions, vessel type, control equipment, and principal dimensions. As is the case for environmental data (see Subsection 3.1.2), vessel datasets must also undergo quality control and validation to ensure reliability. This includes removing incomplete or inconsistent entries, resolving duplicated or invalid records, and supplementing missing particulars using external fleet databases, classification society documents, or port authority information. Together, these datasets allow for a comprehensive characterization of traffic patterns and vessel-specific properties.

From the cleaned and preprocessed dataset, vessel types and dimensional characteristics relevant to each O-D route are directly derived. This results in a validated and comprehensive representation of the vessels that actually use each route and therefore form the basis for selecting design vessels. Consequently, ensuring that the design vessels selected for analysis are both representative and operationally realistic.

Selecting Representative Design Vessels

Design vessels must capture the maneuvering behavior and navigational constraints associated with the vessel types that govern each O-D route. The selection process follows three methodological steps.

1. First, the governing vessel types are identified for each O-D route using the validated traffic dataset. Governing types are those that dominate operational relevance or impose maneuvering constraints due to their dimensions, loading conditions, or superstructure geometry. Examples include tankers, container vessels, general cargo vessels, ro-ro vessels, bulk carriers, and cruise ships, depending on the specific traffic composition. This step ensures that the selection process reflects the actual fleet expected to transit the barrier.
2. According to the experience of maritime pilots, different vessel types exhibit distinct maneuvering dynamics, necessitating differentiated risk assessments. Therefore, second, the governing vessel types are categorized according to their sensitivity to the environmental forcing mechanisms accounted for in the definition of the worst navigable scenarios (see Subsection 3.1.2). As such, the sensitivity categories may include wind-sensitive vessels (e.g., vessels with large windage areas), current-sensitive vessels (e.g., deep-draught vessels highly influenced by hydrodynamic forces), and wave-sensitive vessels. This classification links vessel selection directly to the environmental conditions under which the simulations will be conducted.
3. Third, for each O-D route and for each sensitivity category, the method selects the vessel with the largest combination of length, beam, and draught observed in the traffic dataset, i.e. the governing design vessels. In many practical applications, this results in one design vessel per sensitivity category, per O-D route. However, additional vessels may be required if different dimensional extremes are identified within the same sensitivity category. For example, when the vessel with the largest length (in a certain sensitivity category) is not the vessel with the greatest beam or draught. To ensure consistency with operational experience, maritime pilots should be involved in validating the identification of governing vessel types, the sensitivity categorization, and the final selection of design vessels.

Representing Design Vessels in the Simulation Model

Once the design vessels have been selected, the method requires representing them in the ship maneuvering simulation model in a manner that faithfully reflects their maneuvering characteristics. The manner in which the design vessels can be represented depends on the capabilities of the simulation model.

If the model allows user-defined vessel parameters, the relevant characteristics necessary to parameterize vessel behavior within the assessment method, such as principal dimensions, displacement, loading condition, propulsion configuration, rudder type, and wind coefficients, can be specified directly based on authoritative vessel data. If the model uses a library of pre-calibrated or pre-validated vessel models, the method requires selecting the vessel model that most closely matches the design vessel in terms of dimensions, windage, displacement, and maneuvering performance. Any deviations between

the design vessel and the available vessel model must be documented. Once a vessel model has been selected to represent a given design vessel, that same vessel model must be used consistently in all simulation scenarios involving that design vessel, ensuring that any differences in results arise from changes in barrier configuration rather than changes in vessel representation.

3.1.4. Physical Maneuvering Indicators

The physical maneuvering indicators discussed in Section 2.4, heading, course over ground, drift angle, and swept path, provide a quantitative representation of a vessel's dynamic behavior as it transits the barrier. These indicators capture how a vessel responds to the spatial layout, environmental forcing, and navigational constraints along its trajectory.

From a methodological perspective, physical maneuvering indicators do not require selecting values, thresholds, or categories. Their role in the method is functional: they form the basis for defining and computing the quantitative assessment metrics presented in Subsection 3.1.6. For this reason, it is essential to monitor the development of these indicators in space and time during each simulated transit, for example through plots of drift angle versus distance, or swept path versus time. The methodological requirement that follows is therefore directed at the simulation model. The chosen ship maneuvering simulation model must support extraction of the physical maneuvering indicators for each of the simulated scenarios, with sufficient temporal and spatial resolution to allow their use in the computation of the assessment metrics.

In summary, while no input choices are required for the physical maneuvering indicators themselves, the simulation model must provide consistent access to these indicators, as they form a foundational component of the quantitative nautical safety assessment method.

3.1.5. Ship Maneuvering Simulation Model

As discussed in Section 2.5, the ship maneuvering simulation model forms the computational core of the assessment method. It generates vessel trajectories under the spatial, environmental, and operational conditions defined in the preceding subsections and provides the physical maneuvering indicators required to compute the quantitative assessment metrics (see Subsection 3.1.6). The choice of simulation model must therefore be justified in relation to the characteristics and comparative considerations presented in Section 2.5.

Justification for Using Fast-Time Simulation

Based on the considerations presented in Section 2.5, this method employs a fast-time ship maneuvering simulation model. Fast-time simulation offers several methodological advantages essential for a comparative navigational safety assessment.

First, fast-time simulation is computationally efficient and inexpensive compared to real-time or high-fidelity simulation approaches. The assessment requires a large number of simulation scenarios, involving multiple O-D routes, design vessels, environmental conditions, and alternative barrier configurations. Performing these scenarios using a real-time simulation model would be impractical due to the associated time, computational demand, and operational costs.

Second, fast-time simulations are fully deterministic. This allows for reproducible and objective comparison of barrier configurations: the vessel's response is governed solely by environmental forcing, vessel characteristics, and control algorithms, without influence from human operators. Real-time simulation, by contrast, introduces variability through pilot behavior, making systematic comparison across scenarios unreliable.

Third, FTS provides a consistent evaluation framework across all scenarios. Identical environmental inputs, vessel characteristics, and control strategies can be applied across the considered barrier configurations, ensuring that differences in outcomes arise only from changes between configurations.

Although real-time simulation is not part of the assessment method developed in this chapter, it may serve as an optional supplementary step in later design stages. Real-time simulation can provide additional validation by allowing maritime pilots to evaluate the feasibility of vessel handling for specific barrier configurations, ensuring navigational credibility through human feedback (PIANC, 2014; IALA, 2022). Lataire et al. (2018) and Verdugo et al. (2018) confirm that combining both methods enhances

both quantitative and qualitative understanding of navigational risk, providing a balanced assessment of vessel-infrastructure interactions. However, this lies outside the scope of the comparative method developed in this chapter and is not required for the computation of the quantitative assessment metrics defined in Subsection 3.1.6.

Functional Requirements of the Simulation Model

To support the assessment method, the chosen fast-time simulation model must meet several functional requirements:

- First, the model must allow implementation of the spatial schematization as defined in Subsection 3.1.1. This includes importing or constructing the navigational geometry, bathymetry, and barrier configurations so that vessel motion is simulated relative to the actual physical environment. This input forms the spatial foundation for the subsequent dynamic interaction of vessels, environmental forces, and barrier structures within the fast-time simulation model.
- Second, the model must allow application of the environmental forcing mechanisms defined in Subsection 3.1.2. This includes specifying wind, current, water level, and wave conditions, and ensuring that these can be applied consistently across all scenarios. For currents specifically, the model must allow to differ the flow field around the barrier elements for each considered configuration.
- Third, the model must represent vessel maneuvering behavior with sufficient fidelity to resolve alignment, turning, drift development, and post-transit stabilization. The model should incorporate hydrodynamic formulations appropriate for the vessel types considered (see Subsection 3.1.3), including the ability to represent inertia, turning response, and control actions.
- Fourth, the model must automatically incorporate shallow water and bank interaction effects (see Subsection 3.1.3) through its hydrodynamic formulations. These effects arise from the combination of vessel geometry (relating to the choice of design vessels), water depth (relating to the defined environmental conditions), and proximity to boundaries (relating to the modeled spatial schematization) and must therefore be represented without requiring user-defined parameters.
- Fifth, the simulation model must support extraction of the physical maneuvering indicators described in Subsection 3.1.4. These indicators must be available for the simulated transit, with sufficient temporal and spatial continuity to allow computation of the assessment metrics.
- Sixth, the simulation model must additionally support extraction of rudder angle plots, rate of turn plots, and spatial overview plots of the vessel trajectories at sufficient spatial and/or temporal resolution to allow computation of the quantitative assessment metrics. This requirement arises from the way in which the quantitative assessment metrics are defined and becomes apparent in Subsection 3.1.6.
- Finally, the model must produce deterministic outputs, enabling reproducible comparisons across vessel types, O-D routes, and barrier configurations. Consistency in model behavior is essential to ensure that differences in simulation outcomes reflect only the conditions defined in the method rather than variability in model execution.

3.1.6. Nautical Safety Assessment Metrics: Framework and Definitions

The first purpose of this subsection is to establish a coherent framework for the development of quantitative assessment metrics used to evaluate navigational safety of vessels sailing in proximity to storm surge barriers. The rationale underpinning this framework lies in the findings from Section 2.6, where it was concluded that quantitative navigational safety indicators in existing literature consistently fall into three recurring families (spatial, temporal, and control), and that vessel passages through storm surge barriers must be analyzed as multi-stage transits, each with its own characteristic safety considerations.

The metrics that follow from the framework serve as quantifiable indicators of nautical safety, and are connected to the model components defined in Subsection 3.1.1, Subsection 3.1.2, Subsection 3.1.3, and Subsection 3.1.4 through the applied ship maneuvering simulation model (see Subsection 3.1.5). These metrics translate the simulated vessel motions into objective measures of navigational safety, providing the analytical foundation for evaluating the nautical safety performance of a storm surge barrier configuration. Because the assessment method must systematically compare the navigational

safety performance of alternative storm surge barrier configurations, the metrics must be reproducible, physically meaningful, and directly comparable across the simulated scenarios. The quantitative assessment metrics are explicitly defined following the presentation of the framework, fulfilling the second purpose of this subsection.

Framework: Margins and Segments

In Subsection 2.6.1, it was found that existing research often conceptualizes nautical safety through measurable spatial, temporal, and control allowances available to a vessel during critical stages of navigation. Accordingly, the framework adopted in the assessment method distinguishes three principal categories of safety margins:

1. *Distance margins*, which describe the physical separation between the vessel and nearby structures, the channel boundary, or the seabed;
2. *Time margins*, which represent the temporal allowance available to the pilot or automated controller to perform a required maneuver before encountering a potential hazard; and
3. *Control margins*, which quantify the extent to which a vessel can be steered or propelled to maintain the desired course, typically expressed through rudder or power usage.

These margin types reflect complementary dimensions of navigational safety: distance relates to spatial clearance, time to reaction capability, and control to maneuvering flexibility. Together, they provide a multidimensional representation of how safely and efficiently a vessel can transit a constrained waterway under defined environmental conditions.

To apply this concept consistently, and account for the fact that assessments of nautical safety in the vicinity of storm surge barrier require a transit-wide perspective incorporating safety considerations across the full extent of the vessel passage (see Subsection 2.6.2), the passage of a vessel is subdivided into three distinct segments, irrespective of whether the vessel is inbound or outbound:

- A. The *approach segment*, representing the portion of the transit before the vessel enters the barrier (see Figure 3.1).
- B. The *crossing segment*, corresponding to the passage of the vessel between the barrier's structural elements (see Figure 3.1).
- C. The *departure segment*, covering the period after the vessel exits the barrier and proceeds toward the next navigational turn or open-water reach (see Figure 3.1).

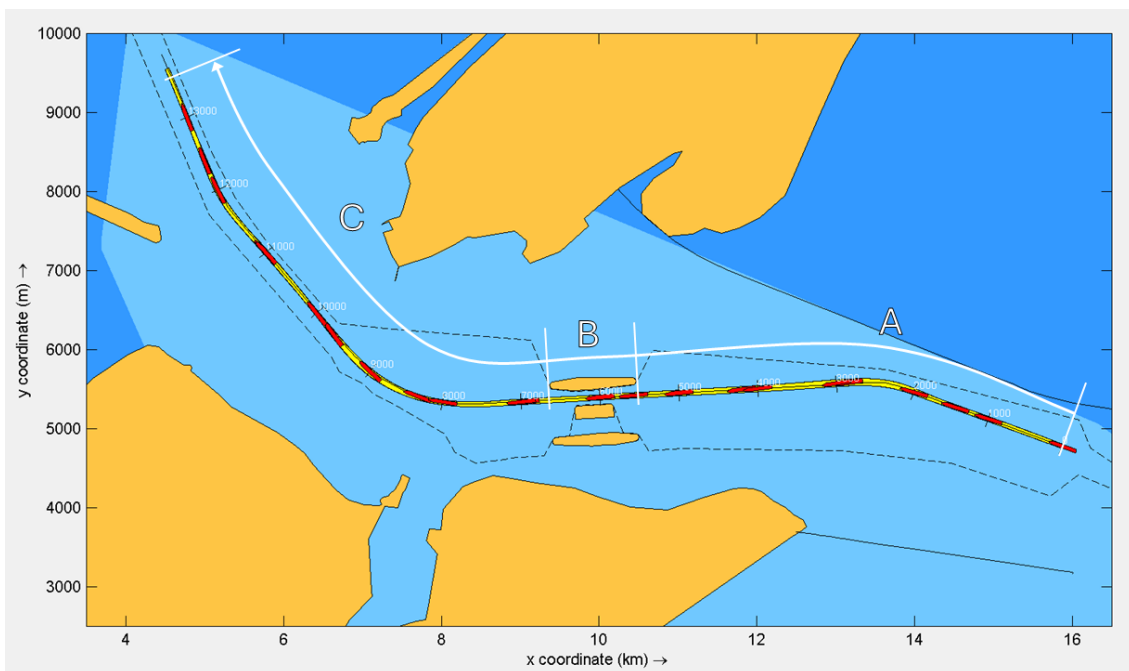


Figure 3.1: The three segments of a vessel passage, transit direction indicated by white arrow.

By combining the three types of safety margins with the three sequential segments of a vessel passage, a structured analytical matrix is obtained. This matrix forms the conceptual backbone of the quantitative assessment metric design, ensuring that each defined metric explicitly captures one aspect of navigational safety (distance, time, or control) within a specific phase of the vessel's trajectory (before, inside, or after the barrier). The resulting framework establishes the quantitative foundation upon which the assessment method relies and is summarized in Table 3.1, which also presents the full set of developed metrics. These metrics, such as *Distance Before Entry*, *Rudder Variability In Barrier*, and *Time After Barrier*, enable a consistent, quantitative evaluation of vessel maneuvering performance derived directly from fast-time simulation outputs. Each metric is therefore traceable to a specific theoretical construct from Chapter 2 and can be objectively reproduced across all of the considered barrier configurations. All assessment metrics are defined in a standardized manner and described in detail later in this subsection.

Table 3.1: Framework for development of nautical safety assessment metrics.

Assessment Metric	Margin Type	Segment of Passage
Distance Before Entry	Distance	Approach
Time Before Entry	Time	Approach
Rudder Range In Barrier	Control	Crossing
Beam Clearance In Barrier	Distance	Crossing
Maximum Drift Angle In Barrier	Control	Crossing
Distance After Barrier	Distance	Departure
Time After Barrier	Time	Departure

Intermezzo: Components of a Vessel Maneuver

Prior to defining the assessment metrics, it is crucial to understand how a vessel maneuvers. For storm surge barrier transits, whether in simulation or reality, vessel maneuvering can be described as a sequence of turns and course-keeping phases. Each maneuver represents a controlled change in the vessel's direction, executed through coordinated adjustments of the rudder and propulsion systems in response to navigational requirements and environmental forces. When a vessel executes a turn, this maneuver can be dissected into four distinct parts, representing a consecutive sequence of *action-response-action-response*:

1. **Initiation of the maneuver:** Turning begins with a deliberate and large adjustment of the rudder (action). This rudder deflection initiates the change in heading and can be clearly observed in a time or distance plot of the rudder angle. The magnitude and rate of this initial input reflect the pilot's intent and the vessel's responsiveness to steering commands.
2. **Development of the turn:** Following the rudder adjustment, the vessel's rate of turn begins to change (response). This relationship can be visualized in a plot of rate of turn versus time or distance. A notable feature of this phase is the latency between the rudder command and the vessel's response, a delay inherent to the hydrodynamic interaction between rudder deflection, propeller wash, and hull motion. The magnitude of this latency varies with vessel type, speed, and environmental conditions.
3. **Completion and counter-rudder phase:** As the vessel approaches its new heading, the rudder is readjusted to reduce or reverse the turning motion (action). This typically involves applying counter-rudder to arrest the turn and stabilize the vessel on its intended course. The counter-rudder action can be identified in rudder angle plots as a rapid deflection opposite to the initial turning direction. The effectiveness of this phase determines how precisely the vessel can align with the desired trajectory. This part of the turning maneuver can be observed in a plot of rudder angle versus time or distance.
4. **Stabilization:** The maneuver concludes once the rate of turn stabilizes near zero following the counter-rudder input, indicating that the vessel has achieved steady-state course-keeping on its new heading (response). This stabilization is visible in rate of turn plots as the return of angular velocity to baseline levels.

In-between turning maneuvers, vessels engage in course-keeping, where the primary objective is to maintain a steady heading along a defined track. During these intervals, only small rudder corrections are required to compensate for environmental disturbances such as wind, current, or bank effects. Effective course-keeping reflects both the vessel's inherent stability and the adequacy of control margins under prevailing conditions. Figure 3.2 illustrates an example passage of a vessel through a storm surge barrier requiring three turning maneuvers, while Figure 3.3 decomposes each of these turning maneuvers into its four constituent parts. This conceptual understanding of how a vessel maneuvers forms the foundation for the subsequent definition of the quantitative assessment metrics. Each metric described later in this subsection is defined on the basis of one or more of these maneuvering components, enabling an objective evaluation of navigational safety through the analysis of rudder activity, rate of turn, and course stability.

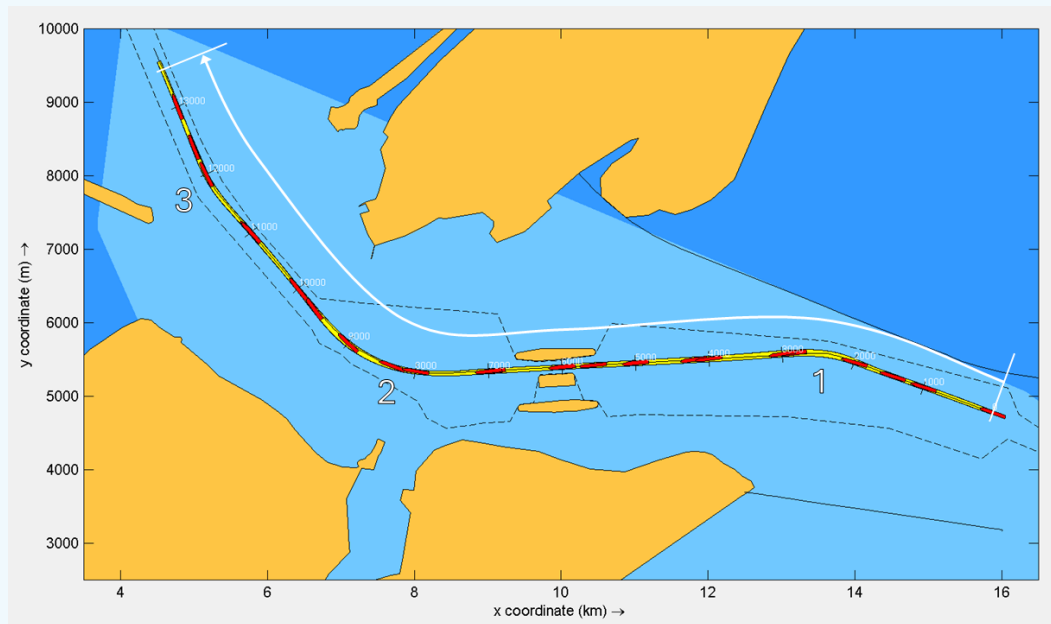
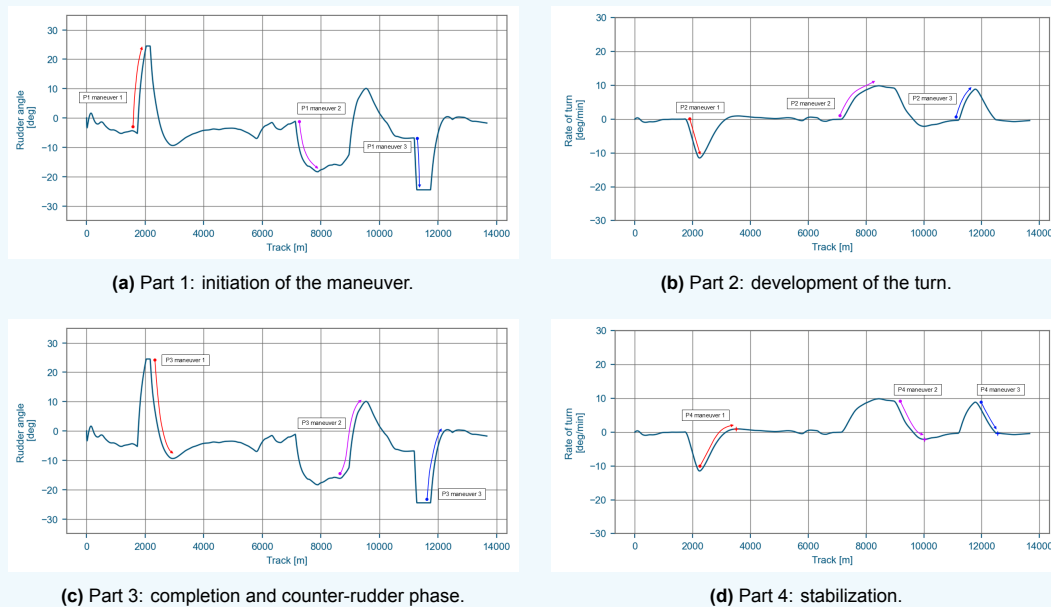


Figure 3.2: Vessel passage requiring the execution of three turning maneuvers (turns indicated by numbers).



(c) Part 3: completion and counter-rudder phase.

(d) Part 4: stabilization.

Figure 3.3: Three turns decomposed into their four parts (corresponding turns shown in Figure 3.2).

Distance Before Entry (Dist. B.E.)

The *Distance Before Entry* is a distance margin that applies to the first segment of the vessel passage, the approach segment. It represents the longitudinal distance (measured along the track) between the point at which a vessel completes its final turning maneuver before the barrier and the entry point of the barrier (the point of barrier entry is depicted in Figure 3.4). In practical terms, it measures how much navigational space is available for the vessel to align itself with the barrier's axis prior to entering the structure. Figure 3.5 provides a graphical representation of the *Distance Before Entry*.

This metric provides a direct indication of the spatial flexibility a vessel possesses prior to barrier entry. A larger *Distance Before Entry* allows more room for the vessel to complete any final course adjustments, stabilize its heading, and respond to environmental effects such as wind, current, or residual drift from the preceding turn. Consequently reducing the likelihood of late corrections and enhancing the predictability and safety of the approach. Conversely, a small *Distance Before Entry* signals that the vessel completes its final turning maneuver before the barrier very close to the barrier itself, leaving minimal spatial margin to correct for deviations in alignment with the barrier, adjust speed or recover from unexpected drift, thereby increasing cumulative maneuvering demand and decreasing navigational safety.

The *Distance Before Entry* therefore reflects a vessel's alignment readiness and contributes to assessing the overall maneuvering safety in the approach phase. It forms one of the key distance-based indicators for the approach segment within the broader framework of navigational safety metrics presented in Table 3.1.

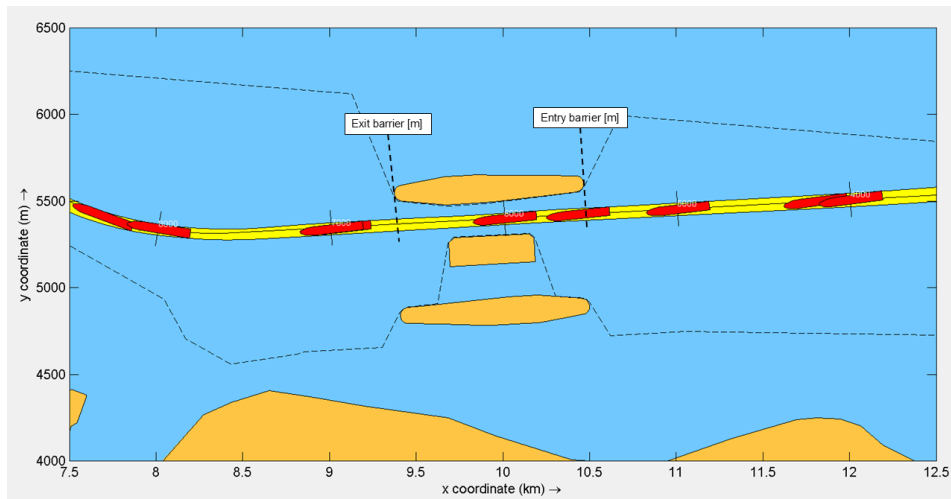


Figure 3.4: Points of barrier entry and barrier exit.

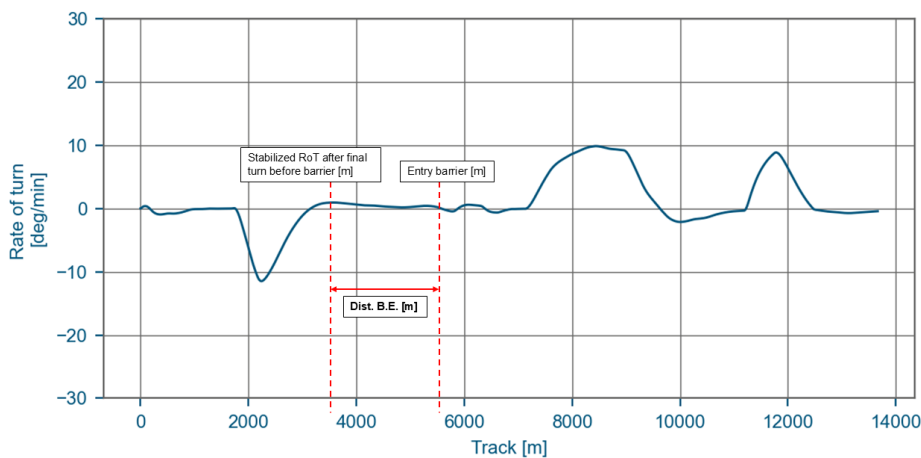


Figure 3.5: Assessment metric visualization: *Distance Before Entry*.

Time Before Entry (Time B.E.)

The *Time Before Entry* is a time margin corresponding to the first segment of the vessel passage, the approach segment. It represents the temporal allowance a vessel has between completing its final turning maneuver before the barrier and reaching the entry point of the barrier (the point of barrier entry is depicted in Figure 3.4). In essence, it quantifies how much time is available for a vessel to achieve and maintain proper alignment with the barrier before entering it. Figure 3.6 provides a graphical representation of the *Time Before Entry*.

This metric complements the *Distance Before Entry* by expressing the same navigational safety margin in temporal rather than spatial terms. A longer *Time Before Entry* allows the vessel more time to stabilize its heading, manage speed, and respond to environmental disturbances such as wind and currents, thereby reducing cumulative maneuvering demand. Conversely, a shorter *Time Before Entry* indicates a more constrained approach, leaving less time for corrective actions before barrier entry, increasing the likelihood of abrupt course or speed adjustments in the immediate vicinity of the structure and thus negatively impacting navigational safety.

The *Time Before Entry* therefore serves as an indicator of maneuvering readiness and response capacity in the approach phase. By relating the spatial distance available to the vessel's speed, it provides an additional dimension to the analysis of how safely a vessel can prepare for entry into the barrier.

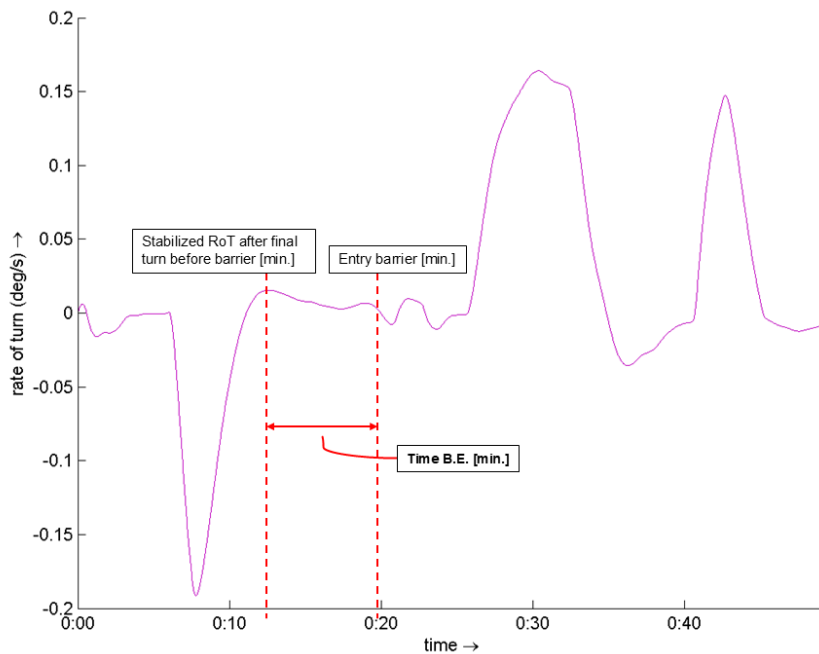


Figure 3.6: Assessment metric visualization: *Time Before Entry*.

Rudder Range In Barrier (Rudder Range I.B.)

The *Rudder Range In Barrier* is a control margin that applies to the second segment of the vessel passage, the crossing segment. It is defined as the range between the minimum and maximum rudder angles applied by the vessel while navigating within the barrier. Figure 3.7 provides a graphical representation of the *Rudder Range In Barrier*. This metric provides an indication of how much rudder activity is required to maintain a stable course during transit through the confined structure.

A large *Rudder Range In Barrier* suggests that significant steering corrections are necessary to compensate for hydrodynamic disturbances such as current-induced yaw, bank effects, or turbulence caused by flow constriction between the barrier's piers. This implies that the vessel experienced greater difficulty maintaining a steady heading and required increased control effort. Conversely, a small *Rudder Range In Barrier* indicates that the vessel could maintain its intended alignment with minimal steering intervention, signifying safer, smoother, and more stable passage conditions.

The *Rudder Range In Barrier* therefore serves as a direct measure of course stability and control demand under confined flow conditions. As a control-based metric, it captures the extent to which

the pilot, or, in simulation, the autopilot algorithm, must use the available rudder authority to preserve the desired track. This makes it particularly relevant for evaluating how different barrier configurations affect the controllability of vessels navigating through them.

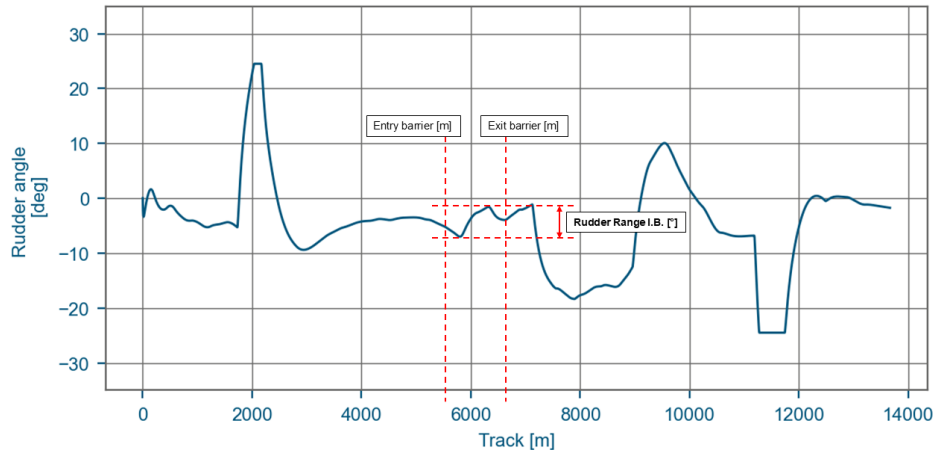


Figure 3.7: Assessment metric visualization: *Rudder Range In Barrier*.

Beam Clearance In Barrier (Beam Clr. I.B.)

The *Beam Clearance In Barrier* is a distance margin associated with the second segment of a vessel's passage, the crossing segment. It is defined as the closest point of approach between the vessel and the barrier structure (i.e. the minimum lateral clearance between the vessel's swept path and the barrier) while transiting within the barrier. This distance is expressed as a multiple of the vessel's beam, thereby normalizing the measure across different vessel sizes and facilitating comparison between simulation scenarios. Figure 3.8 provides a graphical representation of the *Beam Clearance In Barrier*.

This metric directly reflects the lateral spatial safety margin available to a vessel navigating through the barrier. A larger *Beam Clearance In Barrier* indicates that the vessel maintains a greater distance from the structure's boundaries, signifying a reduced susceptibility to hydrodynamic interaction effects such as bank suction and thereby lowering likelihood of contact with the barrier's structural elements, resulting in a safer passage through the barrier. Conversely, a smaller *Beam Clearance In Barrier* implies tighter navigation within the confined channel, heightening sensitivity to steering errors, current-induced drift, and environmental disturbances.

The *Beam Clearance In Barrier* therefore serves as a key indicator of navigational safety and maneuvering space in the most constrained section of the passage. It provides insight into how barrier geometry and environmental conditions influence the vessel's ability to maintain a safe lateral position.

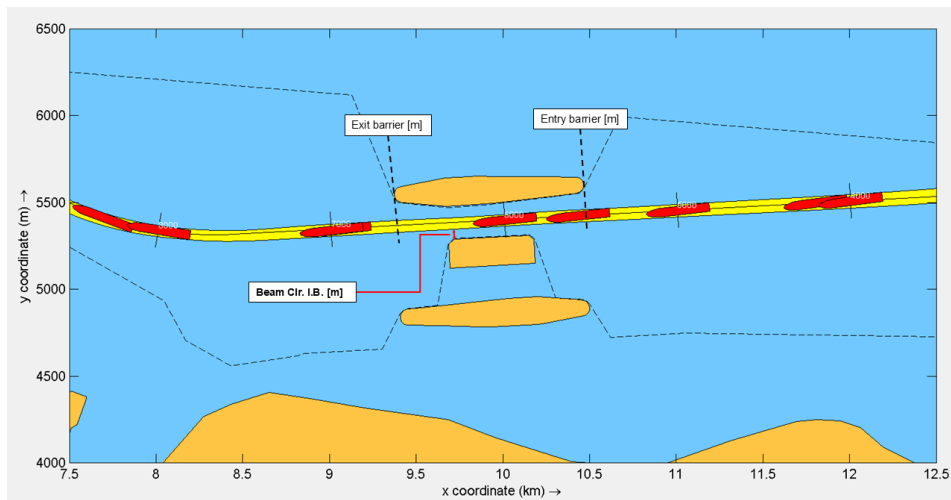


Figure 3.8: Assessment metric visualization: *Beam Clearance In Barrier*. Swept path in yellow.

Maximum Drift Angle In Barrier (Max. DA I.B.)

The *Maximum Drift Angle In Barrier* is a control margin associated with the second segment of a vessel passage, the crossing segment. It is defined as the largest absolute angular deviation between a vessel's heading and its course over ground (i.e. the maximum drift angle) while navigating within the barrier. Figure 3.9 provides a graphical representation of the *Maximum Drift Angle In Barrier*. This parameter quantifies the extent of lateral motion experienced by the vessel relative to its intended forward direction, providing a measure of the vessel's ability to maintain alignment in the confined environment between the barrier.

A large *Maximum Drift Angle In Barrier* indicates that the vessel experienced a greater degree of sideways movement due to environmental forces such as crosscurrents or wind, or as a result of hydrodynamic interactions with the barrier walls. Excessive drift angles reduce the vessel's predictability and increase the likelihood of structural contact, especially in narrow or asymmetric openings, negatively impacting the navigational safety of the barrier passage. Conversely, a small *Maximum Drift Angle In Barrier* reflects stable, well-controlled navigation through the barrier, and sufficient hydrodynamic balance between steering forces and external disturbances. Consequently reducing the probability of lateral deviation, structural contact, and hydrodynamic interaction effects.

This metric therefore serves as a key indicator of lateral control performance and course stability within the barrier. It directly links to the hydrodynamic response of the vessel under the influence of crosscurrents, winds, and bank effects, while also capturing the adequacy of rudder corrections applied to maintain a steady trajectory. Figure 3.9 visualizes this metric, showing the variation in drift angle along the vessel trajectory within the barrier for a representative simulation case.

The *Maximum Drift Angle In Barrier* complements the *Rudder Range In Barrier* by illustrating the outcome of control efforts; whereas rudder range represents the control action applied, the drift angle reflects the resulting vessel response. Together, these two control-based metrics describe how effectively a vessel can counteract environmental forces and maintain safe passage while navigating through the confined barrier structure.

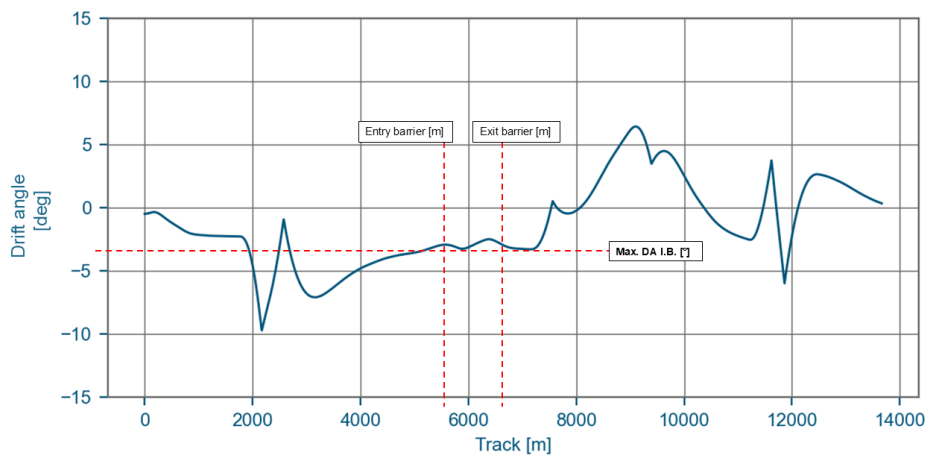


Figure 3.9: Assessment metric visualization: *Maximum Drift Angle In Barrier*.

Distance After Barrier (Dist. A.B.)

The *Distance After Barrier* is a distance margin associated with the third segment of a vessel's passage, the departure segment. It is defined as the longitudinal distance (measured along the track) between the point where a vessel crosses the exit point of the barrier (depicted in Figure 3.4) and the initiation point of the first subsequent turning maneuver. Figure 3.10 provides a graphical representation of the *Distance After Barrier*. This metric captures the spatial allowance available for a vessel to regain alignment and prepare for post-barrier navigation.

A greater *Distance After Barrier* indicates that the vessel has more navigational space to stabilize its course, adjust speed, and prepare for the next turn under the influence of environmental forces such as wind and currents. This extended distance enhances navigational safety by providing sufficient room for the vessel to adjust its course and re-establish alignment well ahead of the next turning maneuver,

thereby reducing cumulative maneuvering demand. Conversely, a smaller *Distance After Barrier* implies that the vessel must initiate a turn shortly after exiting the structure, reducing the space available for realignment and increasing the likelihood of abrupt or unstable maneuvers.

The *Distance After Barrier* therefore represents an important measure of spatial recovery capacity following transit through the confined environment of the barrier. It provides insight into the degree of navigational freedom available to vessels once they re-enter the open channel, making it particularly relevant for assessing the nautical safety implications associated with barrier siting and channel layout.

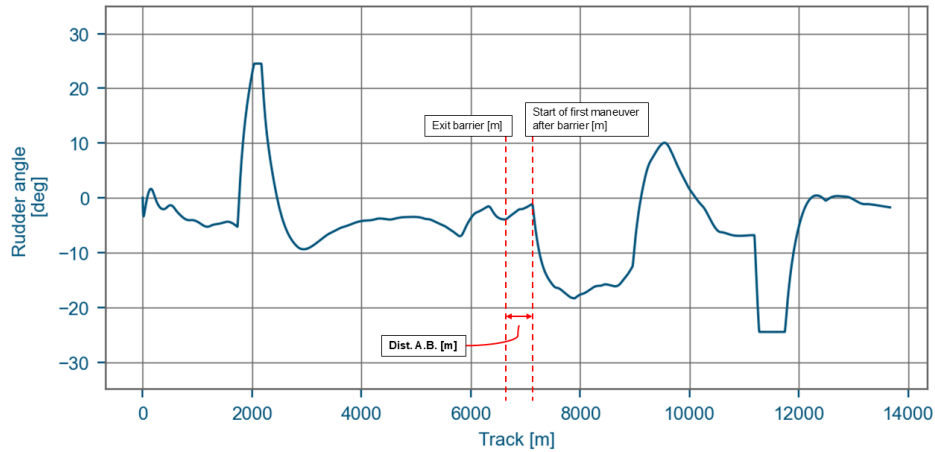


Figure 3.10: Assessment metric visualization: *Distance After Barrier*.

Time After Barrier (Time. A.B.)

The *Time After Barrier* is a time margin associated with the third segment of a vessel's passage, the departure segment. It is defined as the time elapsed between the moment a vessel crosses the exit point of the barrier (depicted in Figure 3.4) and the initiation of the first subsequent turning maneuver. Figure 3.11 provides a graphical representation of the *Time After Barrier*. This metric quantifies the temporal allowance available for a vessel to regain alignment and prepare for the next navigational action following barrier transit.

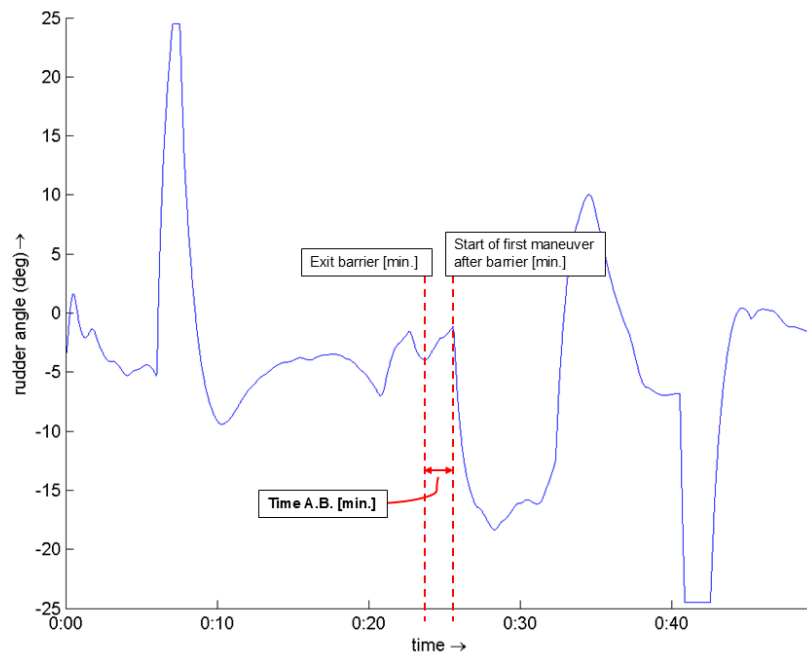


Figure 3.11: Assessment metric visualization: *Time After Barrier*.

A longer *Time After Barrier* indicates that the vessel has more time to stabilize its heading, adjust speed, and correct minor deviations before commencing the next turn. This extended period enhances navigational safety by providing the pilot, or, in the case of simulation, the control algorithm, sufficient time to recover from hydrodynamic effects experienced within the barrier and regain alignment, thereby reducing cumulative maneuvering demand. Conversely, a shorter *Time After Barrier* implies that the vessel must initiate its next maneuver almost immediately upon exiting the structure, leaving limited time for realignment and increasing the likelihood of abrupt control demands.

The *Time After Barrier* therefore represents a measure of temporal recovery capacity, complementing the *Distance After Barrier* by expressing the same navigational margin in temporal rather than spatial terms. Together, these two metrics capture how safely and effectively a vessel can transition from the constrained environment of the barrier to open-channel navigation.

3.1.7. Method Synthesis

Figure 3.12 summarizes the synthesis of the developed assessment method, illustrating how the specified method inputs, modeling components, and outputs are combined into a structured and reproducible workflow. The method is designed to ensure consistent and comparable evaluation of the nautical safety performance of alternative storm surge barrier configurations by applying identical environmental conditions, vessel characteristics, and assessment metrics across all scenarios, such that observed differences in outcomes can be attributed to differences in barrier configuration rather than to methodological inconsistencies. The assessment method defined in this chapter produces one set of quantitative nautical safety assessment metrics per barrier configuration. Accordingly, for an assessment involving three barrier configurations (for example), the assessment metrics are determined three times, each time for a distinct configuration, while the underlying assessment framework remains unchanged. Comparative nautical safety performance is subsequently derived from the systematic comparison of the resulting assessment metrics across configurations.

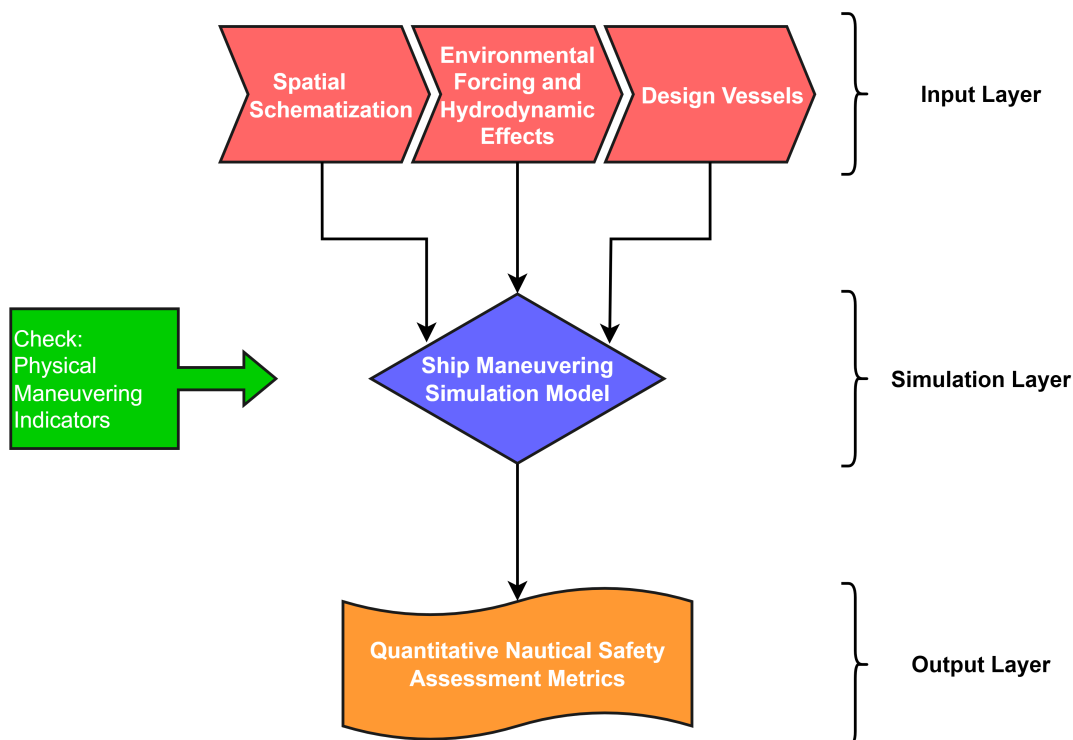


Figure 3.12: Overview of the developed nautical safety assessment method for storm surge barriers.

While the developed framework produces quantitative indicators of maneuvering demand and safety margins, these indicators are not assigned absolute classifications such as “safe” or “unsafe.” Nautical safety is inherently context-dependent and influenced by operational practices and expert judgment, making the definition of universally applicable acceptance thresholds objectively infeasible. Instead,

the assessment metrics are intended to support comparative evaluation and to identify configurations and scenarios that warrant closer scrutiny. By using these quantitative outputs as input for structured pilot discussion, the method combines reproducible analysis with experiential knowledge, enabling informed interpretation without imposing arbitrary or misleading safety classifications. In this way, the method functions as an exploratory and iterative decision-support framework, rather than a prescriptive or normative safety assessment tool.

3.2. Case Study: Bolivar Roads, “The Doorway to Galveston Bay”

To evaluate the validity and practical usefulness of the method developed in Section 3.1, it is applied to a real-world storm surge barrier through a dedicated case study. In this research, the Bolivar Roads barrier, previously introduced in Subsection 1.1.4 as a prominent example of the navigational challenges associated with barrier placement in busy maritime gateways, serves as the test case. The case provides an opportunity to assess the nautical safety performance of multiple barrier configurations and to demonstrate how the proposed method can support early-stage design decisions.

Firstly, Subsection 3.2.1 introduces the Bolivar Roads context at a high level and outlines its relevance as a representative and operationally significant setting for method application. The subsequent subsections briefly describe the rationale for constructing a storm surge barrier at this location, the key elements of the proposed gate system, and the findings of prior navigational evaluations. Together, these elements establish the foundation for implementing the assessment framework for this case, the outcomes of which are presented in Chapter 4.

3.2.1. Context and Significance of Bolivar Roads

Bolivar Roads, a natural navigable strait connecting the Gulf of Mexico with Galveston Bay, located between Galveston Island (to its South) and the Bolivar Peninsula (to its North) on the upper Texas coast, forms the primary maritime gateway to one of the most active port regions in the United States (BTS, 2025). Serving as the entrance to Galveston Bay, this region accommodates the convergence of several key shipping channels that support deep-draught vessel traffic to and from a number of major port facilities. Central to this system are the Houston, Galveston, and Texas City Ship Channels, each of which converges in the vicinity of Bolivar Roads before branching inland toward their respective destinations: the Port of Houston, the Port of Galveston, and the Port of Texas City (USACE, 2021c). These ports, all rely on uninterrupted navigability through this strait for the transit of deep-draught vessels. Amongst these, the Port of Houston is the largest in terms of tonnage, ranking consistently at the top of national port statistics for foreign waterborne commerce (BTS, 2025).

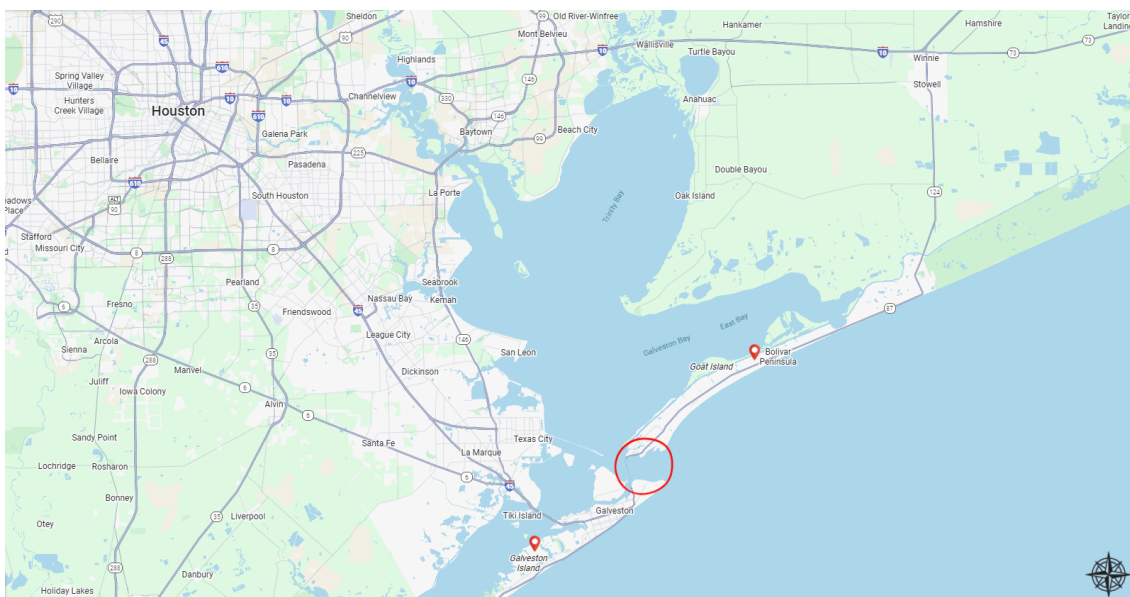


Figure 3.13: Map of the Greater Galveston Bay Area, Bolivar Roads marked with red circle (Google, 2025).

All three ports handle a wide range of cargo types, including dry and liquid bulk, breakbulk, roll-on/roll-off, containers, general and project cargo, refrigerated goods, cruise-related traffic, resins, and crude and refined petroleum products, as well as other petrochemicals (Port of Galveston, 2025; Port of Houston, 2025; Port of Texas City, 2025). The figures in Table 3.2 underscore the scale of maritime operations that rely on uninterrupted navigational access through Bolivar Roads. Given this operational density, Bolivar Roads plays a central role in maintaining the efficiency and reliability of maritime operations across the entire upper Texas coast.

Table 3.2: Facts and figures: ports of Galveston, Houston, and Texas City in 2023 (S&P Global, 2024; BTS, 2025).

	Port of Galveston	Port of Houston	Port of Texas City
<i>Vessel* Arrival Calls 2023</i>	9,116	9,064	768
<i>Total Tonnage 2023 [M tons]</i>	13.0	309.5	29.9
<i>Rank U.S. Ports (by total tonnage)</i>	40	1	21
<i>Rank Texas Ports (by total tonnage)</i>	7	1	6
<i>Operating Revenue [\$M]</i>	67.4	585.0	NP**

*Tankers, Bulk Carriers, Dry Cargo and Passenger Vessels
**Non-Public

3.2.2. The Need for a Storm Surge Barrier at Bolivar Roads

As discussed in Subsection 1.1.4, the Texas coast faces increasing exposure to coastal storms, sea-level rise, and erosion (see Figure 3.14), placing critical economic and social assets at risk and underscoring the need for comprehensive coastal protection. In response to the growing threats, the United States Army Corps of Engineers (USACE) and the Texas General Land Office (GLO) have collaborated to develop solutions that address these challenges. Aiming to strengthen coastal resilience, the *Coastal Texas Study* was launched in 2014 to explore large-scale actions in coastal storm risk management and ecosystem restoration across the entire Texas coast (USACE, 2021c).



Figure 3.14: Hurricane storm surge (l), coastal erosion (m), and relative SLR (r) on the Texas coast (USACE, 2021c).

3.2.3. Bolivar Roads Gate System

For the upper Texas coast, a primary objective is to protect Galveston Bay from storm surges originating from the Gulf of Mexico, by means of the *Gulf Lines of Defense* (see Figure 3.15) (USACE, 2021b). The Bolivar Roads Gate System (see Figure 1.2), of which the reported costs are ca. 14B\$ (USACE, 2021a), is the central feature of the *Gulf Lines of Defense*, comprising the following critical structures:

- A 3 mile long levee segment integrating with the proposed dune system on Bolivar Peninsula.
- A 1 mile long combi-wall linking the levee to the shallow water environmental gates.
- 16 shallow water environmental gates (SWEG), supporting tidal flow and circulation.
- 15 vertical lift gates (VLG) adjacent to navigational sector gates, further aiding natural tidal movement.
- Navigable floating sector gates (SG) to facilitate commercial (2 gates, both 650 feet wide) and recreational (2 gates, both 125 feet wide) vessel passage through Bolivar Roads.



Figure 3.15: Upper Texas coast, Gulf Lines of Defense (USACE, 2021c).

3.2.4. Evaluation Study

In the context of the *Coastal Texas Study*, the Greater Houston Port Bureau emphasizes that the protective measures must be carefully balanced with the need to ensure safe navigation and preserve the economic contributions of the area’s commercial waterways (GHPB, 2023b). To assess this balance, and gain insights into the navigational impacts of the gate complex for the maritime sector, the bureau sponsored a RTS-based evaluation study of the proposed 650-foot-wide (198.12 m) navigable sector gates (see Figure 3.16). The navigational challenges and areas for potential improvement identified during the study are briefly summarized below.

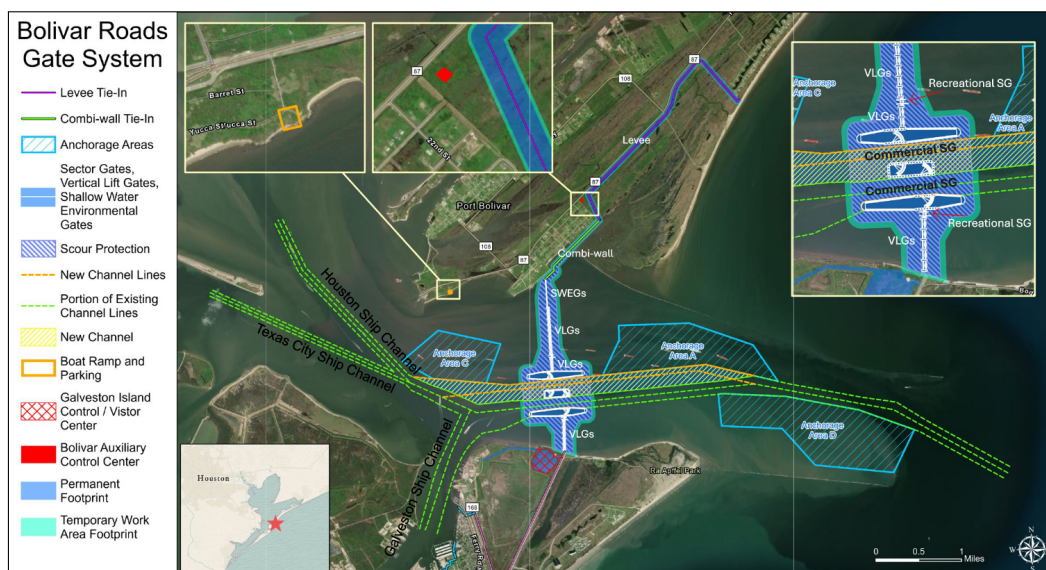


Figure 3.16: Detailed overview of Bolivar Roads Gate System (USACE, 2021c).

Key Findings of the Evaluation Study

The design of the gate complex and its location within the Bolivar Roads area would pose significant navigational hazards for commercial vessels due to the reasons described below (Burkley et al., 2022):

- The gate complex is situated too close to the Houston and Galveston Ship Channels (see Figure 3.16), requiring vessels to execute severe angle turns when entering or exiting these channels.
- The siting of the gate complex is misaligned with prevailing tidal currents, exacerbating hydrodynamic issues such as amplified currents and eddy formation, and complicating navigation for commercial vessels attempting to pass through the gate.
- At 650 feet wide, the gate openings leave little margin for error, requiring precise piloting.
- The asymmetry of the three islands causes uneven shearing forces on vessels when they enter the gates at an angle or without proper alignment, causing them to lose control and dangerously veer off course.

Recommendations of the Evaluation Study

Based on the simulations and their analyses, the following mitigation measures were proposed to address the identified design- and siting-related issues (Burkley et al., 2022):

- Move the gate complex further east within the Bolivar Roads area to increase the distance from the Houston and Galveston Ship Channels, providing vessels with more room to align with the gates.
- Widen the gate openings beyond the current 650 feet to allow greater navigational flexibility.
- Replace the current asymmetrical island design with three symmetrical islands.

4

Results

The results presented in this chapter have been obtained by applying the developed quantitative nautical safety assessment method to the Bolivar Roads storm surge barrier case study introduced in Section 3.2. Based on case-specific inputs, the assessment framework is implemented to evaluate the nautical safety performance of multiple alternative barrier configurations. Vessel maneuvering behavior is simulated using the fast-time ship maneuvering simulation model SHIPMA, under a consistent set of spatial, environmental, and operational assumptions. The resulting simulation outputs are processed using the defined nautical safety assessment metrics, yielding quantitative indicators of spatial, temporal, and control margins for each configuration. Here, the focus lies on the structured presentation of these results and on identifying configuration-dependent differences in maneuvering behavior and safety performance.

4.1. Spatial Schematization

This section presents the spatial schematization that was modeled for the application of the developed assessment method to the Bolivar Roads case study. Following the procedure defined in Section 3.1, the spatial schematization translates the alternative storm surge barrier configurations and governing vessel routes into a consistent geometric representation suitable for simulation-based evaluation. The section describes the governing origin-destination combinations, the chosen geometric domain size, and the nautical and bathymetric layout of the study area including the alternative barrier configurations considered, culminating in the final spatial schematization used in the assessment. Together, these elements define the spatial context within which vessel maneuvering behavior and navigational safety are evaluated in the subsequent analysis.

4.1.1. Governing Origin-Destination Combinations

As can be seen in the nautical chart of Bolivar Roads shown in Figure 4.1 (a full-size image of this nautical chart is provided in Appendix B), the turn leading to the Port of Texas City requires a smaller course change than the turns leading to the Port of Houston and Port of Galveston, and can therefore be assumed to be less challenging. Furthermore, Table 3.2 shows that the Ports of Houston and Galveston are also the governing ports when considering the number of vessel arrivals. For these reasons, origin/destination Texas City was deemed irrelevant.

Consequently, the origins/destinations considered in the assessment were:

1. Port of Houston, of which the corresponding routes are: IB-HOU (Inbound-Houston) and OB-HOU (Outbound-Houston).
2. Port of Galveston, of which the corresponding routes are: IB-GAL (Inbound-Galveston) and OB-GAL (Outbound-Galveston).

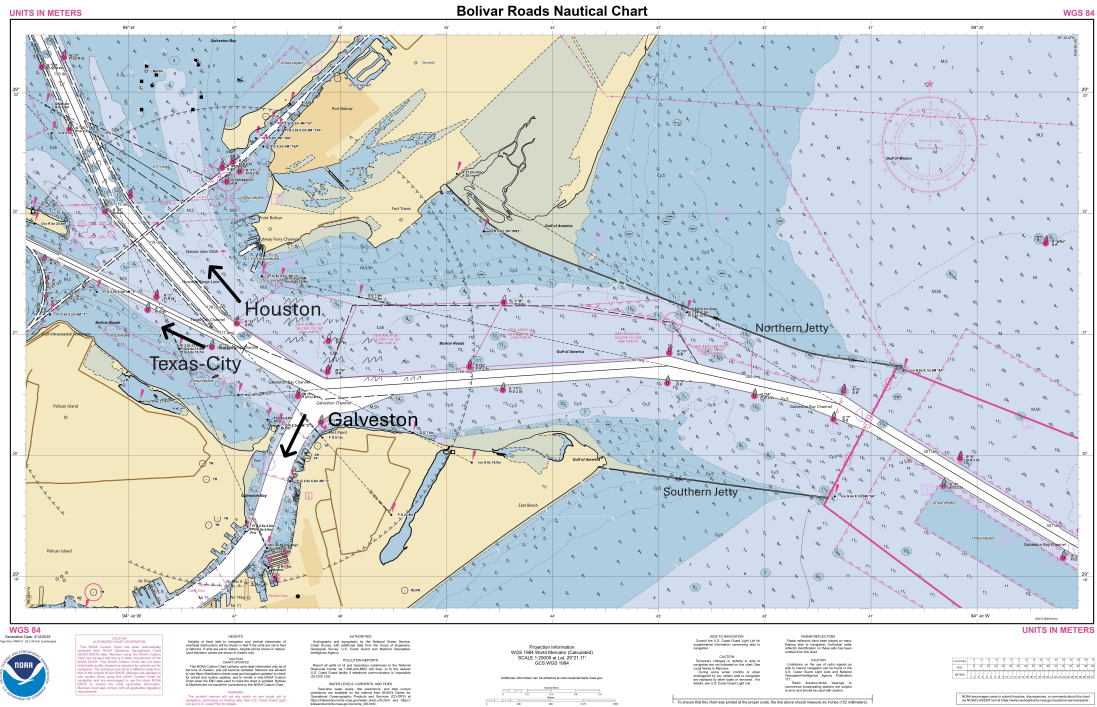


Figure 4.1: Nautical chart of Bolivar Roads (NOAA, 2025a).

4.1.2. Geometric Domain Size

The base map used as a starting point in the modeling of the spatial schematization is shown in Figure 4.2. The grid shown in this figure defines the geometric domain size. The lateral extent of the domain allows the inclusion of all navigable channel boundaries, jetties, levees, breakwaters, harbour basins, and shoreline features that define or constrain maneuvering space. As will become evident in Subsection 4.1.3, the longitudinal extent of the geometric domain includes at least one significant course change or bend upstream and downstream of the barrier along each of the two considered O-D routes.

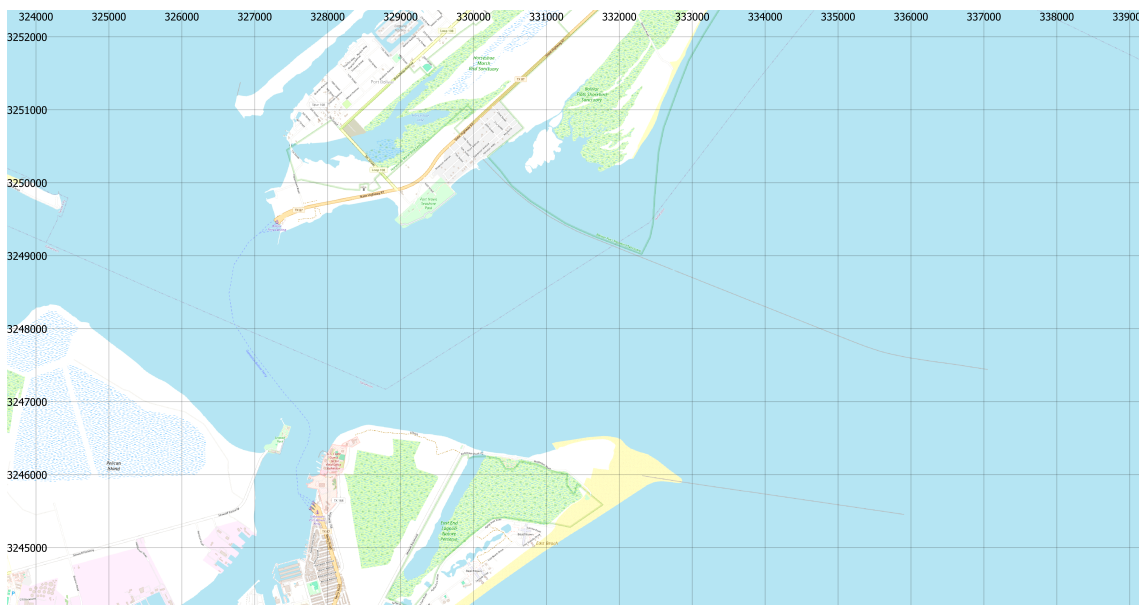


Figure 4.2: Base map of Bolivar Roads, CRS = EPSG:32615 - WGS84 / UTM zone 15N [m]; (from QGIS).

4.1.3. Nautical and Bathymetric Layout

Alternative Barrier Configurations

Although the design of the alternative barrier configurations is not strictly a component of the assessment method defined in Section 3.1, the process through which these alternative configurations came to fruition for the Bolivar Roads case is summarized below.

The development of alternative barrier configurations was carried out in joint effort, by representatives of the Houston Pilots Association, the Galveston-Texas City Pilots Association, TU Delft, Texas A&M University, Rijkswaterstaat, Haskoning, USACE, Gulf Coast Protection District, and other key stakeholders. These configurations were defined and refined through a series of dedicated workshops. The collaborative process ensured that the configurations reflected both engineering feasibility and navigational practicality, integrating the insights of local maritime experts with design expertise.

In developing the alternative configurations, the focus was deliberately placed on the navigational and geometric characteristics of the barrier rather than on its hydraulic or structural design. Consequently, aspects such as gate type, foundation design, and construction materials were excluded from consideration. Instead, the design exploration concentrated on three principal geometric parameters that most strongly influence the way that vessels navigate through the Bolivar Roads area (e.g., where turns have to be made, how sharp these turns are, where vessels enter the barrier, complexity of maneuvers, and how much maneuvering space vessels have at their disposal): gate width, alignment, and siting. These design variables are defined as follows:

- *Gate width* refers to the width of the navigable opening of the storm surge barrier when the gates are fully open.
- *Alignment* denotes the angle of orientation of the barrier relative to a predefined 0° alignment, measured about the structure's center of mass.
- *Siting* describes the geographical position of the barrier's center of mass within the project area, expressed by its horizontal (x) and vertical (y) coordinates.

The combination of these three parameters determines the overall geometry and positioning of the barrier's structural elements, such as its outer islands and navigable openings. Appendix C provides a graphical representation of each of the parameters.

Based on discussions during the stakeholder workshops, a series of consistent design choices was made to aid in the generation of the alternative barrier configurations:

- A review of the baseline design, informed by the findings of Burkley et al. (2022) and the design workshops, indicated that the inclusion of a middle island, as present in the original design of the Bolivar Roads barrier (see Figure 1.2), would pose significant navigational risks (see Subsection 1.1.4 and Subsection 3.2.4). For this reason, the alternative configurations developed during the workshops excluded a middle island, resulting in single-gate, two-way traffic configurations.
- The gate width for all alternative designs was set to 460 meters. This is 100 meters wider than the Maeslantkering, which currently holds the record for the storm surge barrier with the largest gate width (360 meters), but still considered feasible by the workshop attendees.
- Two of the alternative configurations were located further eastward as recommended by Burkley et al. (2022), although with a slightly different siting and alignment.
- A third alternative configuration retained the same horizontal siting (x-coordinate) and alignment as the original baseline configuration, thereby serving as a comparative control.

Ultimately, the workshops yielded a total of three alternative barrier configurations. As such, the assessment method was applied to comparatively assess the nautical safety performance of four barrier configurations: one baseline configuration and three alternatives. Each of these configurations represents a distinct geometric combination of gate width, alignment, and siting. Figure 4.3 depicts the spatial layouts of the baseline configuration and the three alternative configurations developed for Bolivar Roads. For reference, the existing dredged channel is also shown. It should be noted that this existing dredged channel is not representative of the bathymetric layout in the spatial schematization applied in the assessment method.

Configuration 3 (see Figure 4.3c) is the only layout that does not directly align with the existing dredged channel. Instead, it aligns indirectly with the adjacent channel segments in an attempt to minimize the turning angles required for vessel maneuvers. This design choice reflects an effort by the workshop attendees to improve navigational fluidity and reduce steering efforts near the barrier.

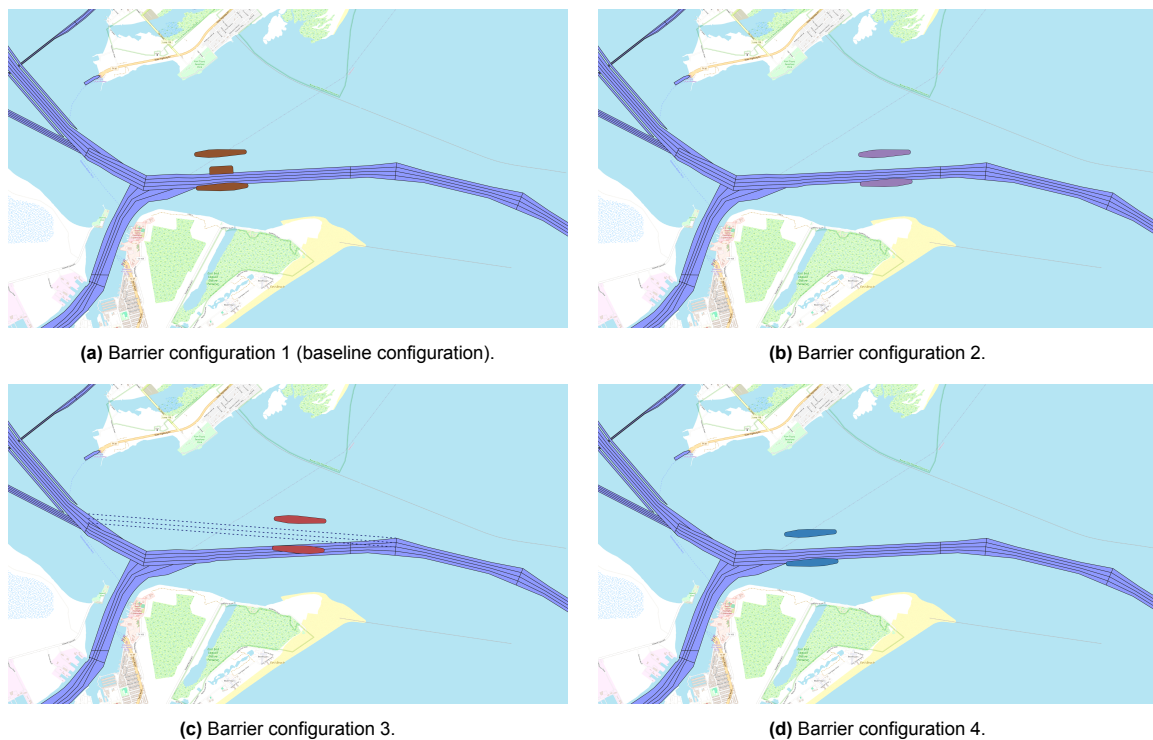


Figure 4.3: Baseline and alternative barrier configurations for Bolivar Roads, on existing dredged channel; (from QGIS).

Table 4.1 summarizes the defining geometric parameters of each of the four barrier configurations shown in Figure 4.3.

Table 4.1: Specification of geometric parameters of barrier configurations developed for Bolivar Roads.

Barrier Configuration	Gate Width [m]	Alignment* [°]	Siting [m]
1	2 x 200	-	(329835.73, 3247497.65)**
2	460	0.00	(331385.25, 3247538.52)**
3	460	6.00 ⌚	(331464.95, 3247729.23)**
4	460	0.00	(329835.73, 3247451.21)**

*relative to barrier configuration 1

**CRS = EPSG:32615 - WGS84 / UTM zone 15N [m] (see Figure 4.4)

Figure 4.4 (CRS = EPSG:32615 - WGS84 / UTM zone 15N [m]) provides a visual overview of all the developed barrier configurations, illustrating their relative positions and orientations within the Bolivar Roads area. Notably, the southern outer island of configuration 1 has the same location as the southern island of configuration 4.

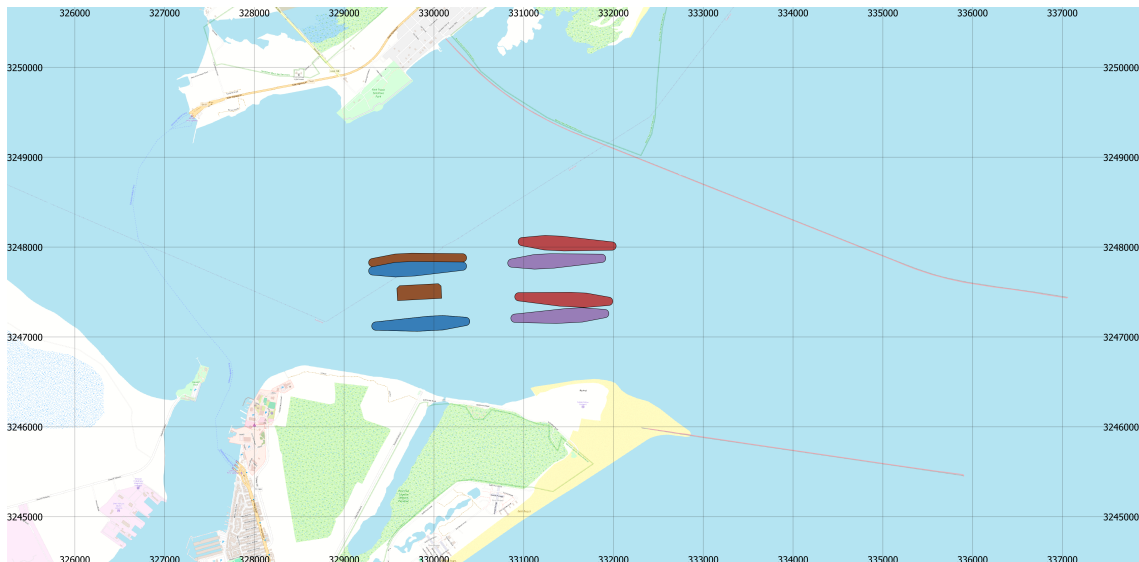


Figure 4.4: Overview of barrier configurations: 1 (brown), 2 (purple), 3 (red), and 4 (blue); (from QGIS).

Nautical and Bathymetric Modeling

The ship channel approach leading to Bolivar Roads is flanked by two jetties (see Figure 4.1) extending into the Gulf of Mexico, with distances of 7.2 km (northern jetty) from the Bolivar Peninsula and 3.62 km (southern jetty) from Galveston Island, that prevent the inflow of sediment into the waterway and protect it from wave penetration (NOAA, 2025a).

Figure 4.1 illustrates the current layout of the existing shipping channels within the Bolivar Roads area, providing nautical, as well as bathymetric information. The Houston Ship Channel follows a northwestward trajectory from the entrance at Bolivar Roads (NOAA, 2025a). It is maintained at a depth of 14 meters relative to mean lower low water (MLLW), with a typical channel width of 400 meters for the channel section near Bolivar Roads and narrower, more inland sections, with widths of 160 meters (NOAA, 2025a). The Galveston Ship Channel, branching south from Bolivar Roads, is similarly maintained at a depth of 14 meters relative to MLLW, with channel widths of up to 426 meters (NOAA, 2025a).

The spatial schematization was executed in QGIS v.3.40.5. Each of the alternative barrier configurations was modeled such that it accurately represents the configurations developed during the series of workshops (detailed earlier in this section), capturing the full set of geometric characteristics summarized Table 4.1.

The nautical and bathymetric layout were constructed using bathymetric and hydrographic data for Bolivar Roads obtained from NOAA³, including the nautical chart shown in Figure 4.1 and Appendix B (full-size image). As the navigational sections of the developed barrier configurations extend beyond the existing dredged channel (see Figure 4.3) the bathymetry modeled in the spatial schematization was extended such that it covers the navigational sections for all of the developed barrier layouts. In this way the spatial schematization portrays the (possible) future bathymetric layout. The extension of the existing bathymetry can be seen in Figure 4.5. As both the Houston and Galveston Ship Channel are currently maintained at a depth of 14 meters with respect to MLLW, this was the bed level assumed in the spatial schematization model. The resulting spatial schematization incorporated the geometric definition of the proposed storm surge barrier configurations, extended dredged fairway layouts, bank positions, jetties, and surrounding land masses across the extent of the geometric domain depicted in Figure 4.2. The final spatial schematization is shown Figure 4.6.

³Electronic Navigational Charts obtained from: <https://devgis.charttools.noaa.gov/pod/>

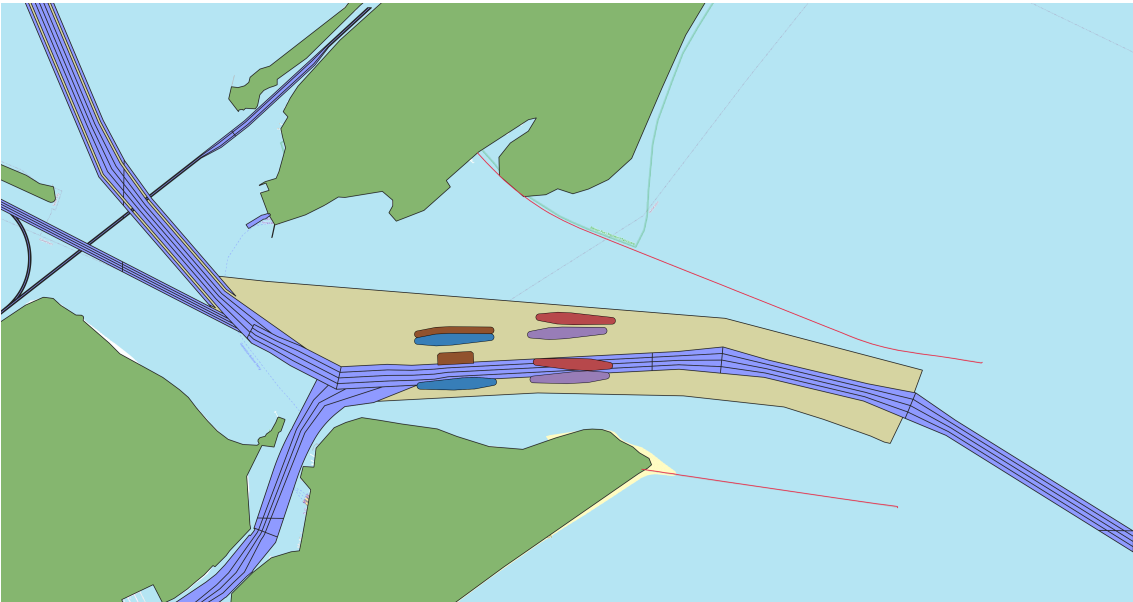


Figure 4.5: Spatial schematization, Bolivar Roads, existing bathymetry (purple) and extension (beige); (from QGIS).

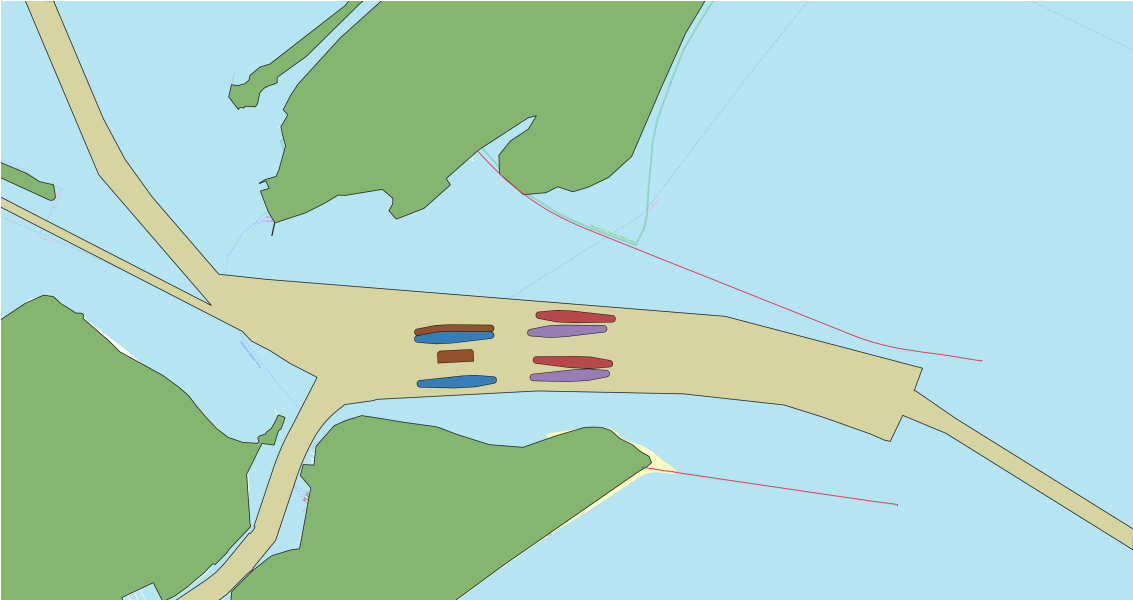


Figure 4.6: Final spatial schematization, Bolivar Roads; (from QGIS).

4.2. Environmental Forcing and Hydrodynamic Effects

This section presents the environmental forcing conditions applied in the assessment of the Bolivar Roads storm surge barrier configurations. Following the procedure defined in Section 3.1, representative wind and current conditions are derived from measured data and translated into a set of consistent environmental scenarios for simulation. The section describes the data sources used, the statistical characterization of wind and current conditions, and the selection of representative forcing scenarios applied across all barrier configurations. These results define the environmental context within which vessel maneuvering behavior is evaluated in the subsequent simulation-based analyses.

4.2.1. Environmental Data Sources and Dominant Forcing Mechanisms

The Bolivar Roads area is instrumented with several environmental monitoring stations that provide real-time and historical data on hydrodynamic and meteorological conditions (NOAA, 2025b). These stations constitute the primary data sources used to define the environmental forcing inputs applied in the assessment method for this case study. Based on an analysis of NOAA data and discussions with maritime experts, it was concluded that the navigational conditions at Bolivar Roads are predominantly governed by two environmental forcing mechanisms: wind and currents. Consequently, wave action was not considered in the present assessment.

Figure 4.7 displays the spatial distribution of wind and current monitoring stations in the Bolivar Roads area. The stations from which the wind and current data were ultimately obtained are indicated by red circles in this figure. The wind station provides continuous measurements of wind speed and direction at standard reference heights, typically updated at six minute and hourly intervals. The current station records current speeds and direction at varying depths, contributing to an understanding of both lateral and longitudinal current profiles within the navigable fairway.

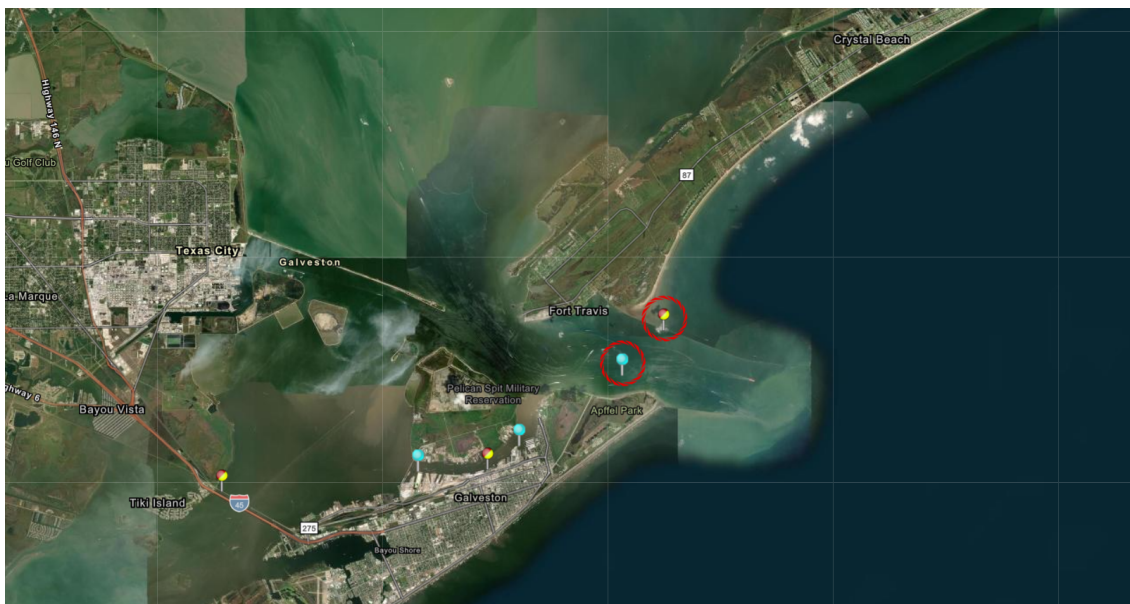


Figure 4.7: Location of current (blue markers) and wind stations (red/yellow markers) at Bolivar Roads (NOAA, 2025b).

In this case study, worst navigable conditions were defined in collaboration with maritime experts using one year (2023) of historical wind and current data. To represent the dominant hydrodynamic regimes influencing vessel passage at Bolivar Roads, two environmental scenarios were defined: one corresponding to flood-tide conditions and one corresponding to ebb-tide conditions, each combined with a representative wind forcing. For both scenarios, the magnitudes of the winds and currents derived from the monitoring stations (circled in red in Figure 4.7) were applied homogeneously across the full extent of the simulation domain. The worst navigable scenarios are described in the following subsections.

4.2.2. Wind

The wind data⁴ used to define the worst navigable conditions can be found in Appendix D. Using this data, the wind rose shown in Figure 4.8 was created in Python. The magnitude of the wind in the worst navigable scenarios was set to 10.0 m/s (19.44 knots). As visible in Figure 4.8, this is representative of the stronger prevailing winds under which vessels would navigate. Experienced shipping pilots report that cross winds tend to have the most significant impact on ship maneuverability because they directly affect course-keeping and alignment. As such, the direction of the wind was chosen such that it acts on the side of vessels as they align themselves with, and maneuver through, the barrier. For inbound vessels this resulted in a wind blowing in the direction of 20.0° (relative to true north). For outbound vessels this resulted in a wind blowing in the direction of 160.0° (relative to true north).

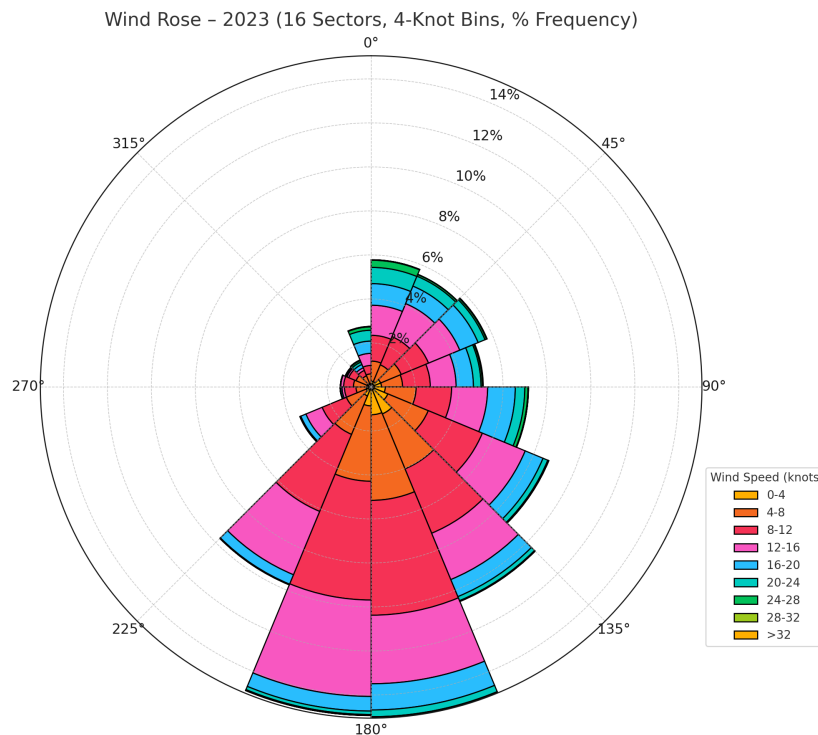


Figure 4.8: Wind rose of measured winds in 2023 (wind direction is the direction from which the wind blows).

4.2.3. Currents

The current data⁵ used to define the worst navigable conditions can be found in Appendix E. Using this data, the current rose shown in Figure 4.9 was created in Python. From the current data it was concluded that the prevailing ebb tidal currents are slightly larger in magnitude than the flood tidal currents (see Figure 4.9). This is reflected in the magnitudes that were chosen for the current forcing. The magnitudes of the currents in the worst navigable scenarios were defined as follows: 0.8 m/s (1.56 knots) for the flood current, and 0.85 m/s (1.65 knots) for the ebb current. According to maritime pilots, these magnitudes are representative of the stronger prevailing currents under which vessels would navigate. The directions of the currents were chosen such that they follow the dredged shipping channels, as observed in supplementary spatial current data⁶, and flow around the structural elements of the corresponding barrier configuration. Due to time and resource constraints, configuration-specific hydrodynamic modeling was not undertaken.

⁴Wind data for year 2023 obtained from: <https://tidesandcurrents.noaa.gov/met.html?id=8771341>

⁵Current data for year 2023 obtained from: <https://tidesandcurrents.noaa.gov/cdata/DataPlot?id=g06010&bin=0&bdate=20251210&edate=20251211&unit=1&timeZone=UTC>

⁶Supplementary current data obtained from: <https://www.admiralty.co.uk/publications/miscellaneous-tidal-publications/admiralty-tidal-stream-atlases>

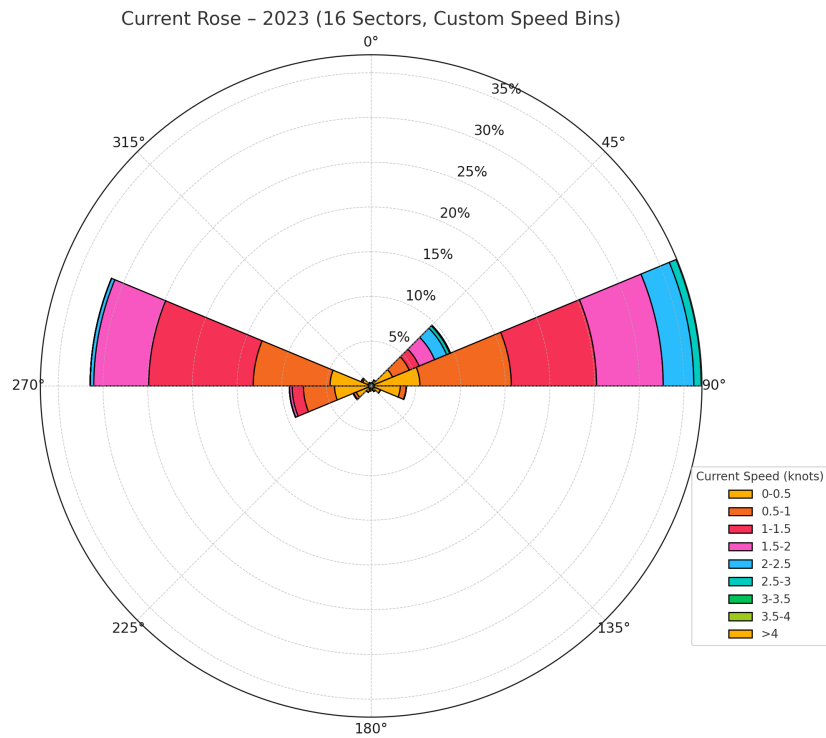


Figure 4.9: Current rose of measured currents in 2023 (current direction is the direction to which the current flows).

According to maritime experts, following currents (see Subsection 2.2.2) lead to the most challenging maneuvering conditions for vessels. Therefore, flood currents were used to define the worst navigable conditions for inbound vessels, and ebb currents were used to define the worst navigable conditions for outbound vessels. This led to a set of 8 current fields: one current field corresponding to ebb currents and one current field corresponding to flood currents, for each of the four configurations. All of the current fields were modeled in QGIS v.3.40.5. Figure 4.10 depicts the flood current field for barrier configuration 1, and Figure 4.11 depicts the ebb current field for barrier configuration 1. The current fields for configurations 2, 3, and 4 can be found in Appendix G.1.

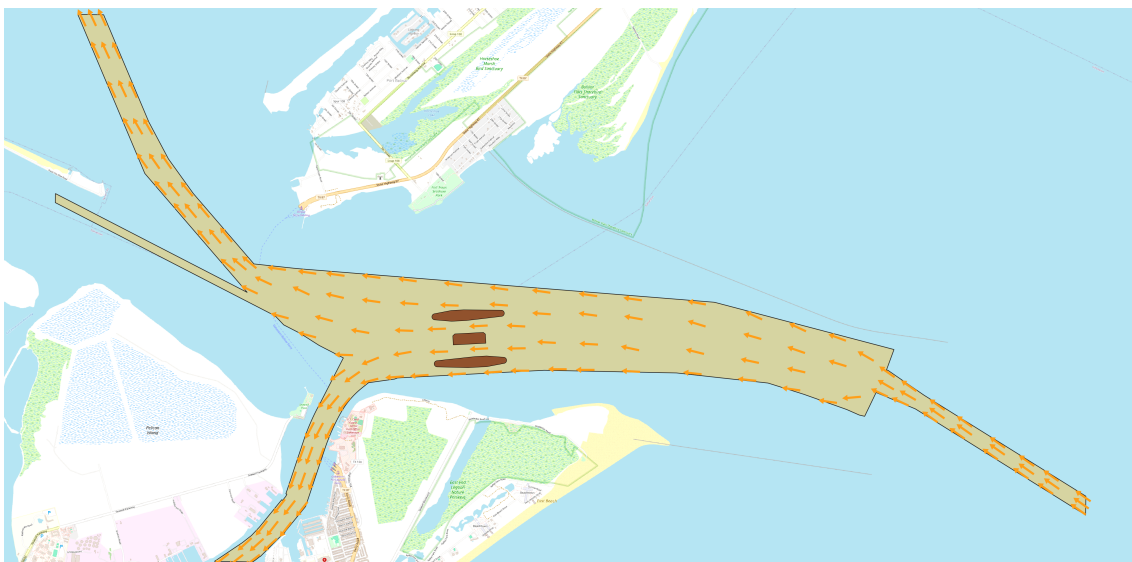


Figure 4.10: Current field: flood current, inbound vessels, configuration 1; (from QGIS).

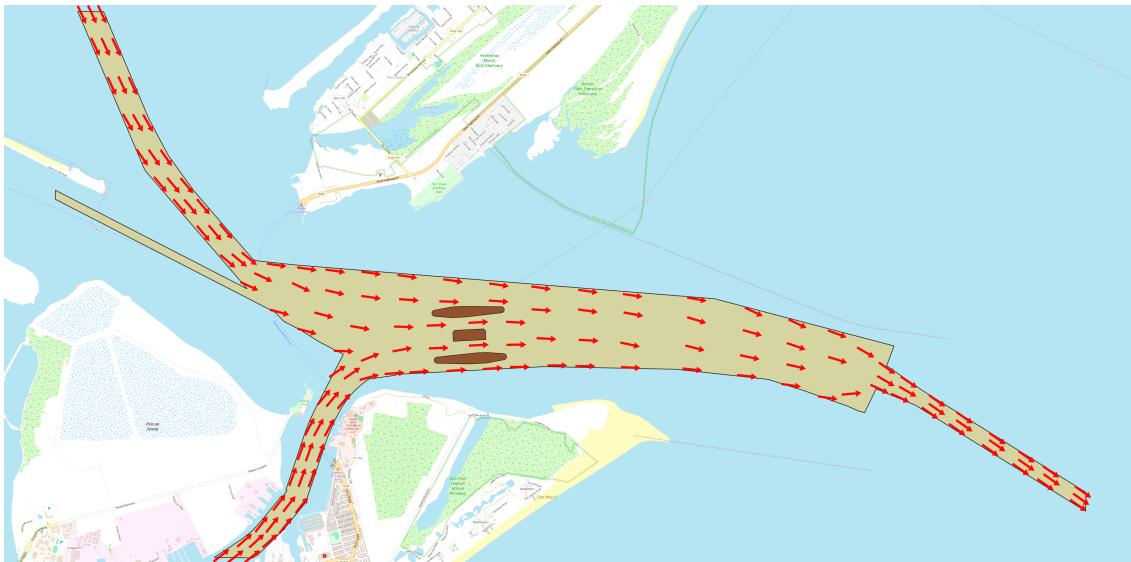


Figure 4.11: Current field: ebb current, outbound vessels, configuration 1; (from QGIS).

4.2.4. Worst Navigable Conditions

The discussions with maritime experts ultimately led to the following set of worst navigable scenarios:

Table 4.2: Worst navigable conditions for Bolivar Roads.

Route*	Tide	Wind Magnitude [m/s]	Wind Direction [°]	Current Magnitude [m/s]	Current Direction [°]
IB	Flood	10.0	20.0	0.8	**
OB	Ebb	10.0	160.0	0.85	**

*IB = inbound, OB = outbound

**for direction of currents please refer to current fields

The magnitudes of the winds and currents, and direction of the winds, shown in Table 4.2, were applied homogeneously across the full extent of the simulation domain.

4.2.5. SHIPMA-Specific Environmental Inputs

Several environmental effects considered in the assessment require a tool-specific representation when implemented in SHIPMA. In the context of this case study, water depth, bank suction, and shallow-water effects are therefore introduced here as relevant environmental influences on vessel maneuvering. Their specific numerical formulation and detailed parametrization depend on the implementation within SHIPMA and are therefore described in Section 4.5.

Water Depth

In SHIPMA, water depth is represented through a combination of the local bathymetry and a prescribed water level. Together, these determine the effective water depth experienced by a vessel during simulation. The selection of water level is constrained by the characteristics and calibration range of the applied vessel models.

Bank Suction

In SHIPMA, bank suction effects are included to account for the interaction between vessels and nearby channel boundaries under confined navigation conditions. The representation of these effects depends on the local bathymetry and vessel position within the fairway.

Shallow Water Effects

Shallow-water effects in SHIPMA arise from the combined specification of vessel draught (defined by the vessel model), bed level (defined in the spatial schematization), and water depth (imposed through the defined water level in the current field input).

4.3. Design Vessels

This section presents the selection of design vessels used in the assessment of navigational safety at Bolivar Roads. Following the procedure defined in Section 3.1, representative vessels were identified based on an analysis of historical Automatic Identification System (AIS) data, with the aim of capturing the dominant vessel types, sizes, and operational characteristics relevant to the considered navigation routes. The section describes the composition of the vessel population, the criteria applied to select representative design vessels, and their sensitivity to environmental forcing mechanisms such as wind and currents. Together, these results define the set of design vessels that form the basis for the subsequent maneuvering simulations and comparative safety assessment.

4.3.1. Identification of Vessel Population

In order to identify the design vessels and select representative vessel models for the simulations, an analysis of AIS data was performed. For this analysis 1 year (2024) of historical AIS data, from Haskoning's AIS platform, was downloaded and imported into QGIS v.3.40.5. The raw dataset was cleaned and missing information, such as an absent LOA, beam, draught or vessel type, was supplemented using the SeaWeb database⁷. The final dataset used in the AIS analysis is visualized in Figure 4.12, in which, to ensure clear visual separation between contextual geographic information and the AIS-derived vessel trajectories, the base map has been rendered in grayscale. To focus the identification of the relevant vessel population on ships that are most critical for the geometric design and navigational safety assessment of the barrier configurations, the AIS dataset was filtered by LOA, and only vessels with LOA's larger than 100 meters were considered.

The analysis of the AIS data indicated that:

- The vessel types most commonly navigating the Houston Ship Channel are: general cargo vessels, chemical/oil/gas products tankers, bulk carriers, container vessels, and ro-ro vessels.
- The vessel types most commonly navigating the Galveston Ship Channel are: chemical/oil/gas products tankers, bulk carriers, ro-ro vessels, refrigerated cargo ships, cruise ships, and container vessels.

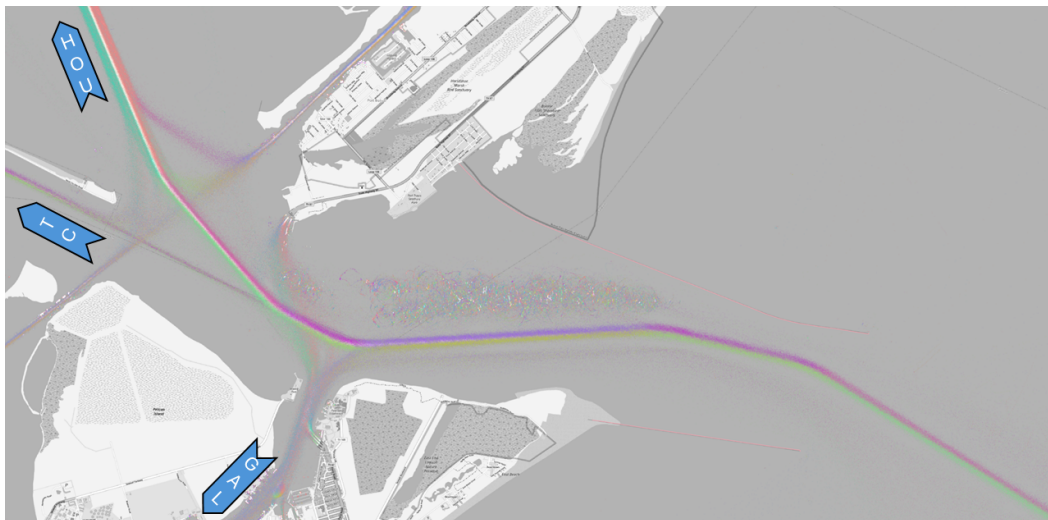


Figure 4.12: Vessel traffic patterns at Bolivar Roads in the year 2024. Categorized per COG; (from QGIS).

4.3.2. Representative Design Vessels

Per origin destination, three design vessels were selected that reflect distinct types of maneuvering behavior given the defined worst navigable environmental conditions (see Table 4.2). To this end, firstly, three sensitivity classes were formulated to represent the environmental forcing mechanisms considered in the worst navigable scenarios: wind sensitive vessels (large windage area), current sensitive vessels (large draught), and vessels susceptible to both wind and currents (large windage

⁷SeaWeb data accessible with login credentials via: <https://maritime.ihs.com/Account2/Index>

area and draught). Next, for each O-D route, the governing vessels types were categorized into one of the sensitivity classes with the help of a maritime pilot. Finally, for each O-D route, the critical vessel (vessel with largest sensitive dimension) within each sensitivity class was chosen, i.e. the governing design vessels. This lead to a collection of one wind sensitive vessel, one current sensitive vessel, and one vessel susceptible to both wind and currents, per O-D route. The selected design vessels and their characteristics are presented in Table 4.3. Images of each design vessel are provided in Appendix F.

Table 4.3: Design vessel characteristics obtained from AIS analysis.

Vessel	MMSI	Origin/Destination	Sensitivity*	LOA [m]	Beam [m]	Draught [m]
Container	215196000	Houston	W & C	363.0	45.6	15.5
Tanker	303294000	Houston	C	287.25	50.0	19.59
Ro-Ro Vessel	403532001	Houston	W	224.96	32.3	9.5
Container	209444000	Galveston	W & C	147.87	23.25	8.5
Tanker	319095200	Galveston	C	277.0	48.0	17.17
Cruise Ship	311000396	Galveston	W	362.12	47.0	9.3

*W = wind, C = currents

4.3.3. Vessel Models for Simulation

The selection of vessel models that represent the identified design vessels is dependent on the implementation of SHIPMA. While Section 4.3 defines the design vessel characteristics at a conceptual level, the corresponding simulation vessel models and their parameterization are specified in Section 4.5.

4.4. Physical Maneuvering Indicators

The fast-time simulation model SHIPMA enables the monitoring and extraction of a range of physical maneuvering indicators at high spatial and temporal resolution during simulated vessel transits. In the context of this case study, SHIPMA was used to record the vessel heading, course over ground, drift angle, and swept path throughout each simulation run. These indicators are not prescribed as inputs to the simulations, but are generated as outputs by the model and can be extracted in both graphical and numerical form. Together, they provide the basis for the computation of the quantitative nautical safety assessment metrics presented in Section 4.6.

4.5. Ship Maneuvering Simulation: SHIPMA

This section presents the ship maneuvering simulations performed using the fast-time simulation model SHIPMA v.7.4 as part of the Bolivar Roads case study. Following the assessment framework defined in Section 3.1, the selected design vessels were simulated under the spatial schematization and representative environmental forcing conditions defined in the preceding sections. The current section describes the simulation setup, including model configuration, boundary conditions, and execution of simulation runs for the alternative storm surge barrier configurations. These simulations generated the vessel maneuvering behavior from which the physical maneuvering indicators and quantitative nautical safety assessment metrics are subsequently derived.

The fast-time simulation model SHIPMA was selected for this study as it is the maneuvering simulation tool routinely applied by Haskoning in their nautical safety assessments. Its use therefore ensures consistency with current engineering practice, while the availability of both the software itself and in-house expertise in model setup, execution, and interpretation enabled a reliable and efficient implementation of the simulation campaign. SHIPMA meets all the functional requirements of a simulation model highlighted in Subsection 3.1.5.

4.5.1. SHIPMA-Specific Input Formats

The following subsection details several simulation input specifications that are tied to the use of SHIPMA. While the underlying physical effects and environmental conditions were defined in the preceding sections, their technical representation and parameterization are discussed here, as they depend on the implementation within the applied simulation model.

Bank Suction

In SHIPMA, bank suction effects are represented through dedicated model formulations that account for the interaction between the vessel and nearby channel boundaries. These effects are activated based on the local bathymetry and vessel position within the fairway, through the definition of bank suction lines that delineate the position of the borders of the modeled dredged channel. As such, the coordinates of these lines follow from the extended bathymetry as modeled in the spatial schematization shown in Figure 4.6. The bank suction lines for each simulation scenario were modeled in QGIS v.3.40.5. Figure 4.13 shows the bank suction lines for IB-HOU routes of barrier configuration 1. All remaining bank suction lines are provided in Appendix G.2.

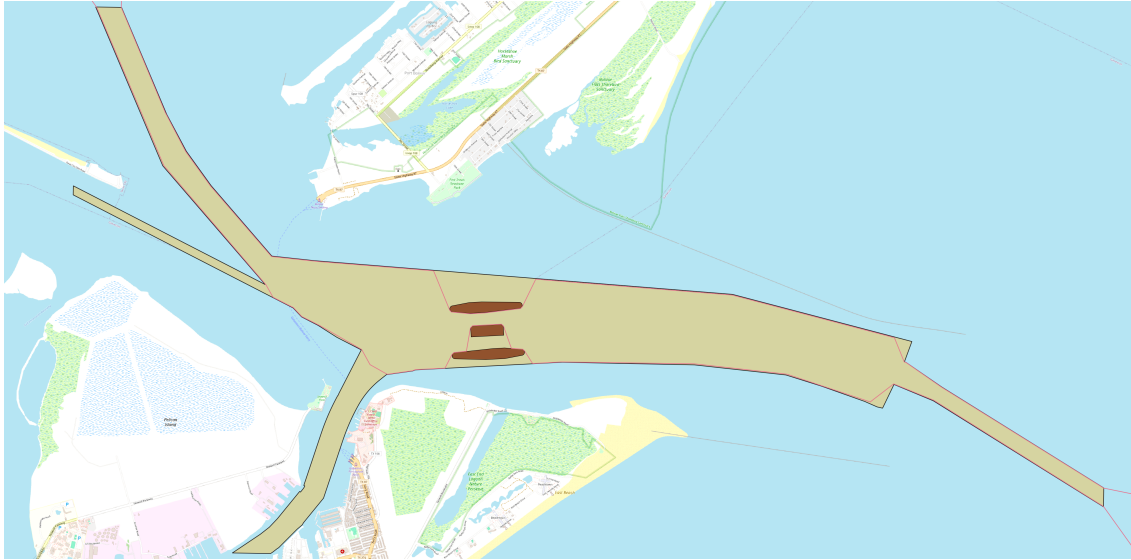


Figure 4.13: Bank suction lines: IB-HOU, configuration 1; (from QGIS).

Vessel Models

Following the determination of the design vessels for each origin/destination, a fitting vessel model was chosen from the library of validated SHIPMA vessel models available at Haskoning. The vessel models were selected such that they represent the characteristics of the identified design vessels (see Table 4.3) as accurately as possible. The chosen vessel models and their characteristics are presented in Table 4.4.

Table 4.4: Characteristics of SHIPMA vessel models.

Vessel	Code	Origin/Destination	Sensitivity*	LOA [m]	Beam [m]	Draught [m]	Max. RPM
Container	con038r1	Houston	W & C	366.0	51.2	13.2	104
Tanker	tan088r1	Houston	C	305.0	53.0	15.5	85
Car Carrier	car004a1	Houston	W	225.0	32.2	10.8	77
Container	con001a1	Galveston	W & C	165.0	25.7	8.2	88
Tanker	tan093r6	Galveston	C	250.0	44.0	13.0	106
Cruise Ship	fer054r1	Galveston	W	338.77	39.03	8.8	100

*W = wind, C = currents

Water Depth

In SHIPMA, the water depth is imposed via the current field input, through the definition of a water level. The sum of this water level and the bed level, as defined in the spatial schematization model, determines the effective water depth experienced by a vessel. All validated SHIPMA vessel models have been calibrated for a range of water depths specific to the particular vessel model: $[d_1, d_2]$. Realistic maneuvering behavior of a vessel model can only be guaranteed within this calibration zone, thus it was essential to define the water level in the current field files such that the final water depth falls within this range. As vessel maneuverability decreases with smaller water depth to draught (h/T)

ratio (measure of under keel clearance, see Section 2.2), the smallest water level possible was taken (representative of the worst navigable conditions) which still allowed for a fair comparison between simulations with different vessel models. This fair comparison was guaranteed by ensuring that the under keel clearance as a percentage of a vessel's draught was equal for all vessels (i.e. same h/T ratio). Consequently, for each specific simulation scenario, the water level prescribed in the current field file needed to be adjusted depending on the applied vessel model (while magnitudes and directions of currents remained unchanged).

The prescribed water levels corresponding to each of the SHIPMA vessel models used in this case study, and the resulting water depths, are summarized in Table 4.5.

Table 4.5: Water level, bottom level and resulting water depth for selected SHIPMA vessel models.

Vessel	Code	Origin/Desination	Water Level [m]	Bed Level [m]	Water Depth [m]	UKC*
Container	con038r1	Houston	1.972	14	15.972	21%
Tanker	tan088r1	Houston	4.755	14	18.755	21%
Car Carrier	car004a1	Houston	-0.932	14	13.068	21%
Container	con001a1	Galveston	-4.078	14	9.922	21%
Tanker	tan093r6	Galveston	1.730	14	15.730	21%
Cruise Ship	fer054r1	Galveston	-3.352	14	10.648	21%

*as a percentage of corresponding vessel draught shown in Table 4.4

Hydrographic survey data indicates that in reality the navigable water depth at Bolivar Roads typically ranges from 14 meters to 16 meters (USACE, 2025). It can therefore be concluded that the water depths in Table 4.5 are of a representative order of magnitude.

4.5.2. Autopilots

SHIPMA has four predefined autopilots, that are suitable for the majority of use cases:

- Autopilot 1: high constant speed with minimum drift angle.
- Autopilot 2: high constant speed with drift angle.
- Autopilot 3: slackening (slowing down).
- Autopilot 4: approach with use of tug/thruster.

In this case study, the simulated vessels were required to navigate through narrow navigational sections (where two way traffic is allowed). This means minimizing the drift angle is essential and as such autopilot configuration 1 was adopted across all simulations to ensure comparability between barrier configurations. This autopilot has been parameterized to reflect realistic pilot behavior for deep-draught vessels transiting through confined estuarine channels under varying tidal and wind conditions (MARIN, n.d.). For details please refer to the SHIPMA v.7.4 User Guide.

4.5.3. Maneuvers

Each barrier configuration was associated with a set of maneuvers representing the expected navigational routes and sailing speeds for inbound and outbound traffic to both the Port of Houston and Port of Galveston. These desired tracks were developed together with a maritime pilot and using the spatial schematization (see Figure 4.6), to ensure alignment with operational practice and the modeled fairways. As vessel traffic at Bolivar Roads currently adheres to starboard-side navigation, it was assumed that this will continue to be the case in the future situation. Each track was designed to test the vessel's ability to execute approach, entry, and exit sequences under representative environmental conditions. Subsequently, the developed tracks were modeled in AutoCAD v.2025. The desired tracks for barrier configuration 1 can be seen in Figure 4.14 (origin/destination Houston) and Figure 4.15 (origin/destination Galveston). Appendix G.3 contains a table of the coordinates of the desired tracks for configuration 1, as well figures and tables of the coordinates of the desired tracks for configurations 2, 3, and 4.



Figure 4.14: Desired tracks: IB-HOU (pink), OB-HOU (green), configuration 1; (from AutoCAD).



Figure 4.15: Desired tracks: IB-GAL (light blue), OB-GAL (red), configuration 1; (from AutoCAD).

For each vessel model, the speed along the track was chosen such that it is representative of the corresponding design vessel's sailing speeds observed in the AIS data, but not higher, as this would overestimate the maneuverability of the vessels. In SHIPMA a vessel's speed is prescribed in terms of an RPM that corresponds to one of the vessel's telegraph settings: dead slow, slow, half, harbour full, and sea full. For all vessels the prescribed telegraph setting was set to *slow*, in correspondence with the opinions of maritime experts. The sailing speeds for each vessel model (in terms of RPM as well as knots) are shown in Table 4.6.

Table 4.6: RPM setting, speed and RPM usage per vessel.

Vessel	Origin/Destination	RPM	Speed [kn]	Max. RPM	RPM Usage*
Container	Houston	39 (Slow)	9.2	104	37.50%
Tanker	Houston	32 (Slow)	6.0	85	37.65%
Car Carrier	Houston	40 (Slow)	9.1	77	51.95%
Container	Galveston	45 (Slow)	9.1	88	51.14%
Tanker	Galveston	47 (Slow)	7.0	106	44.34%
Cruise Ship	Galveston	47 (Slow)	10.2	100	47.00%

*RPM that a vessel uses divided by the maximum RPM capacity of the vessel

By applying identical maneuver definitions across alternative configurations where possible (the segments of the desired tracks through the barrier naturally differ across configurations), the analysis ensured that differences in navigational performance could be attributed solely to geometric and hydrodynamic variations rather than to inconsistencies in route design or control logic.

4.5.4. Initial Conditions

Across all simulation scenarios, the following initial conditions were applied:

- The time step was set to 1.0 sec. and the number of time steps was 6000. This means that 100 minutes of sailing time was simulated, allowing the vessel to reach the final point of the desired track within the simulation duration.
- The vessel's initial heading was chosen such that it is in line with the first segment of the desired track.
- The vessel's initial speed was chosen such that it is equal to the speed along the track defined in Table 4.6. This means that for all vessels the initial speed was set to the RPM corresponding to the *slow* telegraph setting. Thus, vessels did not enter the simulation domain from a stationary position. This is representative of real life situations.
- The starting position of the vessel was equal to the first coordinate of the desired track.

4.5.5. Simulation Cases

A simulation case (S.C.) is a specific combination of input parameters. The combination of input parameters chosen to define a case is dependent on what the end goal of the simulations is. In this case study the interest lay in assessing how different barrier configurations impact navigational safety. To this end, for each of the six considered vessels, eight cases were defined. One inbound transit for each of the four considered barrier configurations, and one outbound transit for each of the four considered barrier configurations. This resulted in a total of 48 different simulation cases, each of which represents one distinct simulation, providing the basis for a structured, quantitative evaluation of navigational safety performance across the four storm surge barrier configurations developed for Bolivar Roads. All of the defined cases are presented in Table 4.7.

Collectively, the vessel models, spatial schematization, worst navigable environmental scenarios, autopilots, maneuvers, and simulation cases form the complete hierarchical structure of the SHIPMA model set-up.

Table 4.7: SHIPMA simulation case matrix.

S.C.	Route	Configuration	Water Depth [m]	Wind (dir. - [m/s])	Current (dir. - [m/s])	RPM**
<i>Container Vessel (con038r1)</i>						
1	IB-HOU	1	15.972	20.0° - 10.0	* - 0.8	39 (Slow)
2	IB-HOU	2	15.972	20.0° - 10.0	* - 0.8	39 (Slow)
3	IB-HOU	3	15.972	20.0° - 10.0	* - 0.8	39 (Slow)
4	IB-HOU	4	15.972	20.0° - 10.0	* - 0.8	39 (Slow)
5	OB-HOU	1	15.972	160.0° - 10.0	* - 0.85	39 (Slow)
6	OB-HOU	2	15.972	160.0° - 10.0	* - 0.85	39 (Slow)
7	OB-HOU	3	15.972	160.0° - 10.0	* - 0.85	39 (Slow)
8	OB-HOU	4	15.972	160.0° - 10.0	* - 0.85	39 (Slow)
<i>Tanker (tan088r1)</i>						
9	IB-HOU	1	18.755	20.0° - 10.0	* - 0.8	32 (Slow)
10	IB-HOU	2	18.755	20.0° - 10.0	* - 0.8	32 (Slow)
11	IB-HOU	3	18.755	20.0° - 10.0	* - 0.8	32 (Slow)
12	IB-HOU	4	18.755	20.0° - 10.0	* - 0.8	32 (Slow)
13	OB-HOU	1	18.755	160.0° - 10.0	* - 0.85	32 (Slow)
14	OB-HOU	2	18.755	160.0° - 10.0	* - 0.85	32 (Slow)
15	OB-HOU	3	18.755	160.0° - 10.0	* - 0.85	32 (Slow)
16	OB-HOU	4	18.755	160.0° - 10.0	* - 0.85	32 (Slow)
<i>Car Carrier (car004a1)</i>						
17	IB-HOU	1	13.068	20.0° - 10.0	* - 0.8	40 (Slow)
18	IB-HOU	2	13.068	20.0° - 10.0	* - 0.8	40 (Slow)
19	IB-HOU	3	13.068	20.0° - 10.0	* - 0.8	40 (Slow)
20	IB-HOU	4	13.068	20.0° - 10.0	* - 0.8	40 (Slow)
21	OB-HOU	1	13.068	160.0° - 10.0	* - 0.85	40 (Slow)
22	OB-HOU	2	13.068	160.0° - 10.0	* - 0.85	40 (Slow)
23	OB-HOU	3	13.068	160.0° - 10.0	* - 0.85	40 (Slow)
24	OB-HOU	4	13.068	160.0° - 10.0	* - 0.85	40 (Slow)
<i>Container Vessel (con001a1)</i>						
25	IB-GAL	1	9.922	20.0° - 10.0	* - 0.8	45 (Slow)
26	IB-GAL	2	9.922	20.0° - 10.0	* - 0.8	45 (Slow)
27	IB-GAL	3	9.922	20.0° - 10.0	* - 0.8	45 (Slow)
28	IB-GAL	4	9.922	20.0° - 10.0	* - 0.8	45 (Slow)
29	OB-GAL	1	9.922	160.0° - 10.0	* - 0.85	45 (Slow)
30	OB-GAL	2	9.922	160.0° - 10.0	* - 0.85	45 (Slow)
31	OB-GAL	3	9.922	160.0° - 10.0	* - 0.85	45 (Slow)
32	OB-GAL	4	9.922	160.0° - 10.0	* - 0.85	45 (Slow)
<i>Tanker (tan093r6)</i>						
33	IB-GAL	1	15.730	20.0° - 10.0	* - 0.8	47 (Slow)
34	IB-GAL	2	15.730	20.0° - 10.0	* - 0.8	47 (Slow)
35	IB-GAL	3	15.730	20.0° - 10.0	* - 0.8	47 (Slow)
36	IB-GAL	4	15.730	20.0° - 10.0	* - 0.8	47 (Slow)
37	OB-GAL	1	15.730	160.0° - 10.0	* - 0.85	47 (Slow)
38	OB-GAL	2	15.730	160.0° - 10.0	* - 0.85	47 (Slow)
39	OB-GAL	3	15.730	160.0° - 10.0	* - 0.85	47 (Slow)
40	OB-GAL	4	15.730	160.0° - 10.0	* - 0.85	47 (Slow)
<i>Cruise Ship (fer054r1)</i>						
41	IB-GAL	1	10.648	20.0° - 10.0	* - 0.8	47 (Slow)
42	IB-GAL	2	10.648	20.0° - 10.0	* - 0.8	47 (Slow)
43	IB-GAL	3	10.648	20.0° - 10.0	* - 0.8	47 (Slow)
44	IB-GAL	4	10.648	20.0° - 10.0	* - 0.8	47 (Slow)
45	OB-GAL	1	10.648	160.0° - 10.0	* - 0.85	47 (Slow)
46	OB-GAL	2	10.648	160.0° - 10.0	* - 0.85	47 (Slow)
47	OB-GAL	3	10.648	160.0° - 10.0	* - 0.85	47 (Slow)
48	OB-GAL	4	10.648	160.0° - 10.0	* - 0.85	47 (Slow)

*for direction of currents please refer to flow fields

**for each vessel, the initial RPM and RPM along the track are equal

4.5.6. Simulation Outputs

Each simulation case produces a set of output files that can be visualized directly in SHIPMA and exported in both graphical and numerical form. Consistent structuring of case outputs was essential for determining the values of the assessment metrics across each of the barrier configurations. In this case study the output files contained:

- Temporal histories of vessel motion (rate of turn and speed).
- Temporal histories of control actions (rudder angle).
- Spatial histories of vessel motion (drift angle, swept path, rate of turn, and speed).
- Spatial histories of control actions (propeller revolutions, and rudder angle).
- Spatial histories of forces (wind, hull, bank suction, and rudder) and the corresponding moments.
- Spatial overview plots depicting the vessel passage from the first to the last point of the desired track.
- Zoom-ins of the spatial overview plots focusing on the part of the passage during which the vessel sails in between the barrier (i.e. the crossing segment).

The simulation outputs described above constitute the primary input for the determination of the quantitative nautical safety assessment metrics presented in the subsequent section. By extracting vessel behavior at predefined locations along the transit, the outputs enable consistent and reproducible determination of the metrics used to compare the navigational safety performance of the considered storm surge barrier configurations.

4.6. Nautical Safety Assessment Metrics

This section presents the outcomes of the quantitative nautical safety assessment metrics for all simulated cases and barrier configurations. Following the procedures defined in Section 3.1, the metrics are derived from the simulation outputs described in Section 4.5 and are reported consistently across vessels, environmental scenarios, and configurations. An overview of the metric values for all simulation cases is provided in Table 4.8, while Figures 4.16–4.19 present the assessment metrics in graphical form to facilitate comparison across simulation cases. For transparency and reproducibility, the detailed determination of the assessment metrics for simulation case 1 is documented in Appendix H. The section concludes with a descriptive, metric-by-metric comparison of nautical safety performance across barrier configurations, highlighting observed differences and patterns, while broader interpretation and implications for design decision-making are addressed in Chapter 5.

The complete set of SHIPMA output plots used for the determination of the nautical safety assessment metrics for all simulation cases is provided in *Annex A: SHIPMA Output Plots*.

4.6.1. Presentation of Nautical Safety Assessment Metrics

In Table 4.8 and Figure 4.16a, a negative value of *Dist. B.E.* indicates that the vessel has not completed the final approach turn prior to reaching the point of barrier entry. In such cases, the vessel has already passed the defined barrier entry point while the turn toward the barrier opening is still ongoing. Negative *Dist. B.E.* values thus reflect situations in which the vessel enters the barrier before achieving a stabilized approach alignment. The *Time B.E.* for these cases has therefore been set to 0.00 minutes. An example of a simulation case for which this occurred is S.C. 29 (highlighted in gray in Table 4.8). Figure 4.20 shows the zoom-in of the spatial overview plot for this simulation case, focusing on the crossing segment.

Table 4.8: Outcomes of quantitative nautical safety assessment metrics, per barrier configuration.

S.C.	Dist. B.E.	Time B.E.	Rudder Range I.B.	Beam Clr. I.B.	Max. DA I.B.	Dist. A.B.	Time A.B.
<i>Configuration 1</i>							
1	1991 m	7.57 min.	[-7.33°, -1.33°]	1.13-B	-3.37°	482 m	1.75 min.
5	50 m	<0.20 min.	[-6.67°, 0.89°]	1.05-B	-1.63°	2560 m	8.79 min.
9	2247 m	11.49 min.	[-16.89°, 0.22°]	1.21-B	-1.85°	558 m	3.03 min.
13	50 m	<0.30 min.	[-12.67°, 5.33°]	1.09-B	-0.87°	2650 m	13.13 min.
17	2144 m	8.71 min.	[-17.11°, -6.89°]	2.39-B	-2.17°	659 m	2.80 min.
21	24 m	<0.20 min.	[-13.11°, -5.11°]	2.19-B	-1.18°	2751 m	11.03 min.
25	2356 m	7.98 min.	[-13.33°, -5.11°]	3.49-B	-1.09°	183 m	<0.70 min.
29	-1133 m	0.00 min.	[-20.00°, 12.67°]	2.24-B	10.33°	2832 m	9.15 min.
33	2376 m	11.63 min.	[-12.00°, 0.00°]	1.75-B	-1.62°	81 m	<0.40 min.
37	67 m	<0.20 min.	[-8.67°, 1.78°]	1.75-B	-0.98°	2695 m	12.04 min.
41	2225 m	6.38 min.	[-12.31°, -3.60°]	1.64-B	-2.61°	0 m	0.00 min.
45	-188 m	0.00 min.	[-8.72°, -2.56°]	1.80-B	-1.41°	2636 m	7.53 min.
<i>Configuration 2</i>							
2	558 m	1.84 min.	[-6.67°, -3.33°]	1.39-B	-4.13°	1865 m	6.76 min.
6	1598 m	5.37 min.	[-6.89°, -4.44°]	1.52-B	-3.26°	995 m	3.52 min.
10	558 m	2.59 min.	[-12.22°, -6.89°]	1.35-B	-2.61°	1941 m	10.34 min.
14	1624 m	7.87 min.	[-12.67°, -7.33°]	1.47-B	-2.07°	1085 m	5.18 min.
18	558 m	2.21 min.	[-14.22°, -10.00°]	2.62-B	-2.72°	2043 m	8.72 min.
22	1624 m	6.30 min.	[-6.00°, -1.56°]	2.82-B	-1.18°	1161 m	4.58 min.
26	959 m	3.33 min.	[-10.89°, -6.89°]	4.04-B	-1.30°	1786 m	6.06 min.
30	343 m	1.14 min.	[-8.44°, -4.00°]	4.30-B	-0.87°	1255 m	4.11 min.
34	561 m	2.52 min.	[-8.22°, -5.33°]	2.07-B	-2.06°	1676 m	8.13 min.
38	1488 m	6.63 min.	[-9.11°, -4.89°]	2.21-B	-1.63°	1138 m	5.05 min.
42	561 m	1.44 min.	[-10.51°, -9.23°]	2.66-B	-3.15°	1589 m	4.68 min.
46	1334 m	3.58 min.	[-10.00°, -7.95°]	2.66-B	-2.07°	1059 m	3.02 min.
<i>Configuration 3</i>							
3	472 m	1.62 min.	[-8.44°, -3.11°]	1.39-B	-3.48°	2930 m	10.48 min.
7	2477 m	8.52 min.	[-6.67°, -2.22°]	1.52-B	-2.83°	959 m	3.22 min.
11	446 m	2.37 min.	[-12.89°, -8.89°]	1.47-B	-1.63°	2982 m	15.70 min.
15	2554 m	12.94 min.	[-11.33°, -2.22°]	1.47-B	-1.52°	1021 m	5.04 min.
19	1062 m	4.32 min.	[-16.22°, -10.89°]	2.82-B	-1.91°	3082 m	12.84 min.
23	2503 m	10.28 min.	[-12.89°, -7.33°]	2.82-B	-1.32°	1123 m	4.44 min.
27	1002 m	3.28 min.	[-14.22°, -8.00°]	4.04-B	-0.87°	1020 m	3.50 min.
31	40 m	<0.10 min.	[-7.78°, -3.11°]	4.30-B	-0.65°	1164 m	3.77 min.
35	1022 m	4.82 min.	[-9.11°, -6.00°]	2.07-B	-1.32°	918 m	4.40 min.
39	1183 m	5.13 min.	[-7.78°, -2.44°]	2.21-B	-1.20°	1059 m	4.55 min.
43	383 m	0.99 min.	[-11.03°, -9.49°]	2.66-B	-2.61°	819 m	2.50 min.
47	1081 m	3.00 min.	[-8.97°, -5.13°]	2.66-B	-1.74°	982 m	2.76 min.
<i>Configuration 4</i>							
4	2058 m	7.57 min.	[-9.11°, -2°]	1.27-B	-4.02°	313 m	1.26 min.
8	27 m	<0.20 min.	[-7.33°, -2.89°]	1.52-B	-3.26°	2558 m	8.77 min.
12	2417 m	10.29 min.	[-14.67°, -2.89°]	1.35-B	-2.28°	339 m	1.86 min.
16	27 m	<0.30 min.	[-13.33°, -3.56°]	1.47-B	-2.28°	2622 m	12.99 min.
20	2135 m	8.95 min.	[-13.78°, -11.56°]	2.62-B	-2.28°	465 m	2.09 min.
24	1 m	<0.20 min.	[-13.33°, -6.89°]	2.82-B	-2.06°	2724 m	10.87 min.
28	2357 m	8.18 min.	[-10.44°, -8.89°]	4.04-B	-1.09°	226 m	<0.80 min.
32	-1103 m	0.00 min.	[-17.11°, 18.22°]	4.04-B	10.33°	2801 m	9.08 min.
36	2439 m	11.40 min.	[-9.78°, -4.89°]	2.07-B	-1.91°	118 m	<0.60 min.
40	77 m	<0.20 min.	[-8.89°, 0.22°]	2.07-B	-2.07°	2684 m	11.94 min.
44	2051 m	5.97 min.	[-11.54°, -7.95°]	2.50-B	-2.93°	18 m	<0.10 min.
48	-217 m	0.00 min.	[-10.00°, -2.56°]	2.66-B	-2.28°	2605 m	7.53 min.

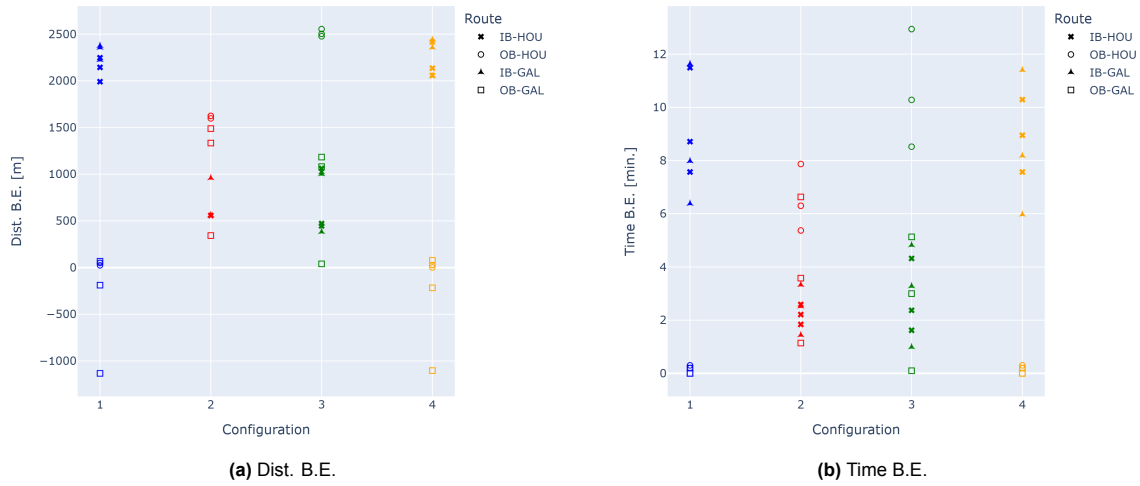


Figure 4.16: *Dist. B.E.* and *Time B.E.*, per configuration, all simulation cases (from Python).

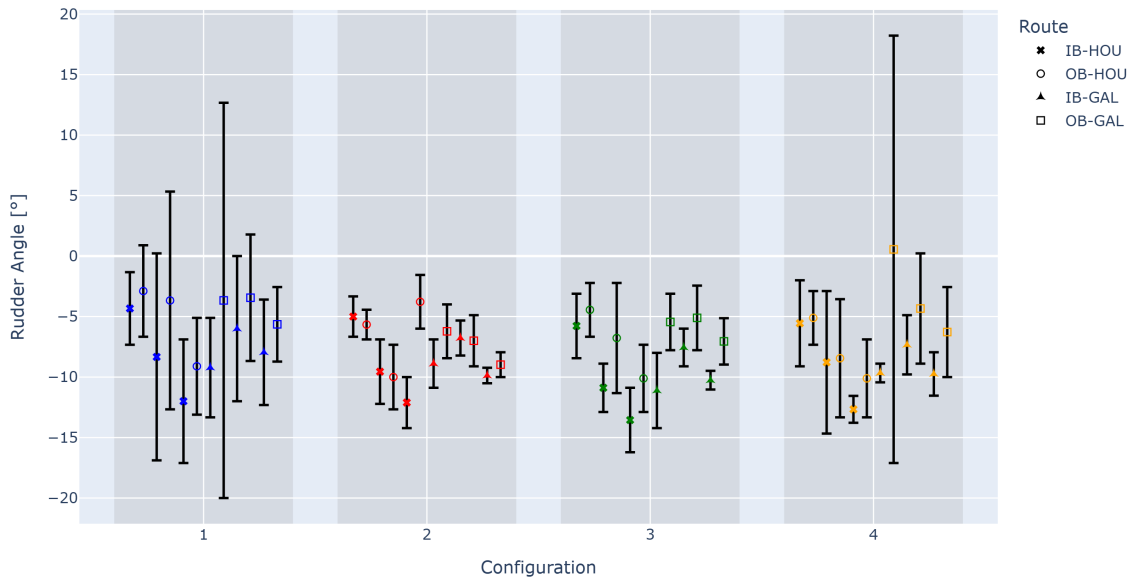


Figure 4.17: *Rudder Range I.B.*, per configuration, all simulation cases (from Python).

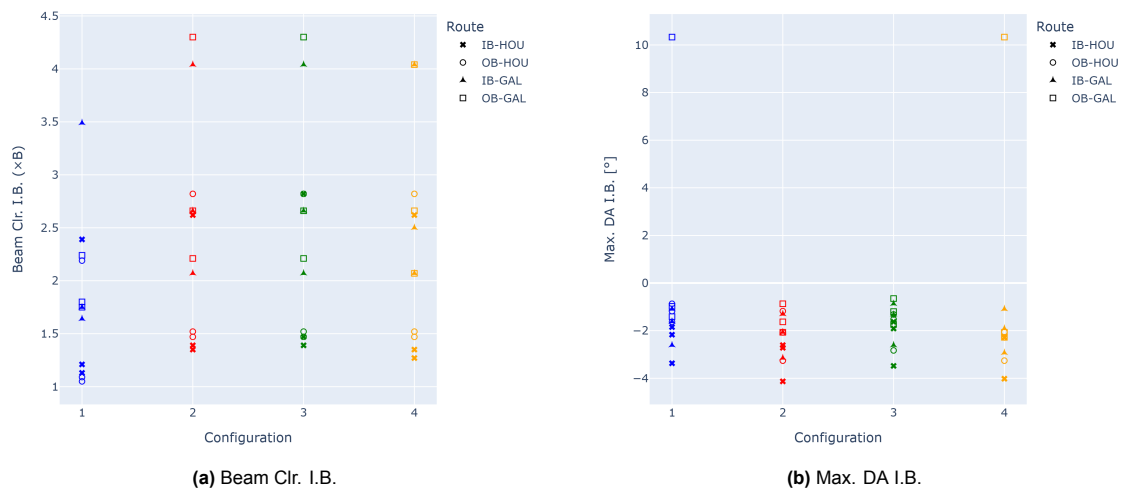


Figure 4.18: *Beam Clr. I.B.* and *Max. DA I.B.*, per configuration, all simulation cases (from Python).

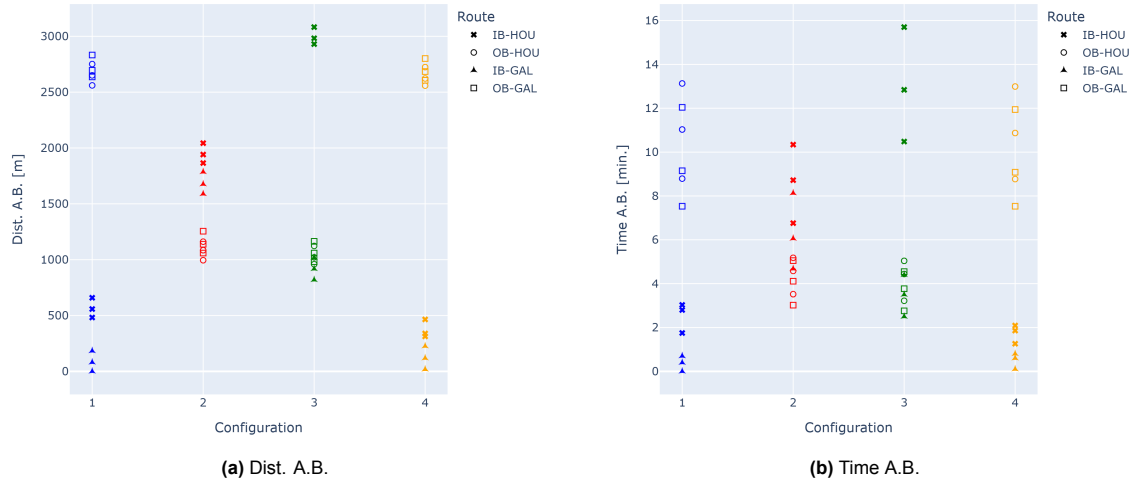


Figure 4.19: *Dist. A.B.* and *Time A.B.*, per configuration, all simulation cases (from Python).

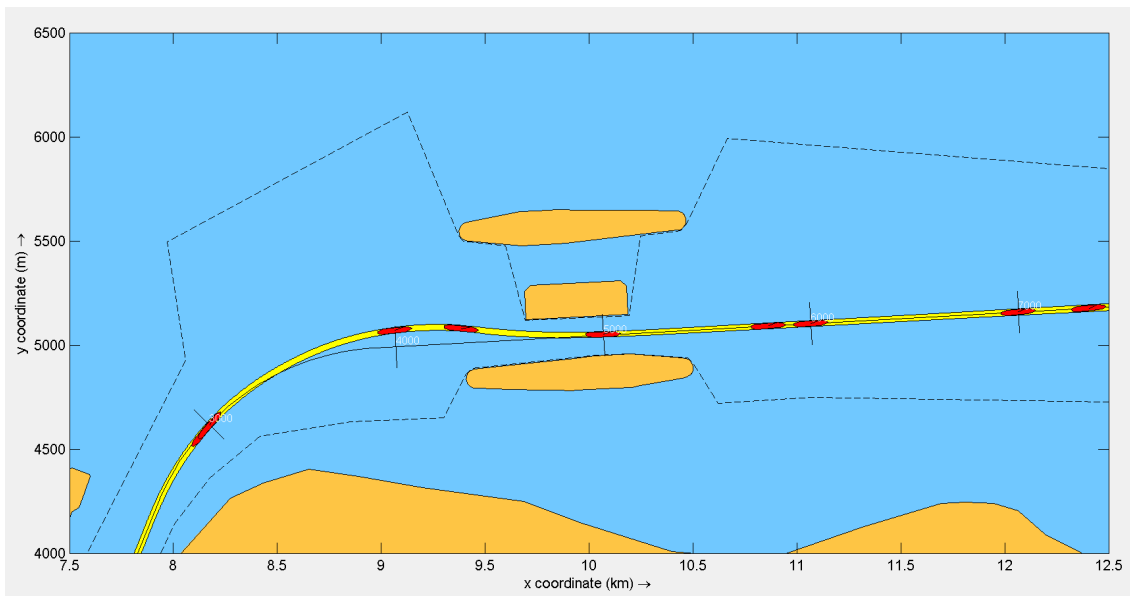


Figure 4.20: S.C. 29: zoom-in of spatial overview plot, crossing segment (from SHIPMA).

4.6.2. Descriptive Analysis of Assessment Metric Outcomes

The descriptive analysis presented below is based on the quantitative assessment metrics reported in Table 4.8 and their graphical representation in Figures 4.16–4.19. Together, the table and figures enable systematic comparison of metric outcomes across barrier configurations and simulation cases. While Table 4.8 provides a complete numerical overview of the assessment results, the figures emphasize relative patterns, variability, and the occurrence of extreme values, thereby facilitating a clear and consistent description of configuration-dependent differences in vessel maneuvering behavior. The analysis remains descriptive in nature and documents the observed outcomes captured by the assessment metrics, without introducing interpretative judgments.

Dist. B.E./Time B.E.

Figure 4.16 presents the *Distance Before Entry* (Figure 4.16a) and *Time Before Entry* (Figure 4.16b) for all simulation cases, grouped by barrier configuration. The paired plots show a consistent correspondence between spatial and temporal margins, with configurations exhibiting larger *Dist. B.E.* values also exhibiting larger *Time B.E.* values, and configurations exhibiting smaller *Dist. B.E.* values exhibiting smaller *Time B.E.* values. Given the metric definitions presented in Subsection 3.1.6, this is to be expected.

Notable observations with regard to these assessment metrics are as follows:

- All negative values of *Dist. B.E.* (0.00 [min.] values of *Time B.E.*), reflecting cases in which the vessel enters the barrier before completion of the final approach turn, correspond to OB-GAL routes of configurations 1 and 4.
- For *Dist. B.E./Time B.E.* the worst performing simulation cases all correspond to OB-GAL routes.
- Configurations 1 and 4 display a comparably wide spread in values of *Dist. B.E.* and *Time B.E.* Comparing identical simulation cases (only differing in barrier configuration), there are only minor differences in *Dist. B.E./Time B.E.* values of configuration 1 and 4. Apparently, removal of the middle island has negligible effect on *Dist. B.E.* and *Time B.E.*
- Placing the barrier further eastward (comparing configurations 2/3 vs. 1/4) induces smaller values of *Dist. B.E./Time B.E.* for IB routes, and larger values of *Dist. B.E./Time B.E.* for OB routes.
- Configuration 2 exhibits the smallest spread in both *Dist. B.E.* and *Time B.E.* The difference in siting/alignment between configuration 2 and 3 has a positive effect on the *Dist. B.E./Time B.E.* of OB-HOU routes corresponding to configuration 3, but a negative effect on OB-GAL routes corresponding to configuration 3. Consequently, the spread of *Dist. B.E./Time B.E.* values of configuration 3 is larger than that of configuration 2.
- Configurations 1/4 exhibit large *Dist. B.E./Time B.E.* (combined with small *Dist. A.B./Time A.B.*) for IB routes, but small *Dist. B.E./Time B.E.* (combined with large *Dist. A.B./Time A.B.*) for OB routes.
- For configurations 2/3 there is more equality (smaller differences) between the magnitudes of *Dist. B.E./Time B.E.* and *Dist. A.B./Time A.B.* for both IB and OB routes.

Rudder Range I.B.

Figure 4.17 presents the *Rudder Range In Barrier* for all simulation cases, grouped by storm surge barrier configuration. The figure clearly highlights configuration-dependent differences in the magnitude and variability of rudder usage during the crossing segment.

Notable observations with regard to this assessment metric are as follows:

- For configurations 1/4, the largest *Rudder Range I.B.* corresponds to an OB-GAL route.
- Configurations 1/4 exhibit larger and more fluctuating *Rudder Ranges I.B.* compared to configurations 2/3. The *Rudder Ranges I.B.* of configurations 2/3 are notably smaller and less varying, indicating a systematically lower and more consistent steering demand across the simulated cases for these configurations. Apparently, placing the barrier further eastward (comparing configurations 2/3 vs. 1/4) causes there to be less rudder activity in the barrier (i.e. during the crossing segment), while the effect of removing the middle island (comparing configuration 1 vs. 4) is less pronounced.

Beam Clr. I.B.

Figure 4.18a presents the *Beam Clearance In Barrier* for all simulation cases, grouped by barrier configuration. The figure clearly highlights configuration-dependent differences in the minimum lateral clearances observed during the crossing segment.

Notable observations with regard to this assessment metric are as follows:

- Removal of the middle island (comparing configuration 1 vs. 4) has a positive effect on *Beam Clr. I.B.*, with configuration 4 exhibiting larger values for identical simulation cases (only differing in barrier configuration).
- *Beam Clr. I.B.* is influenced less by the placement further east (comparing configurations 2/3 vs. 4), but there is still a slight positive influence.
- The *Beam Clr. I.B.* values observed for configurations 2/3 are clearly higher than the values observed for configuration 1.
- The difference in siting/alignment between configuration 2 and 3 has minimal effect on *Beam Clr. I.B.* values.

Max. DA I.B.

Figure 4.18b presents the *Maximum Drift Angle In Barrier* for all simulation cases, grouped by barrier configuration. Notable observations with regard to this assessment metric are as follows:

- Configurations 1 and 4 each exhibit a single pronounced outlier for *Max. DA I.B.*, both of which correspond to an OB-GAL route.
- Besides the two isolated extreme cases, the spread of *Max. DA I.B.* values is quite comparable across configurations, suggesting similar variability in drift behavior during the crossing segment for the majority of simulations.
- Excluding the two outliers, it could be said that *Max. DA I.B.* is less influenced by geometry, and more dominated by environment.

Dist. A.B./Time A.B.

Figure 4.19 presents the *Distance After Barrier* (Figure 4.19a) and *Time After Barrier* (Figure 4.19b) for all simulation cases, grouped by barrier configuration. The paired plots show a consistent correspondence between spatial and temporal margins, with configurations exhibiting larger *Dist. A.B.* values also exhibiting larger *Time A.B.* values, and configurations exhibiting smaller *Dist. A.B.* values exhibiting smaller *Time A.B.* values. Given the metric definitions in Subsection 3.1.6, this is to be expected.

Notable observations with regard to these assessment metrics are as follows:

- For *Dist. A.B.* of configuration 2, IB routes perform slightly better than OB routes.
- Configurations 1 and 4 display a comparably wide spread in values of *Dist. A.B.* and *Time A.B.* Comparing identical simulation cases (only differing in barrier configuration), there are only minor differences in *Dist. A.B./Time A.B.* values of configuration 1 and 4. Apparently, removal of the middle island has negligible effect on *Dist. A.B.* and *Time A.B.*
- Placing the barrier further eastward (comparing configurations 2/3 vs. 1/4) induces smaller values of *Dist. A.B./Time A.B.* for OB routes, and larger values of *Dist. A.B./Time A.B.* for IB routes.
- Configuration 2 exhibits the smallest spread in both *Dist. A.B.* and *Time A.B.* The difference in siting/alignment between configuration 2 and 3 has a positive effect on the *Dist. A.B./Time A.B.* of IB-HOU routes corresponding to configuration 3, but a negative effect on IB-GAL routes corresponding to configuration 3. Consequently, the spread of *Dist. A.B./Time A.B.* values of configuration 3 is larger than that of configuration 2.
- Configurations 1/4 exhibit large *Dist. A.B./Time A.B.* (combined with small *Dist. B.E./Time B.E.*) for OB routes, but small *Dist. A.B./Time A.B.* (combined with large *Dist. B.E./Time B.E.*) for IB routes.
- For configurations 2/3 there is more equality (smaller differences) between the magnitudes of *Dist. A.B./Time A.B.* and *Dist. B.E./Time B.E.* for both IB and OB routes.

Overall

- The maneuvering behavior for configuration 2 is most predictable, exhibiting the narrowest distribution for almost all of the assessment metrics.
- Across the assessment metrics, OB-GAL routes are routinely among the worst performing, particularly for barrier configurations 1 and 4.
- Compared to all other assessment metrics, *Max. DA I.B.* is influenced less by geometry. With the exception of two outliers, it seems that environment dominates for *Max. DA I.B.* For all other assessment metrics differences in geometry are dominant over environment.

The descriptive analysis presented above shows that the developed assessment metrics are capable of capturing clear and systematic differences in navigational safety performance across the considered storm surge barrier configurations, and that these differences can be attributed to certain changes in geometry where applicable. Taken together, the results demonstrate that the selected metrics provide a coherent and sufficiently differentiated description of maneuvering outcomes across the simulated cases, thereby offering a robust basis for subsequent reflection on the assessment method and its application.

5

Discussion

This chapter discusses the results of this study by reflecting on both the developed quantitative nautical safety assessment method (as presented in Chapter 3) and its application to the Bolivar Roads case study (as presented in Chapter 4). The discussion explicitly distinguishes between limitations inherent to the assessment framework itself and limitations arising from its application to a specific real-world context. The chapter first adopts a critical, self-undermining perspective by examining the methodological and case-specific choices made and interpreting their implications for the validity and scope of the results. Building on this reflection, the chapter then proceeds to position the contribution of the developed method within the broader context of nautical safety assessment and storm surge barrier design, clarifying its intended use, added value, and relevance for early-stage design decision-making.

5.1. Limitations

This study has several limitations that frame the interpretation and applicability of its findings. Below, the limitations regarding the developed method's components are discussed, as well as the limitations regarding the manner in which the method was applied in the Bolivar Roads case study.

5.1.1. Methodological Choices

The assessment method developed and presented in this report is the outcome of a series of deliberate methodological choices. While these choices were necessary to ensure feasibility and internal consistency of the method, they also introduce limitations that directly influence the interpretation and robustness of the results. A critical reflection on these methodological decisions is therefore required to clarify the boundaries within which the findings should be understood.

One of the fundamental methodological choices concerns the scope of the developed framework. The method focuses exclusively on the maneuverability of a single vessel transiting a barrier system and does not account for traffic situations in which multiple vessels interact simultaneously. As a result, important aspects of nautical safety related to vessel-vessel interactions are excluded. In practice, encounters between vessels increase maneuvering complexity and may impose constraints that are not present during isolated transits. Hydrodynamic interactions between passing vessels can introduce critical risks, possibly leading to loss of controllability, collisions, or allisions with gate structures. Furthermore, the presence of other vessels may force ships to deviate from idealized approach routes, altering alignment and available maneuvering space. Because such interaction effects are outside the scope of the method, the results should be interpreted as representing single-vessel maneuvering demands only, with additional traffic-related risks requiring separate assessments. In addition, the framework deliberately isolates nautical safety performance and does not incorporate other design objectives such as cost, operational efficiency, or throughput, which must therefore be evaluated separately.

Another key methodological constraint concerns the spatial schematization of the navigational environment. The spatial representation used in the simulations necessarily reflects an anticipated future layout of the waterway. However, only an approximation of the future spatial configuration can be made at

early design stages. Actual future conditions may differ due to decisions by port authorities, changes in traffic patterns, or morphodynamic processes such as sediment transport and siltation. If such developments are not accurately reflected in the modeled schematization, relevant constraints on maneuvering space may be overlooked, potentially leading to overly optimistic or overly pessimistic assessments of nautical safety performance. Anchorage areas illustrate this limitation particularly clearly. These zones can significantly constrain available maneuvering space by introducing stationary obstacles (vessels) in the vicinity of the barrier, thereby influencing approach routes and navigational strategies. However, anchorage locations are often determined only after barrier design decisions have been made. For this reason, anchorage areas are not included as standard components of the spatial schematization. If their future locations are known for all barrier configurations considered in the assessment, the inclusion of anchorage areas in the spatial schematization would be advisable.

Environmental forcing and hydrodynamic effects constitute another area where methodological simplifications affect interpretation. Configuration-specific hydrodynamic current fields are not modeled as part of the framework due to time and resource constraints. Consequently, barrier-induced flow patterns that may negatively affect maneuverability are not explicitly captured. Visibility-related factors, such as fog or nighttime conditions, are likewise excluded, despite their known influence on nautical safety. These omissions mean that certain adverse conditions affecting real-world navigation are not represented in the simulations.

The method defines a limited number of “worst navigable” environmental scenarios to represent critical conditions. This approach assumes that if a configuration is navigable under these worst-case conditions, it will also be navigable under calmer conditions. However, the inverse is not necessarily true: a configuration that performs unsatisfactorily under worst-case conditions may still meet nautical safety requirements if operational constraints or procedures are imposed during such conditions. Moreover, because it is infeasible to cover all possible combinations of environmental parameters, some extreme but plausible scenarios may be excluded. As a result, conclusions regarding safety performance are contingent on the selected environmental scenario envelope.

Uncertainty is further introduced through the representation of design vessels. Only a limited number of representative vessels are considered, and future vessel dimensions and characteristics can only be approximated based on predictive studies and expert judgment. This limitation affects the generalizability of the results.

The reliance on fast-time ship maneuvering simulation models introduces constraints, as these models offer limited representation of human perception. For example, although (electronic) aids to navigation can be included in the spatial schematization, their beneficial effects are closely linked to pilot perception and decision-making, which are only partially represented in fast-time models. As a result, fast-time simulations are well suited for representing routine navigational operations and standard vessel maneuvers, but are poorly equipped to capture exceptional operational scenarios. Situations such as partially blocked gates following an allision or emergency diversion decisions involve human judgment under stress and context-dependent decision-making, which are more appropriately assessed using RTS. Consequently, the developed method is primarily applicable to normal operational navigation scenarios rather than to rare or emergency situations.

Vessel control in FTS is governed by autopilot algorithms, such that the framework implicitly evaluates the compatibility between barrier geometry and a specific control philosophy rather than human navigation in a general sense. While this ensures repeatability, it limits the extent to which adaptive human responses are captured, and any systematic over- or underestimation of control authority propagates directly into the assessment metrics. Within this simplified representation of human navigation and operational context, vessel trajectories follow assumed desired tracks informed by pilot experience. These tracks remain estimates, and actual navigation may differ due to traffic management measures or operational constraints imposed by authorities. In addition, depending on the capabilities of the selected FTS-model, design vessels may need to be represented by pre-calibrated vessel models rather than fully customized representations, potentially introducing discrepancies between the defined design vessel characteristics and simulated maneuvering behavior.

Finally, the quantitative nautical safety assessment metrics focus on measurable spatial, temporal, and control margins. While these metrics capture maneuvering feasibility, they do not account for comfort

or operability considerations that are often associated with perceived safety. Maneuvers that are physically feasible may still impose excessive accelerations or forces on crew, passengers, or equipment, which are not reflected in the current metrics and would require additional indicators and simulation capabilities. Moreover, while validation of the results involves expert judgment and pilot consultation, the developed assessment method does not prescribe how the quantitative metric outcomes should be used or interpreted within such validation sessions.

In addition to the methodological limitations discussed above, the multi-step, software-intensive nature of the framework introduces practical constraints, making the assessment process time-consuming and operationally inefficient.

Taken together, these methodological choices enable a structured and reproducible comparison of barrier configurations while simultaneously constraining the interpretation of the results. The findings should therefore be understood as relative indicators of single-vessel maneuvering demands within a defined modeling context, rather than as comprehensive or absolute measures of nautical safety.

5.1.2. Case Study Choices

In addition to the methodological choices discussed in Subsection 5.1.1, the results of the application of the developed method to the Bolivar Roads case are influenced by a series of case study-specific decisions. While these choices were made to ensure feasibility and consistency within the available data and resources, they introduce additional constraints that affect the interpretation and generalizability of the case-specific findings.

A first important case study choice concerns the modeled bathymetry in the spatial schematization. In the current bathymetry, shoals are present outside the dredged channel at several locations (see nautical chart shown in Figure 4.1 or Appendix B). However, as part of the adopted spatial schematization, an extended dredged channel was assumed, implicitly presuming that some of these existing shoals would be removed through future dredging. Whether such dredging will occur in practice is uncertain and may depend on operational or regulatory considerations. Consequently, the modeled navigational environment may offer greater maneuvering space than is available in reality, potentially leading to optimistic assessments of nautical safety performance.

Case-specific assumptions regarding the temporal scope of the input data further influence maneuvering outcomes. The simulations are based on one year of environmental and vessel traffic data, which provides a representative snapshot of typical operating conditions but does not capture long-term variability or rare extreme events outside this window. As a consequence, the assessment reflects current or near-term environmental and traffic conditions rather than forward-looking worst-case scenarios of environmental conditions or vessel characteristics expected in the future. As such, the results may underestimate maneuvering demands if environmental forces or vessel sizes evolve beyond those represented in the used data.

Environmental forcing in the case study was further simplified by applying only two environmental scenarios. While these conditions were selected to represent critical navigational situations, they cannot encompass the full range of wind and current combinations encountered at Bolivar Roads. Moreover, identical worst navigable conditions were applied to both origin-destination combinations (Houston and Galveston), despite differences in approach geometry, channel alignment, and exposure. This simplification may mask route-specific sensitivities and implies that the resulting performance differences are driven primarily by geometric configuration rather than by nuanced environmental effects.

The selection of design vessels represents another case-specific choice with direct implications for the results. Three design vessels were defined per origin-destination combination to represent dominant traffic categories. While this selection captures key vessel classes, it remains an abstraction of the full diversity of the traffic mix at Bolivar Roads. Consequently, the results reflect the behavior of selected representative vessels rather than the most demanding vessel that could realistically transit the barrier.

The representation of these design vessels in the simulation model introduces additional case-specific uncertainty. Design vessels were represented using pre-calibrated vessel models that did not perfectly match the defined design vessel characteristics. Although the discrepancies were small, differences in hydrodynamic behavior and control response may affect simulated trajectories and control margins.

Similarly, water depths used in the simulations were adjusted to fall within the calibration range of the vessel models, resulting in (minor) differences between measured and modeled depths. This adjustment affects under-keel clearance and hydrodynamic response, with potential implications for maneuverability.

Case-specific choices were also made regarding the definition of vessel approach routes. In the application to the Bolivar Roads case, desired vessel tracks were defined as long, channel-aligned approaches originating from the main dredged channel. While this ensured consistency across configurations, alternative approach geometries, such as shorter, off-axis, or curved approaches, were not explicitly represented, for example those that may occur when vessels depart from anchorage areas. Consequently, maneuvering demands associated with such approach routes are not captured in the case study results. More broadly, the application of the method to Bolivar Roads involves implicit assumptions regarding operational context. Pilotage practices, tug assistance policies, speed regimes, and traffic management measures are not explicitly modeled. While these factors play a significant role in real-world navigation, their exclusion reflects a deliberate focus on geometric and environmental influences rather than on operational risk mitigation.

The application of the method to the Bolivar Roads case did not fully adhere to all aspects of the idealized framework described in Chapter 3. Deviations occurred due to data availability, model limitations, and practical constraints, however, these were necessary to enable application of the method in a real-world context. Consequently, the findings should be interpreted as illustrative of the method's application under a specific set of assumptions, data constraints, and simplifications. While the case study provides valuable insight into the relative nautical safety performance of alternative barrier configurations, it does not constitute a definitive or exhaustive assessment of nautical safety at Bolivar Roads, nor does it imply direct transferability of quantitative results to other locations without careful consideration of local conditions.

5.2. Positioning of the Contribution

The limitations discussed in Section 5.1 clarify the boundaries within which the results of this thesis should be interpreted. Subsection 5.1.1 addressed limitations inherent to the developed assessment method itself, which remain applicable regardless of the case to which the method is applied. Subsection 5.1.2 subsequently focused on limitations arising from the application of the method to the Bolivar Roads case study, which constrain the interpretation and generalizability of the case-specific results. Together, these reflections establish a clear distinction between methodological constraints and application-specific choices, and, rather than undermining the relevance of the contribution, they delineate the conditions under which the results are valid. Against this background, this section reflects on the implications of these findings and positions the contribution of the developed method within the broader context of nautical safety assessment for storm surge barrier design.

Storm surge barrier design is inherently characterized by competing objectives, including flood protection, navigational safety, cost efficiency, operational performance, and environmental impact. Developing a single, all-encompassing method capable of optimizing across all these dimensions is therefore impractical. The method developed in this study does not attempt to resolve this broader optimization problem. Instead, it is deliberately positioned as an early-stage evaluation tool, enabling nautical safety considerations to be incorporated explicitly and quantitatively while configuration choices remain open. In current practice, barrier design and nautical safety evaluation are often performed sequentially, with safety assessments serving primarily as verification tools rather than as inputs to design development. Under this approach, configuration-specific navigational challenges may only become apparent once a design is already largely fixed, as illustrated by the Bolivar Roads case. Moreover, such analyses are often qualitative in nature and poorly suited for iterative design exploration. By contrast, the developed framework allows alternative barrier configurations to be compared systematically during the formative stages of design, using quantitative nautical safety assessment metrics, thereby shifting nautical safety assessment from a reactive to a proactive role within the design process.

The choice for fast-time ship maneuvering simulation is central to this positioning. Given the method's intended use in early design stages, fast-time simulation provides an appropriate balance between fidelity and efficiency, enabling systematic exploration of configuration alternatives within reasonable

time and resource constraints. Although fast-time models cannot capture the full complexity of human decision-making or rare emergency scenarios, increasing model fidelity at this stage, for example by employing real-time simulation, would significantly reduce the number of configurations that can be assessed and would therefore be inefficient for early-stage screening. The framework's reliance on standardized control behavior further reinforces its comparative nature: by evaluating vessel response under a consistent control philosophy, differences in performance can be attributed to configuration characteristics rather than to variations in human behavior. While this abstraction limits representation of adaptive pilot responses, it enables fair and reproducible comparison between alternatives and should therefore be regarded not as a weakness, but as a prerequisite for objective comparative assessment.

It is important to emphasize that the quantitative metrics used in the framework do not represent absolute measures of safety. Instead, they describe available maneuvering margins in spatial, temporal, and control dimensions. Nautical safety remains inherently subjective due to the role of human pilots, and no method can fully eliminate this subjectivity. However, by translating simulated vessel behavior into objectively reproducible metrics, the developed framework reduces reliance on purely qualitative judgment and provides a structured basis for informed expert evaluation. Even where absolute metric values are subject to uncertainty, due to modeling assumptions, data limitations, or case-specific simplifications, the relative differences between configurations remain informative. This relative validity is the most crucial aspect of the contribution. The framework is not intended to certify safety, but to support comparative reasoning: identifying configurations that are more, or less demanding from a maneuvering perspective.

A key implication of this philosophy is that the method evaluates intrinsic maneuvering demand rather than operational traffic management strategies. By focusing on single-vessel behavior under standardized conditions, the framework isolates the influence of geometry and environmental forcing on controllability. Aspects such as traffic-level risks, vessel scheduling, or dynamic operational measures are intentionally excluded. This does not imply that these aspects are unimportant; rather, they constitute separate layers of nautical risk that are more appropriately addressed once a configuration has been selected. In this context, configurations that do not meet nautical safety requirements under worst-case navigable conditions may still be acceptable if appropriate operational constraints or procedures are implemented, underscoring that the framework supports design discrimination while leaving room for operational risk mitigation.

The modular structure of the developed method further strengthens its positioning. Components such as hydrodynamic or morphodynamic modeling, anchorage representation, or alternative environmental forcing scenarios can be integrated as additional information becomes available or as design progresses. This flexibility allows the framework to evolve alongside a project, increasing fidelity where justified without abandoning the underlying comparative structure.

From a broader academic and professional perspective, the contribution of the developed framework can be understood in relation to existing approaches to storm surge barrier design and navigational safety assessment. Much of the literature on storm surge barriers frames these structures primarily as instruments for flood risk reduction, emphasizing hydraulic performance, reliability, and cost-benefit considerations, while navigational safety is typically acknowledged as an important but secondary constraint (Mooyaart & Jonkman, 2017). Historical design practice, exemplified by the development of the Delta Works, similarly reflects a strong emphasis on structural and hydraulic feasibility, while documentation of navigational safety considerations in a quantitative, configuration-comparative form remains limited in the open literature (Walraven et al., 2022). At the same time, research on vessel maneuverability and navigational space has clearly established that geometric constraints strongly govern controllability and alignment behavior (Burmeister, 2020), yet these insights are seldom operationalized in a systematic framework that supports comparison between alternative infrastructure layouts at early design stages. In professional practice, guideline-based approaches, such as those promoted by PIANC, provide essential baseline criteria for safe navigation but offer limited support for discriminating between competing barrier configurations under identical operational assumptions. Against this background, the framework developed in this study can be understood as occupying a complementary position: it does not replace hydraulic design methods, detailed real-time simulation, or established design guidelines, but extends existing concepts by enabling explicit, quantitative, and reproducible

comparison of nautical safety performance across alternative storm surge barrier configurations during early design stages. Capabilities that were previously largely absent from the design process.

Finally, the application of the developed method to the Bolivar Roads case demonstrates that, despite modeling simplifications and data constraints, the framework is capable of capturing meaningful differences in nautical safety performance between alternative barrier configurations using the defined metrics. The transferability of the results therefore lies primarily in the methodological approach and comparative logic, rather than in the absolute numerical values obtained for the case study. For the baseline configuration, the results are consistent with conclusions reported by Burkley et al. (2022), lending confidence to the framework's ability to reproduce previously identified qualitative trends. For alternative configurations, direct validation against existing studies was not possible; nevertheless, the method provides structured and transparent evidence of relative performance differences that would otherwise be difficult to quantify at this stage of design. At the same time, the case study highlights broader institutional and practical implications of applying the framework in practice. Although the individual tools required for implementation are available, their fragmented nature results in an inefficient workflow, helping to explain why quantitative nautical safety assessment is rarely applied systematically in early design stages. By exposing this gap, the developed framework calls attention to the potential value of better-integrated toolchains and underscores the need for clearer responsibility allocation between tool developers and infrastructure designers in ensuring that navigational safety is adequately addressed during design.

Taken together, the developed method occupies a distinct and valuable position within the landscape of nautical safety assessment approaches. It does not replace detailed, human-centered simulations or operational risk analyses, but complements them by enabling early-stage, configuration-specific comparison of maneuvering demands. In doing so, the framework directly addresses the previously identified absence of a systematic and reproducible methodology for configuration-specific nautical safety evaluation during early design stages. Within the clearly defined limitations discussed in Section 5.1, the framework provides capabilities that were previously unavailable, thereby contributing to more informed and transparent storm surge barrier design processes.

6

Conclusion

This chapter concludes the thesis by summarizing the main findings and explicitly answering the research questions formulated in Chapter 1. The conclusions focus on what has been achieved through the development of a quantitative framework for evaluating the nautical safety performance of storm surge barrier configurations during early-stage design, and through its application to the Bolivar Roads case study. By synthesizing the results presented in the preceding chapters, this chapter clarifies the contribution of the research without reintroducing methodological detail or revisiting limitations discussed earlier. The chapter first provides concise, research question-driven conclusions regarding the developed assessment method, its integration into a coherent framework, its application to a real-world case, and the use of its results in comparative nautical safety evaluation. It then outlines directions for future research, highlighting opportunities to further enhance the performance and applicability of the proposed framework.

6.1. Answers to the Research Questions

Below, the sub research questions are covered one by one.

What are the key analytical and conceptual components required for a method that evaluates the nautical safety performance of storm surge barrier configurations at early design stages?

This study concludes that a systematic evaluation of the nautical safety performance of storm surge barrier configurations requires a set of interrelated analytical and conceptual components that jointly translate barrier design characteristics into quantifiable maneuvering safety outcomes. At a conceptual level, the method is grounded in the recognition that, in the context of early-stage storm surge barrier design, nautical safety performance is most directly reflected in vessel maneuverability under constrained geometric and environmental conditions. Rather than attempting to predict accident probabilities or traffic-level risk, the framework focuses on maneuvering demand and available control margins, which are configuration-dependent quantities that represent necessary preconditions for safe navigation.

Analytically, a first essential component is a structured spatial schematization of the navigational environment. This component defines the geometric boundary conditions within which vessels operate, including barrier layout, navigable openings, approach and departure channels, and bathymetric constraints. Spatial schematization establishes the physical context that directly shapes alignment behavior, clearance margins, and recovery capability during barrier transits.

A second key component is the definition of representative design vessels and identification of the governing origin-destination combinations. These elements ensure that the assessment focuses on vessel types and routes that are most sensitive to barrier geometry and environmental forcing, thereby capturing the maneuvering demands that are critical for navigational safety.

Third, the method requires environmental forcing scenarios that represent critical navigational conditions. While exhaustive coverage of all possible conditions is impractical at early design stages, the

definition of representative worst-case navigable scenarios provides a consistent and transparent basis for comparative evaluation across alternative configurations.

Fourth, a suitable ship maneuvering simulation model is required to translate spatial and environmental inputs into vessel trajectories and control behavior. Fast-time simulation enables systematic and reproducible exploration of multiple design alternatives, making it particularly suitable for early design stages.

Finally, the method depends on a set of quantitative nautical safety assessment metrics that express maneuvering performance in terms of spatial, temporal, and control margins. These metrics provide objective, comparable indicators of maneuvering demand, enabling relative assessment of alternative barrier configurations.

Together, these components form a coherent analytical foundation for evaluating nautical safety performance in a structured and reproducible manner, specifically suited to early-stage storm surge barrier design, when configuration and siting decisions remain open to modification.

How can these components be integrated into a coherent and systematic framework for nautical safety assessment?

This study concludes that the analytical and conceptual components identified in sub-research question 1 can be integrated into a coherent and systematic framework by structuring the assessment process as a reproducible, configuration-specific workflow that links design inputs to quantitative nautical safety outcomes in a transparent manner.

At the core of the framework lies a stepwise assessment structure in which the identified components are integrated through an ordered sequence, and barrier configurations are evaluated under identical assumptions. Spatial schematization defines the geometric boundary conditions for each configuration, ensuring that differences in vessel behavior arise from design characteristics rather than inconsistent modeling choices. Within this spatial context, representative design vessels and governing origin-destination combinations are selected to capture the maneuvering demands most sensitive to barrier geometry.

Environmental forcing scenarios are then applied consistently across configurations to ensure comparability. By evaluating all configurations under the same set of critical navigational conditions, the framework enables relative performance differences to be attributed to configuration design rather than to external variability. This consistency is essential for systematic comparison at early design stages.

Ship maneuvering simulation provides the dynamic link between the defined inputs and vessel behavior. Fast-time simulation enables repeated, standardized evaluation of multiple configurations within the information and resource constraints characteristic of early design stages, generating time-dependent vessel trajectories and control actions in a computationally efficient manner. These simulation outputs are subsequently translated into quantitative nautical safety assessment metrics, which express maneuvering performance in terms of spatial, temporal, and control margins.

The integration of these elements into a single workflow ensures that nautical safety performance is assessed in a manner that is both physically grounded and analytically consistent. Importantly, the framework does not seek to produce absolute safety judgments. Instead, it enables relative, configuration-specific comparison by applying identical modeling assumptions and evaluation criteria across alternatives. In doing so, the framework provides a systematic and transparent basis for incorporating nautical safety considerations into early-stage storm surge barrier design and evaluation.

How can this framework be applied to a real-world case to evaluate its practical applicability and performance?

This study concludes that the practical applicability and performance of the developed framework can be evaluated by applying it to a real-world storm surge barrier case in which multiple alternative configurations are assessed under representative navigational conditions. In this thesis, the Bolivar Roads storm surge barrier serves as such a case, enabling the framework to be tested in a complex and operationally relevant setting.

Application of the framework to a real-world case begins with the practical translation of available site-specific information into the standardized inputs required by the method. This includes defining a spatial

schematization that reflects the navigational layout of the area, selecting representative design vessels and governing origin-destination combinations, and specifying environmental forcing scenarios relevant to the local context. These inputs are defined consistently across all configurations to ensure that observed differences in performance are attributable to design choices rather than to inconsistencies in modeling assumptions.

Ship maneuvering simulations are then conducted for each configuration and scenario, generating vessel trajectories and control behavior that reflect the interaction between vessel dynamics, environmental forcing, and barrier geometry. The resulting simulation outputs are processed using the defined quantitative nautical safety assessment metrics, allowing maneuvering performance to be evaluated in terms of spatial, temporal, and control margins.

The application to the Bolivar Roads case demonstrates that the framework can be implemented using available tools and data, and that it is capable of distinguishing between the nautical safety performance of alternative barrier configurations in a transparent, reproducible, and decision-relevant manner for early-stage design comparison. Although the resulting quantitative outcomes are case-specific and subject to the limitations discussed in Chapter 5, the case study confirms that the framework functions as intended: it translates complex navigational interactions into structured, comparable indicators that support early-stage design evaluation.

Accordingly, the real-world application demonstrates the framework's practical usability and illustrates its value as a systematic tool for assessing nautical safety performance in storm surge barrier design.

How can the results obtained from this framework be used to compare the nautical safety performance of multiple storm surge barrier configurations at early design stages?

This study concludes that the primary value of the framework's results lies in their use as structured, quantitative input for expert judgment and stakeholder deliberation, rather than as definitive or standalone safety determinations. By expressing vessel maneuvering behavior in terms of reproducible spatial, temporal, and control margins, the framework translates complex simulation outputs into indicators that can be consistently interpreted and discussed by maritime pilots, designers, and other stakeholders.

The comparative nature of the results enables stakeholders to identify how and where alternative barrier configurations differ in terms of maneuvering demand. These differences can be examined during pilot workshops or validation sessions, particularly at early design stages when configuration options are still under consideration. In such settings quantitative metric outcomes can provide a common reference point for discussing perceived difficulty, controllability, and operational acceptability, supporting informed dialogue by reducing reliance on purely qualitative impressions and by ensuring that comparisons between configurations are grounded in identical assumptions and scenarios.

Importantly, the results do not replace expert judgment. Nautical safety remains inherently subjective due to human decision-making during vessel navigation. Instead, the framework complements expert assessment by offering transparent and reproducible evidence that can be weighed alongside experiential knowledge. In this way, the results facilitate comparison of barrier configurations by structuring and informing pilot and stakeholder discussions, ultimately supporting more robust and defensible design decisions.

6.1.1. Synthesis

Now that the sub research questions have been answered, the main research question can be treated.

How can alternative storm surge barrier configurations be systematically evaluated in terms of their nautical safety performance during early-stage design?

This study concludes that alternative storm surge barrier configurations can be systematically evaluated in terms of their nautical safety performance by applying a configuration-specific, simulation-based assessment framework that translates barrier design characteristics into quantitative indicators of vessel maneuvering demand and supports structured expert judgment.

The developed approach enables systematic evaluation by integrating spatial schematization, representative design vessels, governing routes, and critical environmental scenarios into a consistent ana-

lytical workflow. Fast-time ship maneuvering simulation provides a reproducible means of generating vessel trajectories and control behavior for each configuration under identical assumptions, in a manner suited to the time and information constraints of early-stage design. These simulation outputs are subsequently expressed through quantitative nautical safety assessment metrics that describe spatial, temporal, and control margins during approach, transit, and departure phases. By applying the same scenarios and metrics across configurations, the framework ensures that observed differences in performance can be attributed to design choices rather than to inconsistencies in modeling inputs.

Crucially, the framework does not seek to determine absolute safety or predict accident likelihood. Instead, it supports comparative evaluation by revealing relative differences in maneuvering demand between configurations. These results provide a transparent and objective basis for identifying configurations that impose greater or lesser navigational challenges under defined conditions.

The systematic value of the approach lies not only in the quantitative comparison itself, but also in how the results are used. By presenting maneuvering performance in a structured and reproducible form, the framework facilitates informed discussion among maritime pilots, designers, and other stakeholders. In this role, the results serve as input for expert interpretation and deliberation, reducing reliance on purely qualitative judgment while acknowledging the inherent subjectivity of nautical safety.

Accordingly, alternative storm surge barrier configurations can be systematically evaluated by combining simulation-based analysis with quantitative metrics and structured expert engagement, enabling nautical safety considerations to be incorporated transparently and consistently into early-stage design decision-making.

6.2. Recommendations for Future Research

The discussion presented in Chapter 5 sheds light on a number of critical limitations. However, where limitations lie, so do possibilities for improvement. As such, the following section highlights recommendations for future research informed by the limitations presented in the previous chapter. Not all identified limitations affect the performance of the developed assessment method to the same extent. Future research efforts should therefore be prioritized toward extensions that are expected to yield the largest improvement in the physical realism, interpretability, and decision relevance of the framework, while preserving its suitability for early-stage design evaluation. The recommendations below focus on such high-impact improvements.

1. A first and most impactful direction for future research concerns the integration of configuration-specific hydrodynamic current modeling. In the proposed framework, environmental forcing is represented in a simplified manner, while barrier-induced flow patterns are not explicitly resolved. However, spatial variations in current magnitude and direction near storm surge barriers can have a pronounced effect on vessel controllability, alignment behavior, and required control effort. Coupling the assessment framework with hydrodynamic models that resolve configuration-dependent current fields would significantly enhance the physical realism of the simulated vessel behavior and the resulting assessment metrics. Such integration should be pursued in a modular manner, allowing hydrodynamic detail to be increased without compromising the comparative structure of the method. An extension toward morphodynamic modeling could further improve long-term representation of bathymetric effects on navigation.
2. A second high-impact research direction is the improved representation of human factors and pilot behavior through targeted use of real-time simulation. While fast-time simulation is appropriate for early-stage screening of multiple configurations, it cannot fully capture pilot perception, adaptive decision-making, or comfort-related considerations. Future research should explore hybrid approaches in which real-time simulation is used selectively to interpret, validate, or calibrate results obtained from fast-time simulation, particularly for marginal or extreme cases. This would strengthen the link between quantitative assessment metrics and expert judgment, without undermining the efficiency advantages of the developed framework.
3. A third recommendation concerns the expansion and refinement of the quantitative nautical safety assessment metrics. The current metrics focus on spatial, temporal, and control margins, which are essential indicators of maneuvering feasibility. However, future research could extend the metric set to better capture operability and comfort aspects of navigation, for example through

acceleration-based indicators or other measures reflecting dynamic vessel response. In addition, research into aggregated or multi-dimensional interpretation of metrics could support more intuitive comparison between configurations. One specific avenue for such metric refinement concerns the normalization of maneuvering demand relative to available spatial margins. For example, maximum drift angle within the barrier opening could be evaluated in relation to the available beam clearance, recognizing that a given drift angle does not pose the same level of navigational risk in a wide opening as it does in a constrained one. Such normalized indicators may improve comparability across configurations with different geometric characteristics and reduce the need for ad hoc interpretation of absolute metric values. The formulation and validation of these metrics would require close involvement of maritime pilots to ensure their operational relevance, thereby enhancing the decision relevance of the framework.

4. A fourth avenue for future research is the development of additional assessment layers addressing vessel-vessel interactions and traffic effects. The current framework deliberately focuses on single-vessel maneuvering demand, which is appropriate for early-stage configuration screening. Nevertheless, traffic interactions can be a dominant source of navigational risk in constrained waterways. Future research could explore how traffic-related effects can be incorporated as a complementary assessment layer, applied after initial configuration selection. This would allow the framework to retain its early-design focus while extending its applicability to later design stages and operational evaluations.
5. Finally, future research should address toolchain integration and workflow efficiency. Although the individual tools required to implement the framework are available, their fragmented use results in an inefficient and knowledge-intensive workflow. Improved interoperability between simulation, post-processing, and visualization tools would not directly change the physical accuracy of the method, but would substantially enhance its practical applicability and adoption in design practice. Research into integrated software environments or standardized data interfaces would therefore support broader and more consistent use of quantitative nautical safety assessment in (early-stage) storm surge barrier design.

Together, these research directions provide a focused agenda for advancing the developed framework. By prioritizing improvements that directly affect model performance and decision relevance, future work can build on the contribution of this thesis while maintaining the framework's core strength as a systematic tool for early-stage nautical safety evaluation.

References

- AASHTO. (2020). AASHTO General Design and Location Features. In *AASHTO LRFD Bridge Design Specifications (9th Edition)*.
- Amendola, J., Miura, L. S., Costa, A. H. R., Cozman, F. G., & Tannuri, E. A. (2020). Navigation in Restricted Channels Under Environmental Conditions: Fast-Time Simulation by Asynchronous Deep Reinforcement Learning. *IEEE Access*, 8, 149199–149213. <https://doi.org/10.1109/ACCESS.2020.3015661>
- Bakker, A. M. R., Rovers, D. L. T., & Mooyaart, L. F. (2025). Storm Surge Clusters, Multi-Peak Storms and Their Effect on the Performance of the Maeslant Storm Surge Barrier (The Netherlands). *Journal of Marine Science and Engineering*, 13(2), 298. <https://doi.org/10.3390/jmse13020298>
- BTS. (2025). Maritime and Inland Waterway Transportation. Retrieved September 16, 2025, from <https://www.bts.gov/topics/maritime-and-inland-waterway-transportation>
- Buckers, M. (2017, June). *Minimum entrance width for inland ports* [Master's thesis, Delft University of Technology].
- Burkley, G. B., Webb, D., & Pierce, J. J. (2022, November). *Maritime Implications for Commercial Ship Transits of the Proposed Houston Ship Channel Gate Complex* (tech. rep.). Locus.
- Burmeister, H.-C. (2020). Ensuring Navigational Safety and Mitigate Maritime Traffic Risks While Designing Port Approaches and Ship Maneuvering Areas. In *Handbook of Terminal Planning* (pp. 269–285). Springer Nature.
- Cozzoli, F., Smolders, S., Eelkema, M., Ysebaert, T., Escaravage, V., Temmerman, S., Meire, P., Herman, P. M., & Bouma, T. J. (2017). A modeling approach to assess coastal management effects on benthic habitat quality: A case study on coastal defense and navigability. *Estuarine, Coastal and Shelf Science*, 184, 67–82. <https://doi.org/10.1016/j.ecss.2016.10.043>
- Daniel, R. A., & Paulus, T. M. (2019, July). Managing accidents and failures of hydraulic structures. In M. Kaszynska (Ed.). MATEC Web of Conferences. <https://doi.org/10.1051/mateconf/201928408003>
- De Winter, R. (2018, May). *Designing Ships using Constrained Multi-Objective Efficient Global Optimization* [Master's thesis, Leiden University]. Retrieved November 18, 2025, from <https://www.researchgate.net/doi/10.13140/RG.2.2.21395.12328>
- Deltares. (2018, January). *Overview storm surge barriers* (tech. rep.). Deltares. Retrieved September 27, 2024, from https://kyst.dk/media/srwdyhnp/deltares_2018_overview_storm_surge_barriers_komprimeret.pdf
- Deltares. (2024, October). Two boat collisions in 24 hours highlight the importance of resilient hydraulic structures | Deltares. Retrieved December 13, 2024, from <https://www.deltares.nl/en/news/two-boat-collisions-in-24-hours-highlight-the-importance-of-resilient-hydraulic-structures>
- Dircke, P., Jongeling, T., & Jansen, P. (2011). Navigable Storm Surge Barriers for Coastal Cities: An Overview and Comparison. In *Climate Adaptation and Flood Risk in Coastal Cities*. Routledge. <https://www-taylorfrancis-com.tudelft.idm.oclc.org/chapters/edit/10.4324/9781849776899-10/navigable-storm-surge-barriers-coastal-cities-overview-comparison-piet-dircke-tom-jongeling-peter-jansen>
- Du, P., Ouahsine, A., & Sergent, P. (2018). Influences of the separation distance, ship speed and channel dimension on ship maneuverability in a confined waterway. *Comptes Rendus Mécanique*, 346(5), 390–401. <https://doi.org/10.1016/j.crme.2018.01.005>
- Eloot, K., Verwilligen, J., & Vantorre, M. (2007). A methodology for evaluating the controllability of a ship navigating in a restricted channel. *Archives of Civil and Mechanical Engineering*, 7(3), 91–104. [https://doi.org/10.1016/S1644-9665\(12\)60016-8](https://doi.org/10.1016/S1644-9665(12)60016-8)
- Feizabadi, S., Brannum, S. M., Ghodsian, M., Allahdadi, M. N., & Chaichitehrani, N. (2025). Evaluating the hydrodynamic and transport responses to storm surge barriers in a partially mixed Estuary: A case study of the Hudson–Raritan estuary. *Continental Shelf Research*, 295, 105567. <https://doi.org/10.1016/j.csr.2025.105567>

- Formela, K. (2020). Assessment of the Waterway Variant at the Design Stage in Multiple-criteria Approach. *International Journal on Marine Navigation and Safety of Sea Transportation*, 14(4), 1001–1004. <https://doi.org/10.12716/1001.14.04.27>
- Fossen, T. I. (2011). *Handbook of marine craft hydrodynamics and motion control*. Wiley.
- Friis-Hansen, P. (2008, September). Basic Modelling Principles for Prediction of Collision and Grounding Frequencies. https://www.iala.int/wiki/iwrap/images/2/2b/IWRAP_Theory.pdf
- GHPB. (2023a). Coastal Spine must balance storm protection with safe navigation and long-term economic vitality of the port of Houston. Retrieved July 31, 2025, from https://assets.noviams.com/novi-file-uploads/ghpb/images/Coastal_Barrier/EPCO_IkeDike_Brochure_Final_pdf_11_28_rev-13af9cd3.pdf
- GHPB. (2023b, February). The Greater Houston Port Bureau, Houston Pilots, and the Galveston-Texas City Pilots Present Results from Simulations on Proposed Gate Study by USACE. Retrieved September 20, 2024, from https://assets.noviams.com/novi-file-uploads/ghpb/PDFs-and-Documents/advocacy/cgpd_press_release__2_8_fa-032d0f16.pdf
- Gokarn, R. P. (2024). *A Study of Ship Manoeuvrability*. Springer Nature. Retrieved October 22, 2025, from <https://link.springer.com/10.1007/978-981-97-0625-9>
- Gong, I., Kim, Y., Kim, Y., Park, S., & Kang, N. (2007). Assessment of Shiphandling Difficulty for an Approach Channel of a Harbor. *Coasts and Ports 2007*. <https://search.informit.org/doi/10.3316/informit.811471602645535>
- Google. (2025). Bolivar Roads Google Maps. Retrieved September 16, 2025, from https://www.google.com/maps/place/Bolivar+Roads/@29.3801962,-94.8431809,12.04z/data=!4m6!3m5!1s0x863f75695bf28891:0xc60eeaec1befd924!8m2!3d29.3505133!4d-94.7526949!16s%2Fg%2F1tcwx2xq!5m1!1e4?entry=ttu&g_ep=EgoyMDI1MDkxMC4wIklXMDSoASAFQAw%3D%3D
- Gray, W. O., Waters, J. K., Blume, A. L., & Landsburg, A. C. (2003). Channel Design and Vessel Maneuverability: Next Steps. *Marine Technology and SNAME News*, 40(02), 93–105. <https://doi.org/10.5957/mt1.2003.40.2.93>
- Gucma, S., Gralak, R., & Przywarty, M. (2022). Generalized Method for Determining the Width of a Safe Maneuvering Area for Bulk Carriers at Waterway Bends. *Sustainability*, 14(11). <https://doi.org/10.3390/su14116706>
- Hallegatte, S., Green, C., Nicholls, R. J., & Corfee-Morlot, J. (2013). Future flood losses in major coastal cities. *Nature Climate Change*, 3(9), 802–806. <https://doi.org/10.1038/nclimate1979>
- Hassan, A. (2024). What We Know About the Francis Scott Key Bridge Collapse in Baltimore. *The New York Times*. Retrieved December 18, 2024, from <https://www.nytimes.com/2024/03/26/us/key-bridge-collapse-baltimore-what-to-know.html>
- Hutchison, B. L., Gray, D. L., & Mathai, T. (2003). Maneuvering Simulations – An Application to Waterway Navigability. https://glosten.com/wp-content/uploads/2015/03/2003-10-17-20_SNAME_ApplicationofManeuvering-Simulations-to-EvaluateImpact-of-Proposed-BridgeAlternatives.pdf
- IALA. (2022, June). IALA Guideline - G1058 The use of Simulation as a Tool for Waterway Design and AtoN Planning.
- Jiang, Y., Hou, X.-R., Wang, X.-G., Wang, Z.-H., Yang, Z.-L., & Zou, Z.-J. (2022). Identification modeling and prediction of ship maneuvering motion based on LSTM deep neural network. *Journal of Marine Science and Technology*, 27(1), 125–137. <https://doi.org/10.1007/s00773-021-00819-9>
- Jonkman, S. N., Mooyaart, L. F., Van Ledden, M., Stoeten, K., De Vries, P., Lendering, K., Van der Toorn, A., Willems, A., & Merrell, W. J. (2014). Reconnaissance Level Studies on a Storm Surge Barrier for Flood Risk Reduction in the Houston-Galveston Bay. *Coastal Engineering*, 34. <https://doi.org/10.9753/icce.v34.structures.46>
- Kind, J. (2024, September). *Kosten sluiten Maeslantkering voor de haven en scheepvaart* (tech. rep.). De Waterwerkers. <https://www.deltaprogramma.nl/documenten/2024/12/4/kosten-sluiten-maeslantkering-voor-de-haven-en-scheepvaart>
- Kluijver, M., Dols, C., Jonkman, S. N., & Mooyaart, L. F. (2019). Advances in the Planning and Conceptual Design of Storm Surge Barriers – Application to the New York Metropolitan Area. https://doi.org/10.18451/978-3-939230-64-9_033

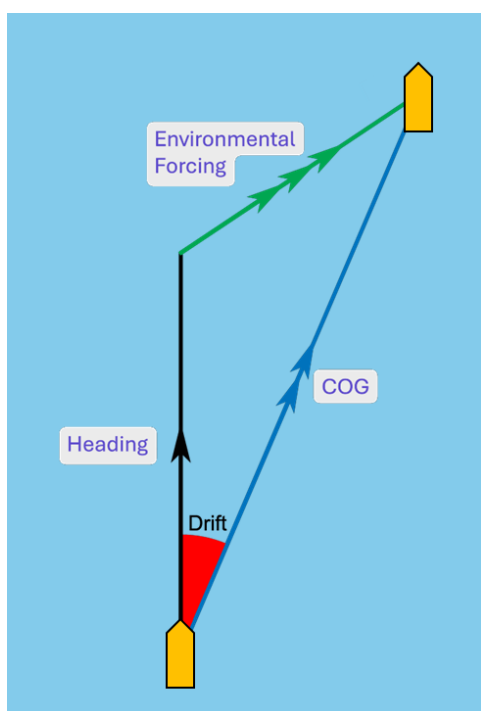
- Knott, M., & Winters, M. (2018). Ship and Barge Collisions with Bridges Over Navigable Waterways. https://coms.events/pianc-panama/data/full_papers/full_paper_46.pdf
- Lataire, E., Vantorre, M., Candries, M., Eloot, K., Verwilligen, J., Delefortrie, G., Chen, C., & Mansuy, M. (2018). Systematic Techniques for Fairway Evaluation based on Ship Manoeuvring Simulations. <https://www.pianc.org/wp-content/uploads/2024/02/34th-World-Congress-Panama-Full-Papers-Inland-Navigation-Part-1.pdf>
- Li, S., Meng, Q., & Qu, X. (2012). An Overview of Maritime Waterway Quantitative Risk Assessment Models. *Risk Analysis*, 32(3), 496–512. <https://doi.org/10.1111/j.1539-6924.2011.01697.x>
- Liu, J. (2020). Tests and Criteria for Inland Vessel Maneuverability. In *Mathematical Modeling of Inland Vessel Maneuverability Considering Rudder Hydrodynamics* (pp. 181–200). Springer Nature. https://doi.org/https://doi-org.tudelft.idm.oclc.org/10.1007/978-3-030-47475-1_7
- Liu, J., Hekkenberg, R., Rotteveel, E., & Hopman, H. (2015). Literature review on evaluation and prediction methods of inland vessel manoeuvrability. *Ocean Engineering*, 106, 458–471. <https://doi.org/10.1016/j.oceaneng.2015.07.021>
- Luo, W., & Zhang, Z. (2016). Modeling of ship maneuvering motion using neural networks. *Journal of Marine Science and Application*, 15(4), 426–432. <https://doi.org/10.1007/s11804-016-1380-8>
- Maljković, M., Pavić, I., Meštrović, T., & Perković, M. (2024). Ship Maneuvering in Shallow and Narrow Waters: Predictive Methods and Model Development Review. *Journal of Marine Science and Engineering*, 12(8). <https://doi.org/10.3390/jmse12081450>
- MARIN. (n.d.). Shipma 7.4 - User Guide.
- Marino, M., Cavallaro, L., Castro, E., Ester Musumeci, R., Martignoni, M., Roman, F., & Foti, E. (2023). New frontiers in the risk assessment of ship collision. *Ocean Engineering*, 274. <https://doi.org/10.1016/j.oceaneng.2023.113999>
- Merkens, J.-L., Reimann, L., Hinkel, J., & Vafeidis, A. T. (2016). Gridded population projections for the coastal zone under the Shared Socioeconomic Pathways. *Global and Planetary Change*, 145, 57–66. <https://doi.org/10.1016/j.gloplacha.2016.08.009>
- Montewka, J., Kujala, P., & Ylitalo, J. (2009). The quantitative assessment of marine traffic safety in the Gulf of Finland, on the basis of AIS data. *The Scientific Journals of the Maritime University of Szczecin*. <https://bibliotekanauki.pl/articles/360151.pdf>
- Mooyaart, L. F., Bakker, A. M. R., Van Den Bogaard, J. A., Rijcken, T., & Jonkman, S. N. (2023). Economic optimization of coastal flood defence systems including storm surge barrier closure reliability. *Journal of Flood Risk Management*, 16(3). <https://doi.org/10.1111/jfr3.12904>
- Mooyaart, L. F., & Jonkman, S. N. (2017). Overview and Design Considerations of Storm Surge Barriers. *Journal of Waterway, Port, Coastal, and Ocean Engineering*, 143(4), 06017001. [https://doi.org/10.1061/\(ASCE\)WW.1943-5460.0000383](https://doi.org/10.1061/(ASCE)WW.1943-5460.0000383)
- Mooyaart, L. F., Jonkman, S. N., De Vries, P., Van der Toorn, A., & Van Ledden, M. (2014). Storm Surge Barrier: Overview and Design Considerations. *Coastal Engineering*, 34. <https://doi.org/10.9753/icce.v34.structures.45>
- Neumann, B., Vafeidis, A. T., Zimmermann, J., & Nicholls, R. J. (2015). Future Coastal Population Growth and Exposure to Sea-Level Rise and Coastal Flooding - A Global Assessment. *PLOS ONE*, 10(3). <https://doi.org/10.1371/journal.pone.0118571>
- NOAA. (2023a). CO-OPS Current Station Data | Galveston Bay Entr Channel LB11. Retrieved September 17, 2025, from <https://tidesandcurrents.noaa.gov/cdata/DataPlot?id=g06010&bin=0&bdate=20250916&edate=20250917&unit=1&timeZone=UTC>
- NOAA. (2023b). Meteorological Observations | 8771341 Galveston Bay Entrance, North Jetty, TX. Retrieved September 17, 2025, from <https://tidesandcurrents.noaa.gov/met.html?id=8771341>
- NOAA. (2025a). Bolivar Roads Nautical Chart. <https://devgis.charttools.noaa.gov/pod/>
- NOAA. (2025b). CO-OPS Map - NOAA Tides & Currents. Retrieved September 16, 2025, from <https://tidesandcurrents.noaa.gov/map/>
- Orton, P., Fernald, S., Marcell, K., Brooks, B., Van Prooijen, B., & Chen, Z. (2019, December). *Surge Barrier Environmental Effects and Empirical Experience Workshop Report (Workshop Report)*. National Estuarine Research Reserve System Science Collaborative. <https://nerrssciencecollaborative.org/resource/surge-barrier-environmental-effects-and-empirical-experience-workshop-report>

- Orton, P., Ralston, D., Van Prooijen, B., Secor, D., Ganju, N., Chen, Z., Fernald, S., Brooks, B., & Marcell, K. (2023). Increased Utilization of Storm Surge Barriers: A Research Agenda on Estuary Impacts. *Earth's Future*, 11(3). <https://doi.org/10.1029/2022EF002991>
- PIANC. (2005, March). *PIANC - Design of Movable Weirs and Storm Surge Barriers* (tech. rep.). PIANC. Retrieved November 27, 2024, from http://www.anast.ulg.ac.be/doc/WG26_Final_Report_V6_2.pdf
- PIANC. (2014). *PIANC - Harbour Approach Channels Design Guidelines* (tech. rep.). PIANC.
- PIANC. (2022). *PIANC - Ship Dimensions and Data for Design of Marine Infrastructure* (tech. rep.). PIANC. <https://www.pianc.org/publication/ship-dimensions-and-data-for-design-of-marine-infrastructure/>
- Port of Galveston. (2025). Port of Galveston, TX - Official Website. Retrieved September 16, 2025, from <https://www.portofgalveston.com/>
- Port of Houston. (2025). Port Houston | The International Port of Texas. Retrieved September 16, 2025, from <https://porthouston.com/>
- Port of Texas City. (2025). The Port of Texas City. Retrieved September 16, 2025, from <https://tctr.com/>
- Qiy, N. M. (2008, June). *Approach channels: Risk- and simulation-based design* [PhD Thesis]. Delft University of Technology. <https://resolver.tudelft.nl/uuid:f892ffbc-e2f3-4fdb-bafb-b6d05006ea1b>
- Reuters. (2024). Mosel river in Germany closed to shipping after lock accident. Retrieved December 13, 2024, from <https://www.reuters.com/world/europe/mosel-river-germany-closed-shipping-after-lock-accident-2024-12-10/>
- Shigunov, V. (2020). Practical assessment of manoeuvrability in adverse conditions. *Ocean Engineering*, 203. <https://doi.org/10.1016/j.oceaneng.2020.107113>
- S&P Global. (2024, November). Sea-Web The Ultimate Marine Online Database. Retrieved September 16, 2025, from <https://www.spglobal.com/market-intelligence/en/solutions/sea-web-maritime-reference>
- Sutulo, S., & Guedes Soares, C. (2021). Review on Ship Manoeuvrability Criteria and Standards. *Journal of Marine Science and Engineering*, 9(8). <https://doi.org/10.3390/jmse9080904>
- Thomas, B. S., & Sclavounos, P. D. (2007). Optimal-control theory applied to ship maneuvering in restricted waters. *Journal of Engineering Mathematics*, 58, 301–315. <https://doi.org/10.1007/s10665-006-9130-6>
- Tian, K., Wen, Y.-Q., Zhu, M., Lei, T., Wang, S.-Y., & Huang, Y.-M. (2025). Hybrid modeling and online prediction of 4-DOF ship maneuvering motion in disturbed waters. *Ocean Engineering*, 341. <https://doi.org/10.1016/j.oceaneng.2025.122566>
- Trace-Kleeberg, S., Haigh, I. D., Walraven, M., & Gourvenec, S. (2023). How should storm surge barrier maintenance strategies be changed in light of sea-level rise? A case study. *Coastal Engineering*, 184. <https://doi.org/10.1016/j.coastaleng.2023.104336>
- USACE. (2021a, August). *Appendix D-22: Cost Engineering Report* (tech. rep.). USACE. Retrieved November 26, 2024, from https://www.swg.usace.army.mil/Portals/26/CTX_MR_AppendixD_Annex22%20%28MM%20Cost%20Summary%29_1.pdf
- USACE. (2021b, August). *Coastal Texas Protection and Restoration Feasibility Study - Executive Summary* (tech. rep.). USACE. Retrieved November 11, 2024, from https://www.swg.usace.army.mil/Portals/26/Coastal%20TX%20Executive%20Summary_FINAL_20210827.pdf
- USACE. (2021c, August). *Coastal Texas Protection and Restoration Feasibility Study Final Report* (tech. rep.). USACE. https://www.swg.usace.army.mil/Portals/26/Coastal%20TX%20Protection%20and%20Restoration%20FINAL%20Feasibility%20Report_20210827.pdf
- USACE. (2025, August). *Bolivar Roads Hydrographic Survey* (tech. rep.). USACE. https://www.swg.usace.army.mil/Portals/26/Missions/Operations/Navigation/HydroSurveyData/02_GTCH/GA/GA_04_IBC.pdf
- Vader, H., Bakker, A. M. R., Jonkman, S. N., Van den Boomen, M., Van Baaren, E., & Diermanse, F. L. M. (2023). A framework for assessing the remaining life of storm surge barriers. *Structure and Infrastructure Engineering*, 20(12), 2022–2034. <https://doi.org/10.1080/15732479.2023.2177874>
- Van Ledden, M., Lansen, A., De Ridder, H., & Edge, B. (2012). Reconnaissance Level Study Mississippi Storm Surge Barrier. *Coastal Engineering*, (33). <https://doi.org/10.9753/icce.v33.structures.69>

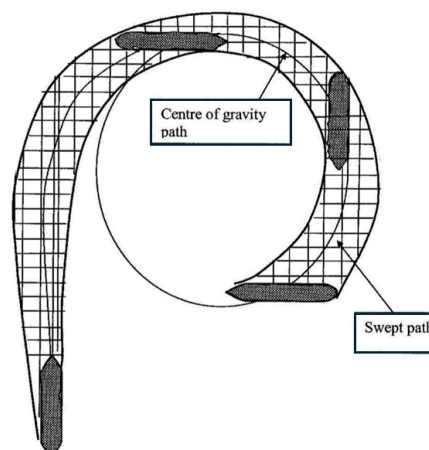
- Vantorre, M., Eloat, K., Delefortrie, G., Lataire, E., Candries, M., & Verwilligen, J. (2017, April). Maneuvering in Shallow and Confined Water (J. Carlton, P. Jukes, & Y. S. Choo, Eds.). <https://doi.org/https://doi-org.tudelft.idm.oclc.org/10.1002/9781118476406.emoe006>
- Verdugo, I., Atienza, R., Cal, C., Iribarren, J. R., Pecharroman, L., & Ayuso, C. (2018). Towards a Complete Design of the Manoeuvring Areas Additional Factors Involved in the Detailed Design.
- Wakita, K., Maki, A., Umeda, N., Miyauchi, Y., Shimoji, T., Rachman, D. M., & Akimoto, Y. (2022). On neural network identification for low-speed ship maneuvering model. *Journal of Marine Science and Technology*, 27, 772–785. <https://doi.org/10.1007/s00773-021-00867-1>
- Walraven, M., Vrolijk, K., & Kothuis, B. (2022). Design, maintain and operate movable storm surge barriers for flood risk reduction. In *Coastal Flood Risk Reduction* (pp. 271–286). Elsevier. <https://doi.org/https://doi-org.tudelft.idm.oclc.org/10.1016/B978-0-323-85251-7.00020-2>
- Wang, Z., Kim, J., & Im, N. (2023). Non-parameterized ship maneuvering model of Deep Neural Networks based on real voyage data-driven. *Ocean Engineering*, 284. <https://doi.org/10.1016/j.oceaneng.2023.115162>
- Xiao, F., Ligteringen, H., Van Gulijk, C., & Ale, B. (2014). Comparison study on AIS data of ship traffic behavior. *Ocean Engineering*, 95, 84–93. <https://doi.org/10.1016/j.oceaneng.2014.11.020>
- Zagonjoli, M., Baart, F., Ten Hove, D., Hermans, M., Van Sloten, J., Nelisse, M., & Van de Laar, P. (2024, March). *Aanvaarrisico en -belasting - Protocol voor de verwerking van AIS-data* (tech. rep.). Kennisprogramma Natte Kunstwerken. https://www.nattekunstwerkenvandetoekomst.nl/wp-content/uploads/2024/03/KpNK-2023-KV1.3-kunstwerk-b003_KENNISBIJDRAGE_Protocol-verwerking-AIS-data-aanvaarrisico-en-belastingen-DEF_20240320.pdf
- Zhang, M., Kujala, P., Musharraf, M., Zhang, J., & Hirdaris, S. (2023). A machine learning method for the prediction of ship motion trajectories in real operational conditions. *Ocean Engineering*, 283. <https://doi.org/10.1016/j.oceaneng.2023.114905>



Physical Maneuvering Indicators



(a) Heading, course over ground, and drift angle.



(b) Swept path.

Figure A.1: Physical maneuvering indicators.

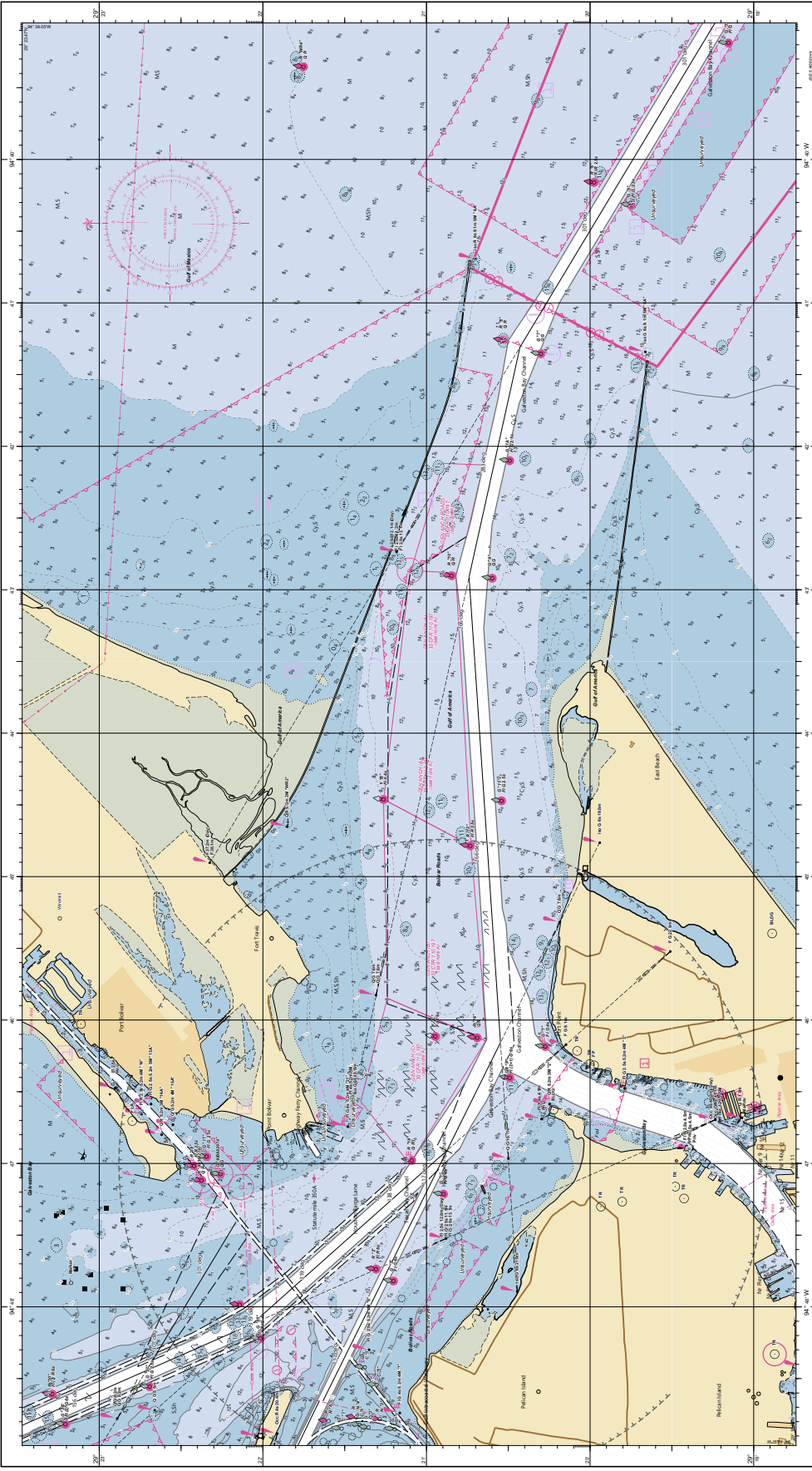
B

Bolivar Roads Nautical Chart

Bolivar Roads Nautical Chart

WGS 84

UNITS IN METERS



WGS 84
For more information, visit www.noaa.gov



INTERNATIONAL CHARTS OFFICE (ICHO)
 1:50,000 Scale
 ICHO Chart No. 11000
 ICHO Chart No. 11000
 ICHO Chart No. 11000
 ICHO Chart No. 11000

NOAA
 National Oceanic and Atmospheric Administration
 1:50,000 Scale
 NOAA Chart No. 11000
 NOAA Chart No. 11000
 NOAA Chart No. 11000

NOAA
 National Oceanic and Atmospheric Administration
 1:50,000 Scale
 NOAA Chart No. 11000
 NOAA Chart No. 11000
 NOAA Chart No. 11000

NOAA
 National Oceanic and Atmospheric Administration
 1:50,000 Scale
 NOAA Chart No. 11000
 NOAA Chart No. 11000
 NOAA Chart No. 11000

NOAA
 National Oceanic and Atmospheric Administration
 1:50,000 Scale
 NOAA Chart No. 11000
 NOAA Chart No. 11000
 NOAA Chart No. 11000

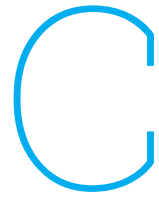
NOAA
 National Oceanic and Atmospheric Administration
 1:50,000 Scale
 NOAA Chart No. 11000
 NOAA Chart No. 11000
 NOAA Chart No. 11000

NOAA
 National Oceanic and Atmospheric Administration
 1:50,000 Scale
 NOAA Chart No. 11000
 NOAA Chart No. 11000
 NOAA Chart No. 11000

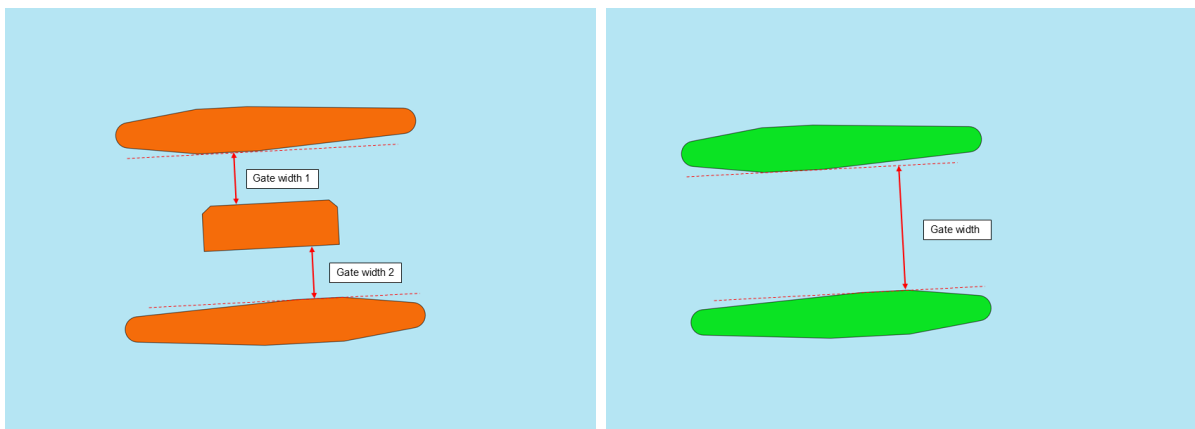
NOAA
 National Oceanic and Atmospheric Administration
 1:50,000 Scale
 NOAA Chart No. 11000
 NOAA Chart No. 11000
 NOAA Chart No. 11000

UNITS IN METERS

A graphical scale bar indicating distances in meters, ranging from 0 to 1000 meters.



Geometric Barrier Design Parameters



(a) Double gate barrier design.

(b) Single gate barrier design.

Figure C.1: Geometric parameter visualization: gate width.



(a) An example alignment.

(b) Another example alignment.

(c) One more example alignment.

Figure C.2: Geometric parameter visualization: alignment. Gate width and siting of the barriers are identical across the figures.

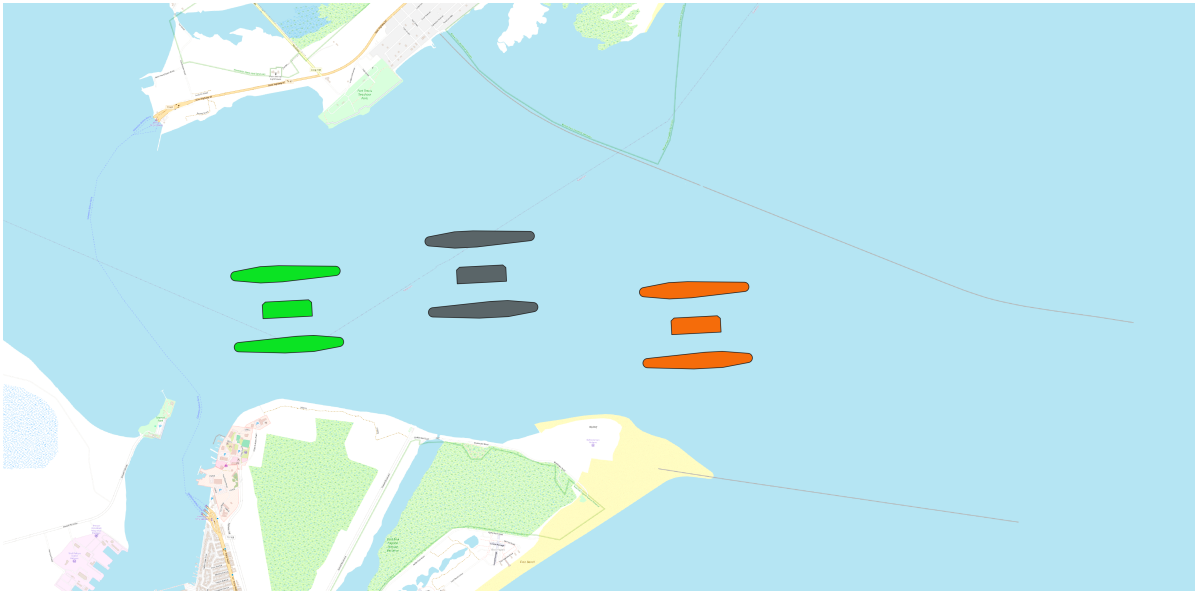


Figure C.3: Geometric parameter visualization: siting. Gate width and alignment are identical across the barriers.

D

Wind Data Bolivar Roads 2023

In all figures presented below, the wind direction is the direction from which the wind blows.

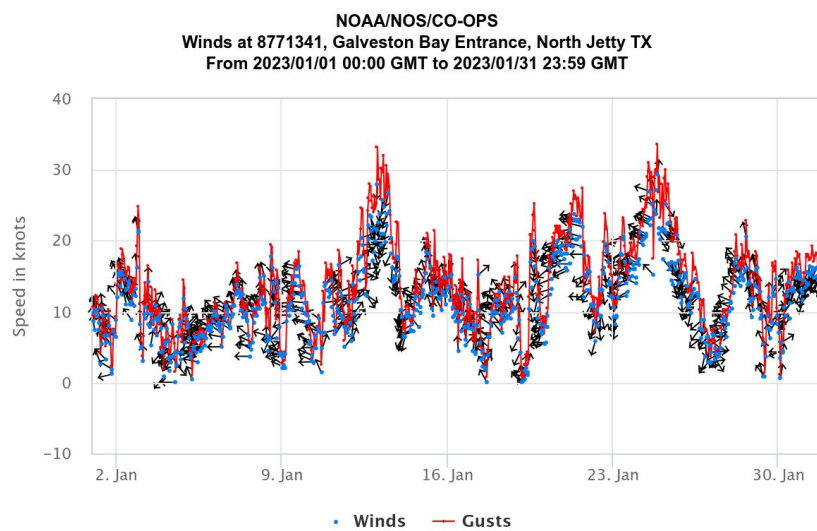


Figure D.1: Speed and direction of measured winds, January 2023 (NOAA, 2023b).

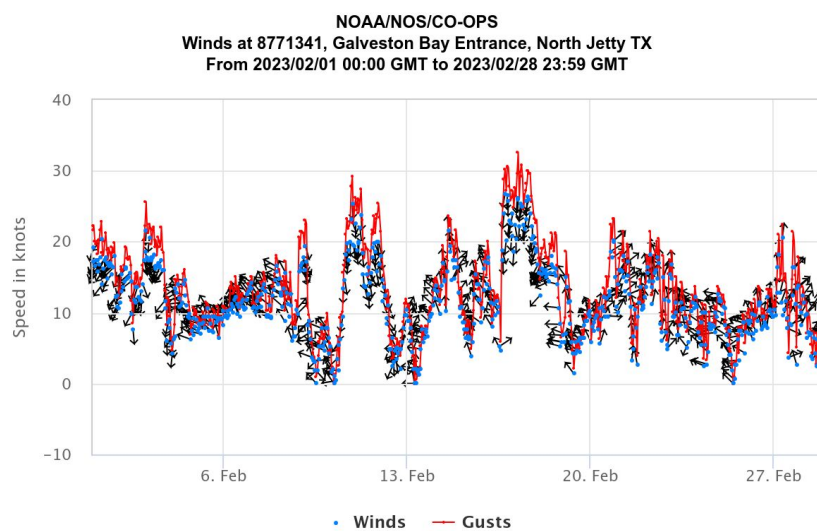


Figure D.2: Speed and direction of measured winds, February 2023 (NOAA, 2023b).

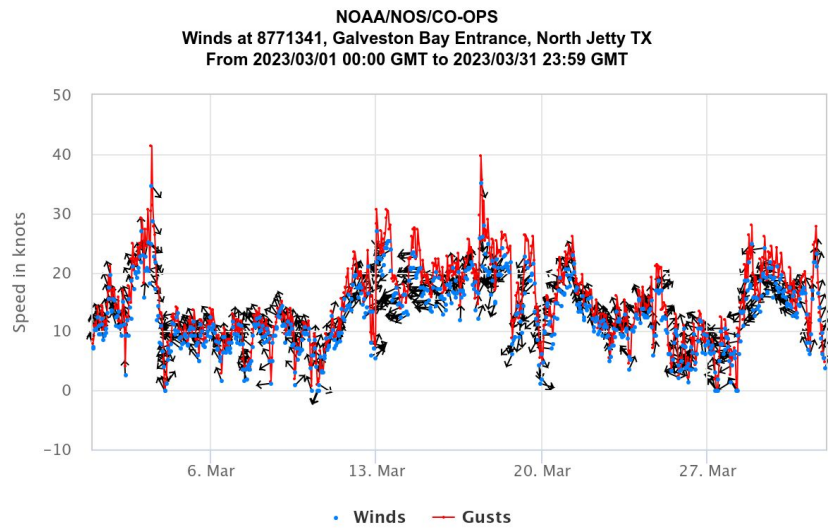


Figure D.3: Speed and direction of measured winds, March 2023 (NOAA, 2023b).

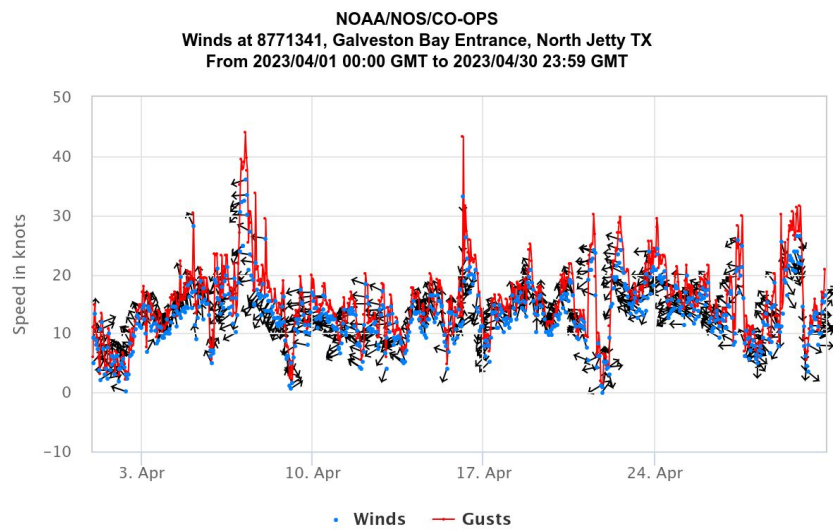


Figure D.4: Speed and direction of measured winds, April 2023 (NOAA, 2023b).

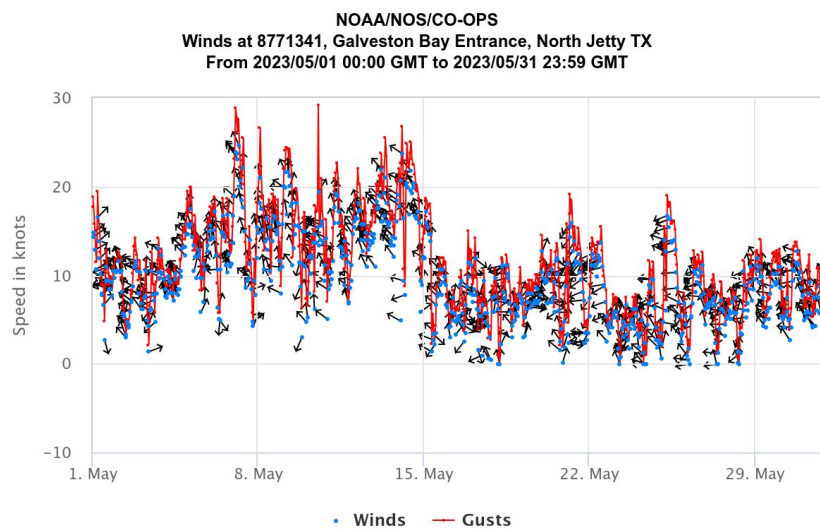


Figure D.5: Speed and direction of measured winds, May 2023 (NOAA, 2023b).

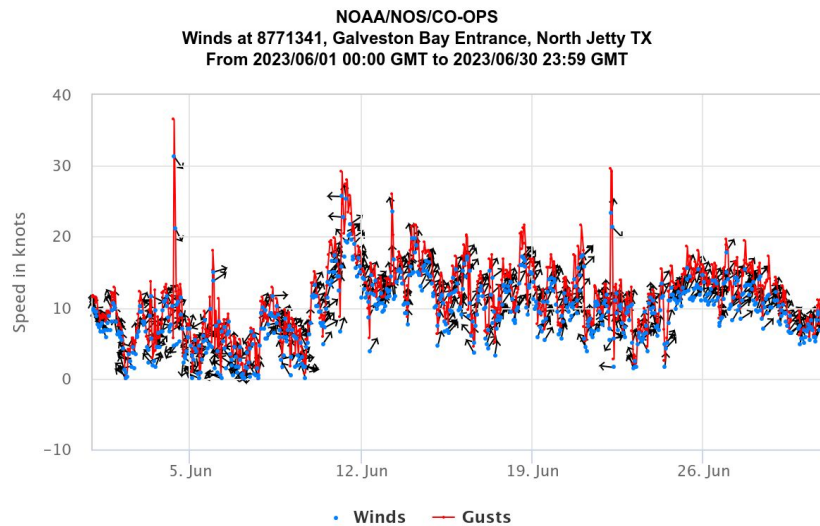


Figure D.6: Speed and direction of measured winds, June 2023 (NOAA, 2023b).

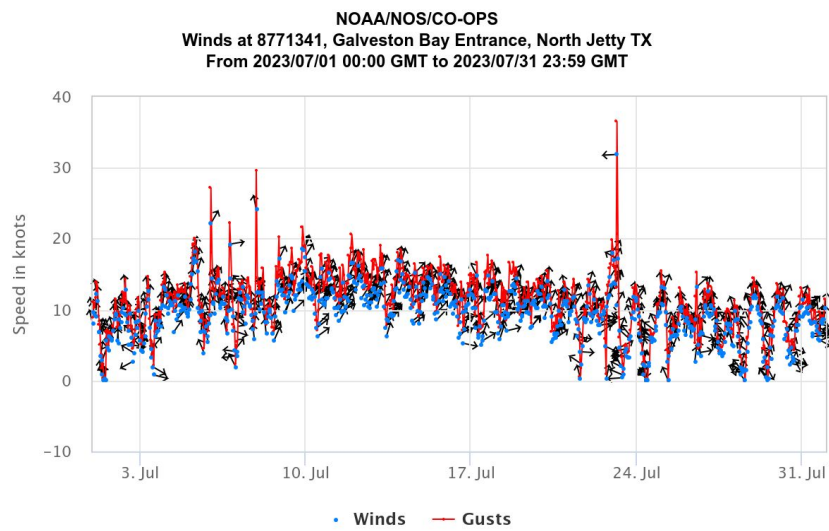


Figure D.7: Speed and direction of measured winds, July 2023 (NOAA, 2023b).

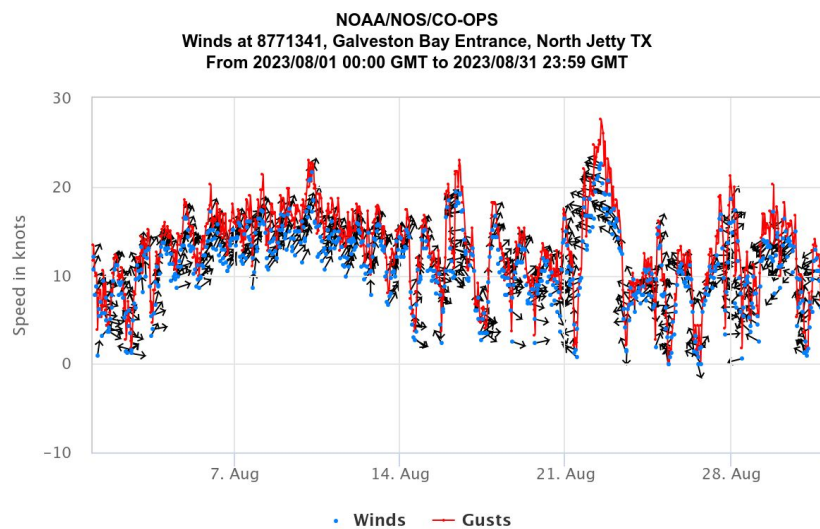


Figure D.8: Speed and direction of measured winds, August 2023 (NOAA, 2023b).

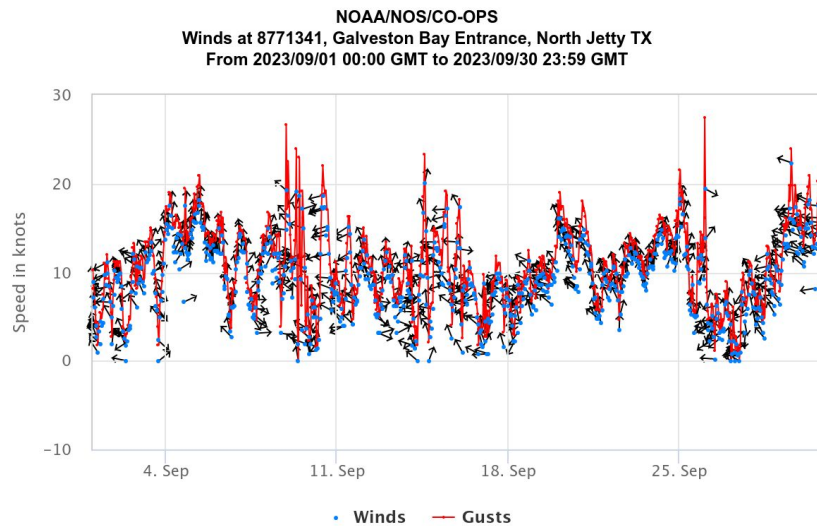


Figure D.9: Speed and direction of measured winds, September 2023 (NOAA, 2023b).

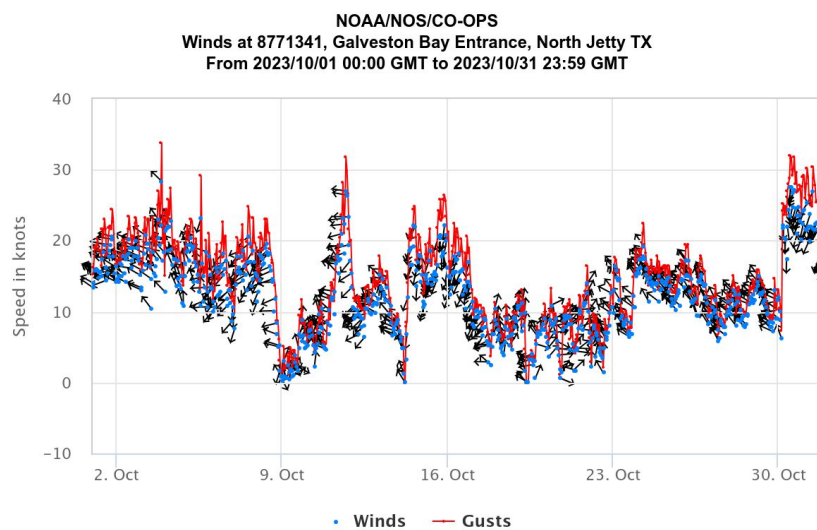


Figure D.10: Speed and direction of measured winds, October 2023 (NOAA, 2023b).

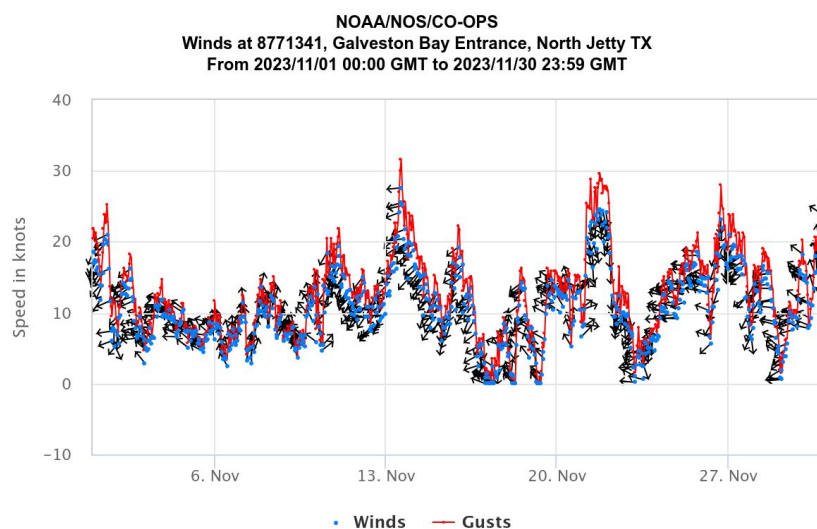


Figure D.11: Speed and direction of measured winds, November 2023 (NOAA, 2023b).

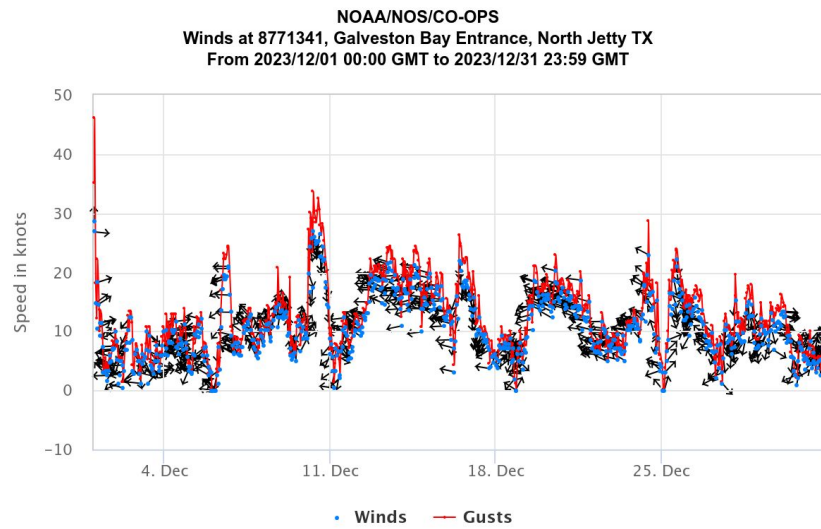


Figure D.12: Speed and direction of measured winds, December 2023 (NOAA, 2023b).



Current Data Bolivar Roads 2023

In all figures presented below, the current direction is the direction to which the current flows.

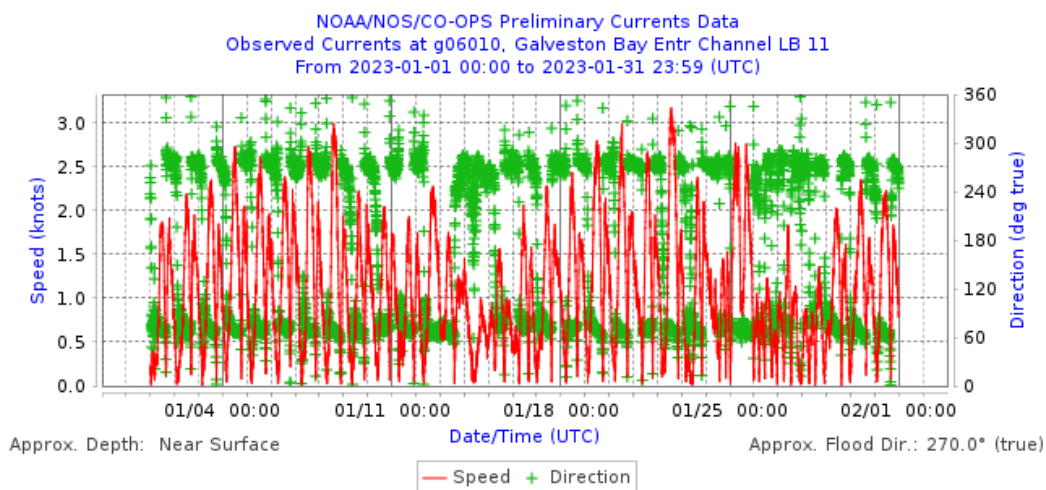


Figure E.1: Speed and direction of measured currents, January 2023 (NOAA, 2023a).

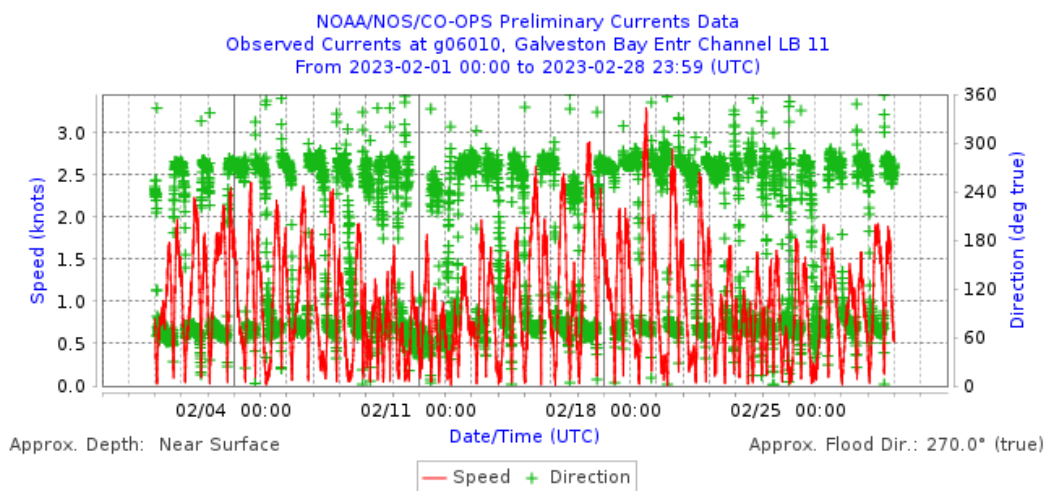


Figure E.2: Speed and direction of measured currents, February 2023 (NOAA, 2023a).

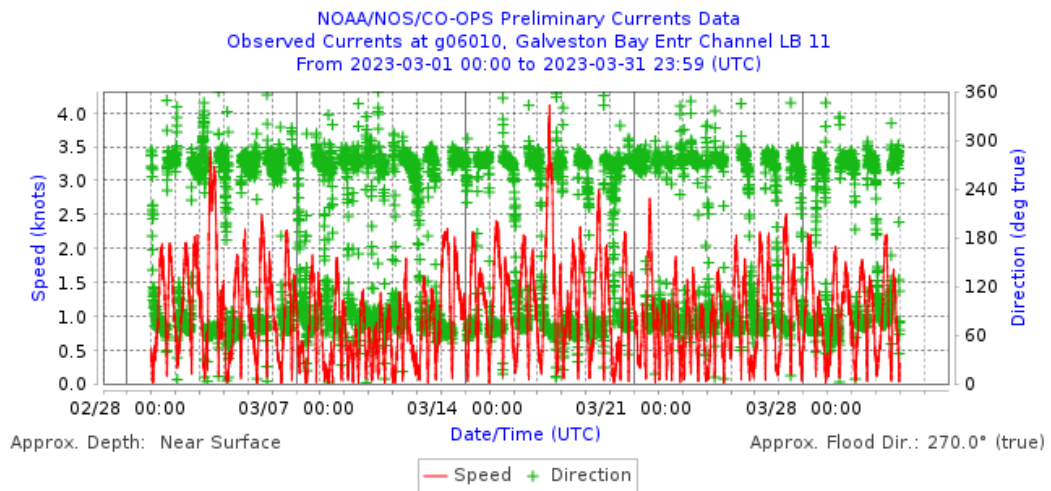


Figure E.3: Speed and direction of measured currents, March 2023 (NOAA, 2023a).

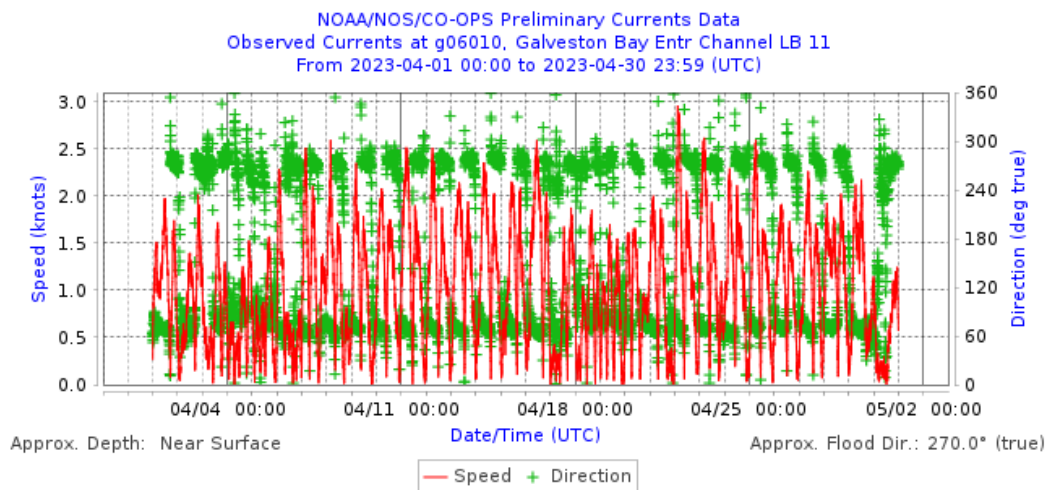


Figure E.4: Speed and direction of measured currents, April 2023 (NOAA, 2023a).

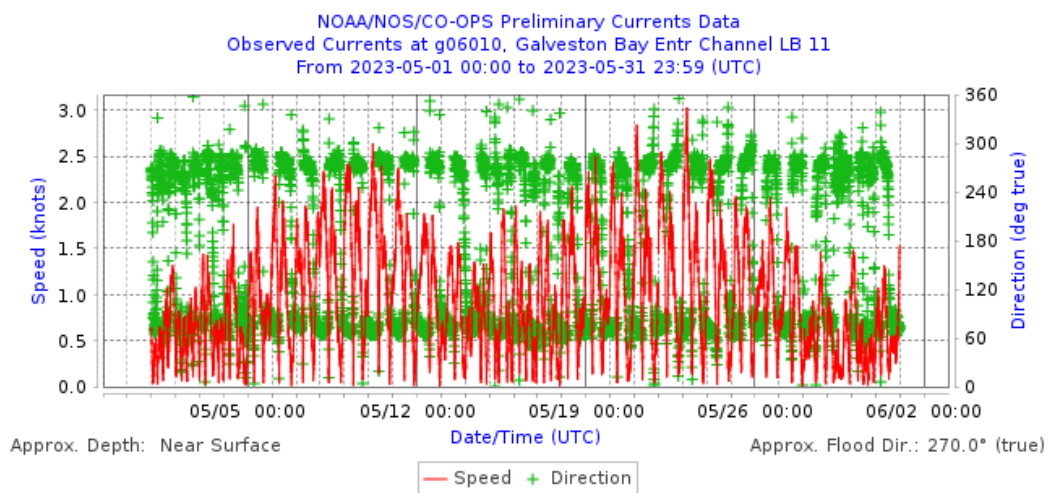


Figure E.5: Speed and direction of measured currents, May 2023 (NOAA, 2023a).

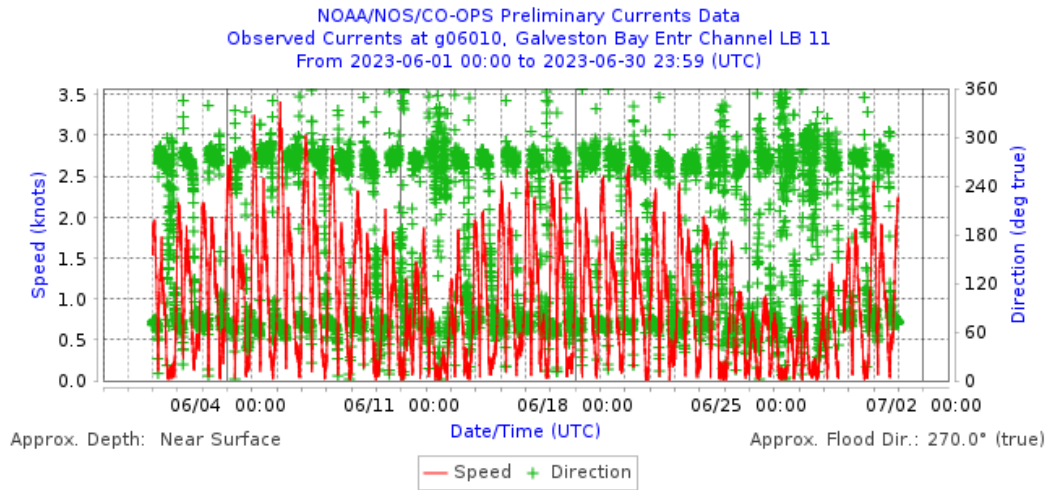


Figure E.6: Speed and direction of measured currents, June 2023 (NOAA, 2023a).

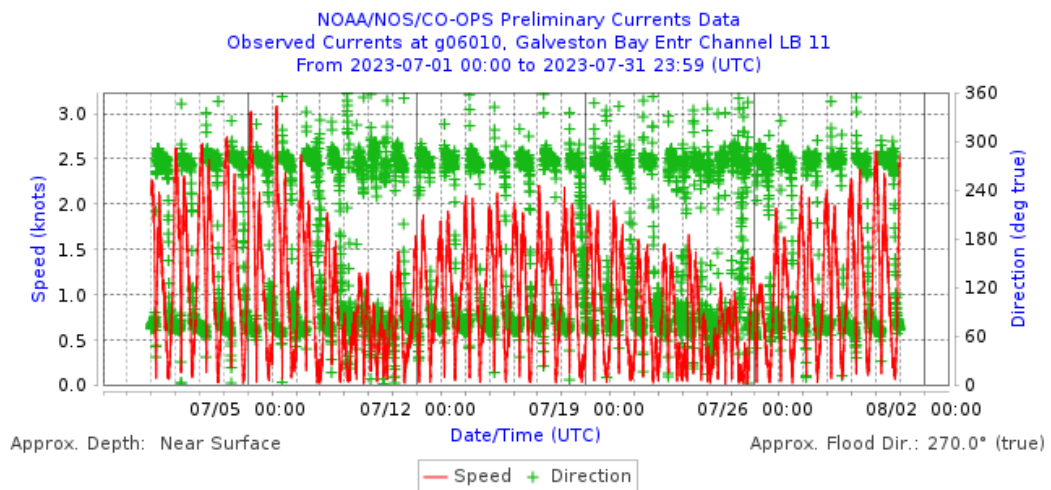


Figure E.7: Speed and direction of measured currents, July 2023 (NOAA, 2023a).

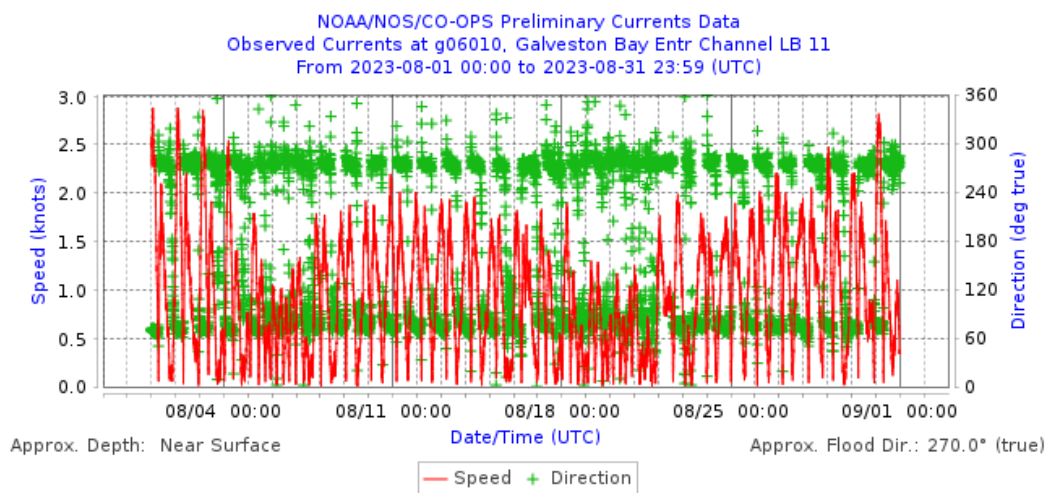


Figure E.8: Speed and direction of measured currents, August 2023 (NOAA, 2023a).

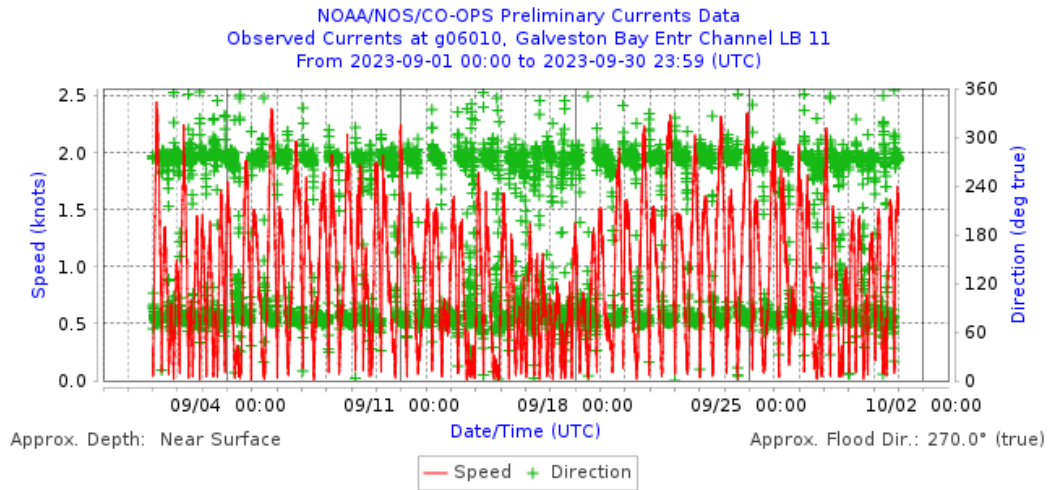


Figure E.9: Speed and direction of measured currents, September 2023 (NOAA, 2023a).

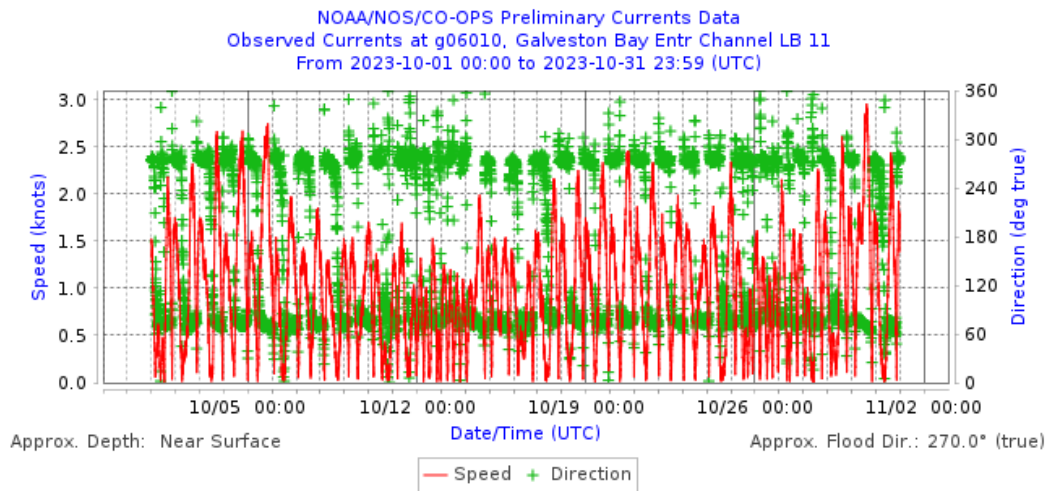


Figure E.10: Speed and direction of measured currents, October 2023 (NOAA, 2023a).

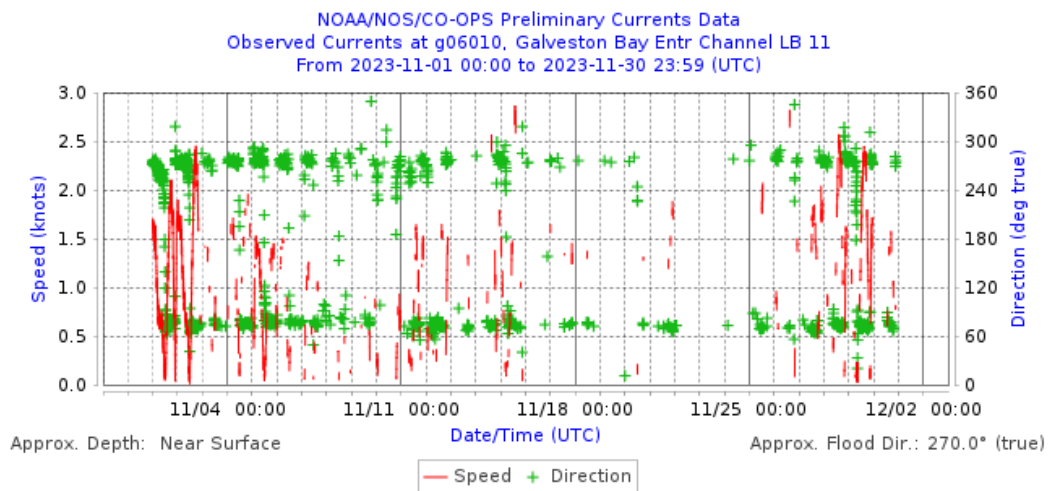


Figure E.11: Speed and direction of measured currents, November 2023 (NOAA, 2023a).

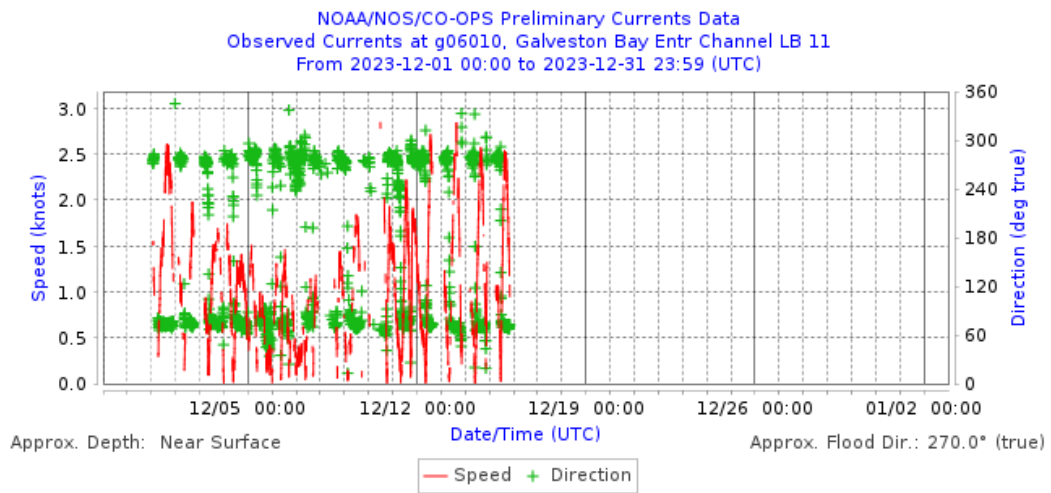


Figure E.12: Speed and direction of measured currents, December 2023 (NOAA, 2023a).

F

Design Vessels Bolivar Roads



Figure F.1: Design vessel: Houston, container, MMSI 215196000.



Figure F.2: Design vessel: Houston, tanker, MMSI 303294000.



Figure F.3: Design vessel: Houston, ro-ro vessel, MMSI 403532001.



Figure F.4: Design vessel: Galveston, container, MMSI 209444000.



Figure F.5: Design vessel: Galveston, tanker, MMSI 319095200.



Figure F.6: Design vessel: Galveston, cruise ship, MMSI 311000396.

G

Supplemental SHIPMA Set-Up Figures

G.1. Current Fields

Configuration 2

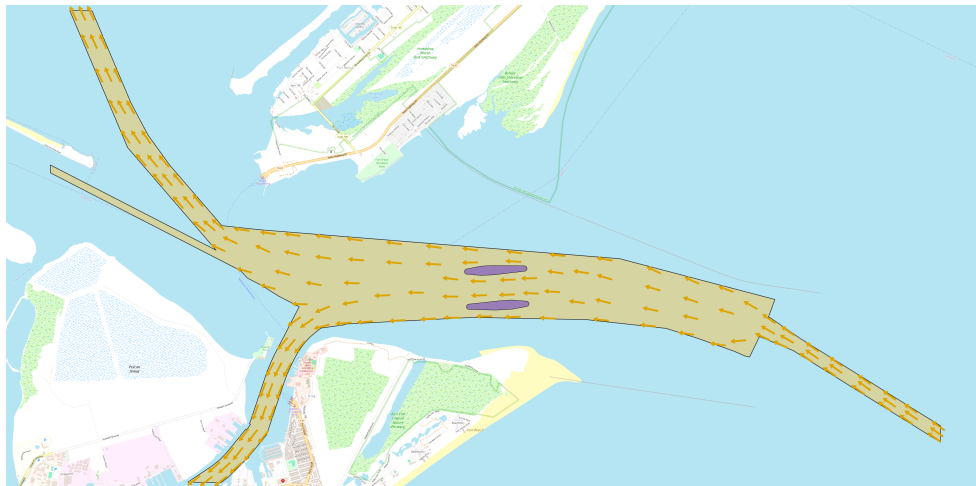


Figure G.1: Current field: flood current, inbound vessels, configuration 2; (from QGIS).

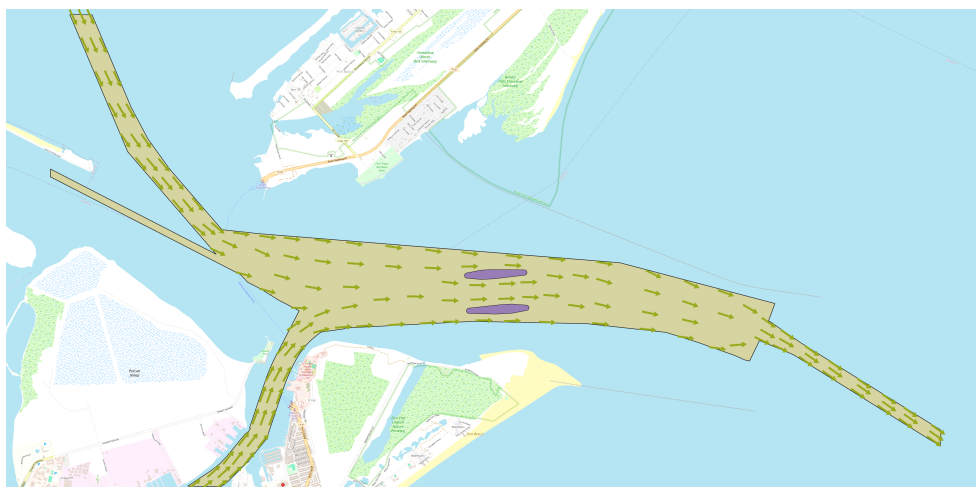


Figure G.2: Current field: ebb current, outbound vessels, configuration 2; (from QGIS).

Configuration 3

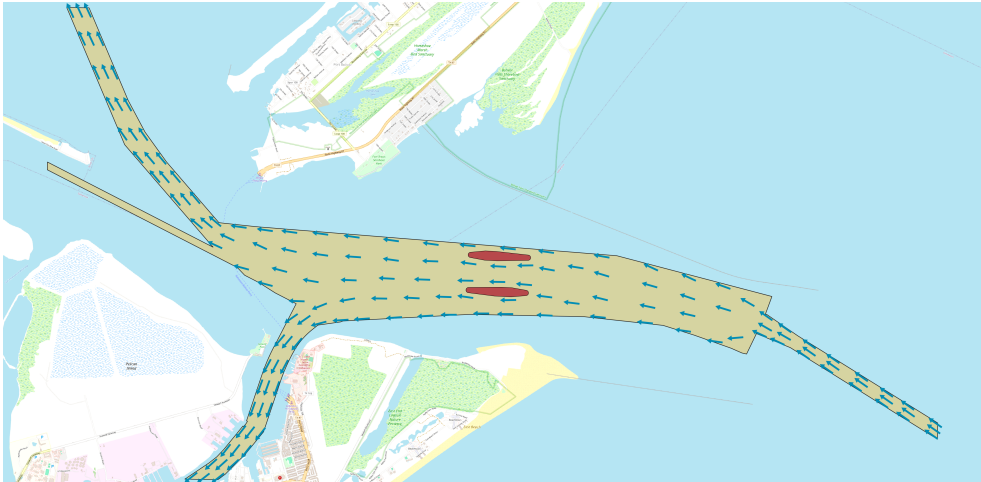


Figure G.3: Current field: flood current, inbound vessels, configuration 3; (from QGIS).

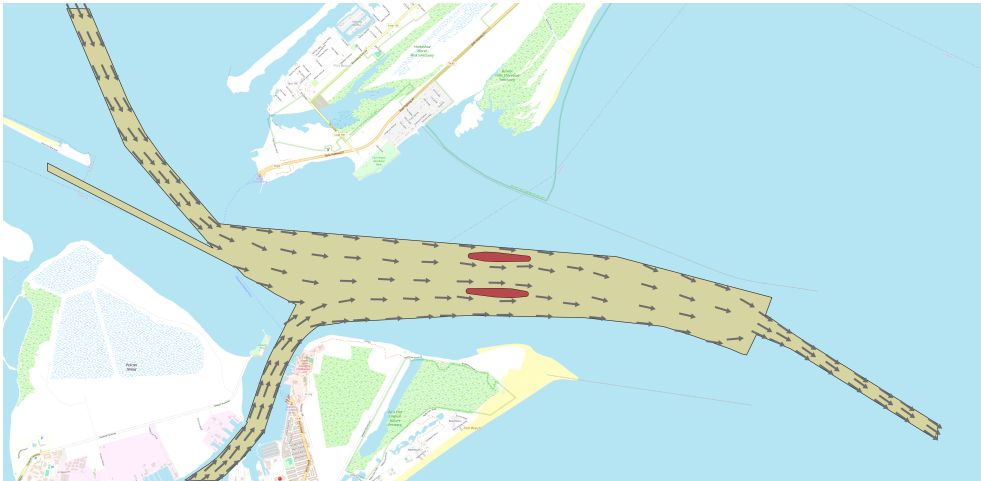


Figure G.4: Current field: ebb current, outbound vessels, configuration 3; (from QGIS).

Configuration 4

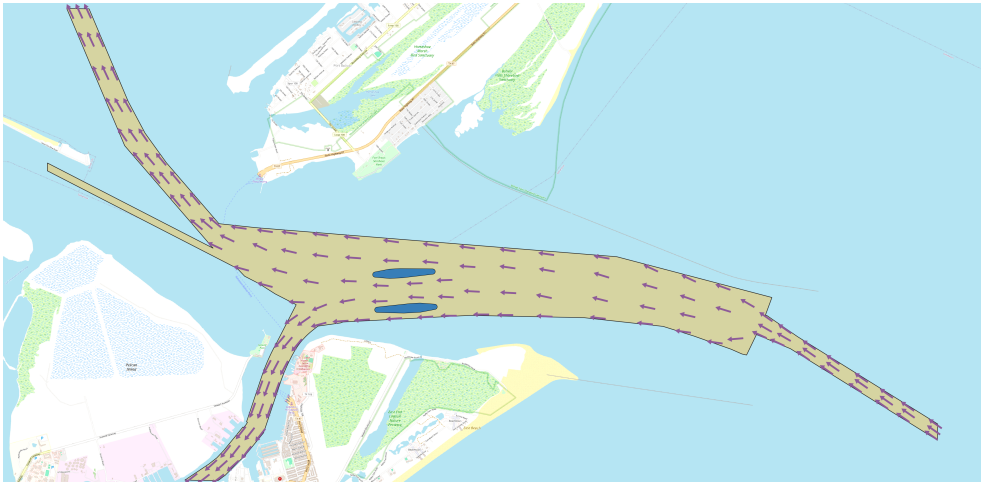


Figure G.5: Current field: flood current, inbound vessels, configuration 4; (from QGIS).

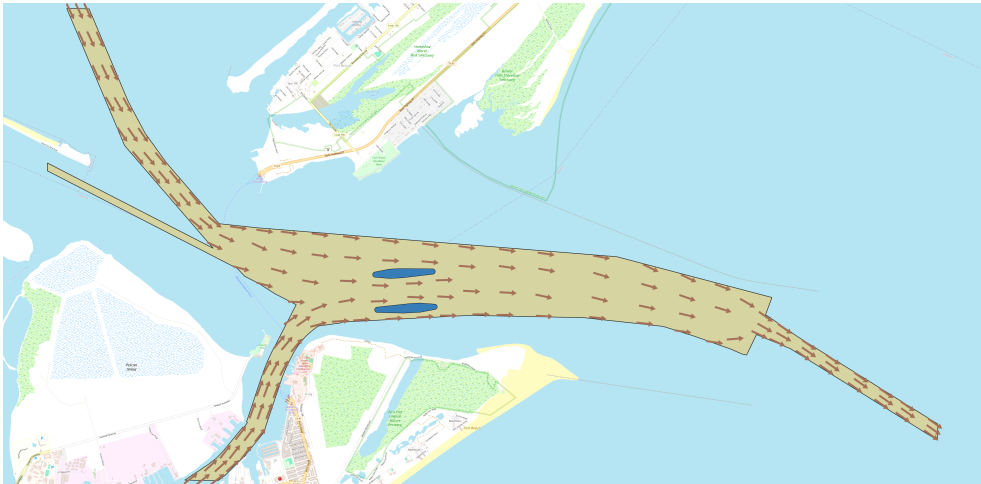


Figure G.6: Current field: ebb current, outbound vessels, configuration 4; (from QGIS).

G.2. Bank Suction

Configuration 1

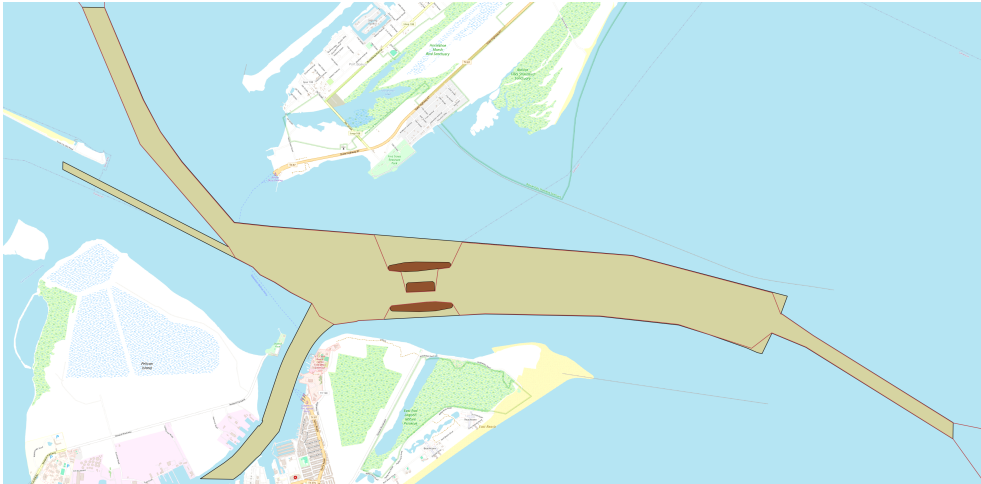


Figure G.7: Bank suction lines: OB-HOU, configuration 1; (from QGIS).

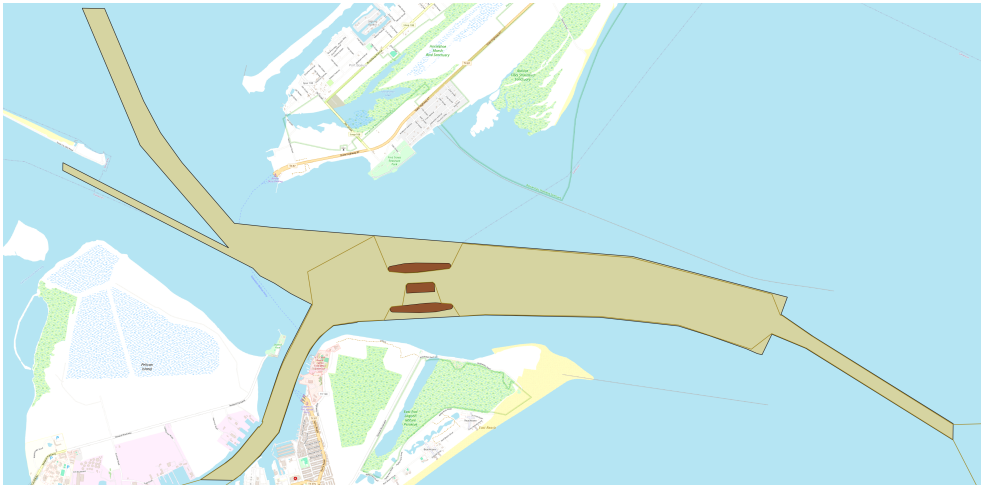


Figure G.8: Bank suction lines: IB-GAL, configuration 1; (from QGIS).

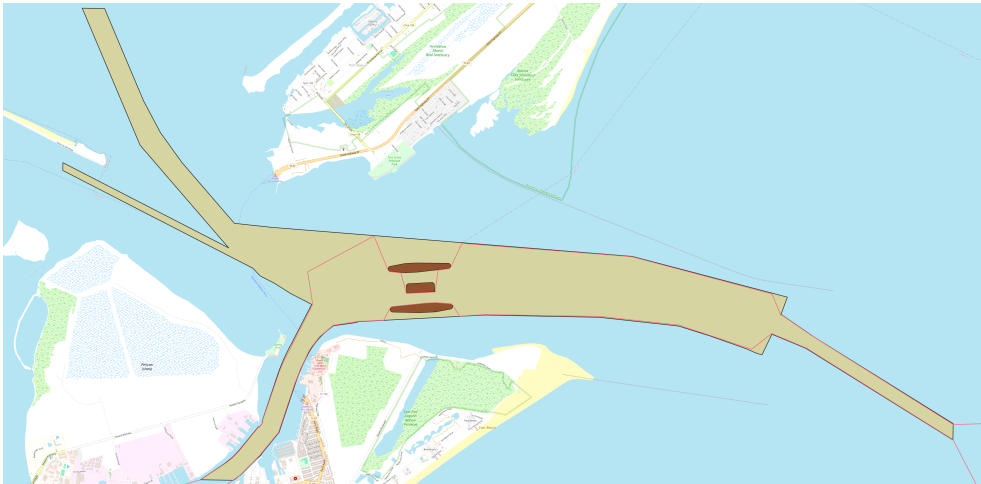


Figure G.9: Bank suction lines: OB-GAL, configuration 1; (from QGIS).

Configuration 2

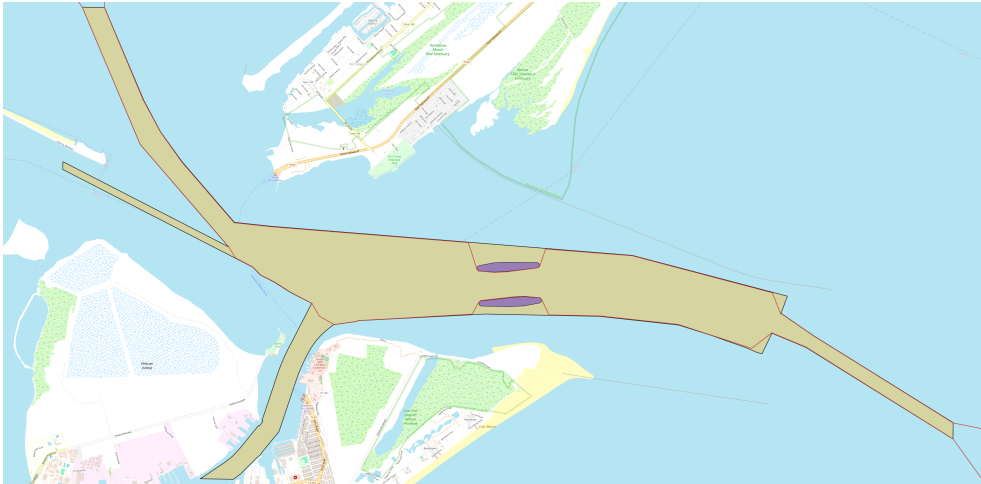


Figure G.10: Bank suction lines: IB/OB-HOU, configuration 2; (from QGIS).

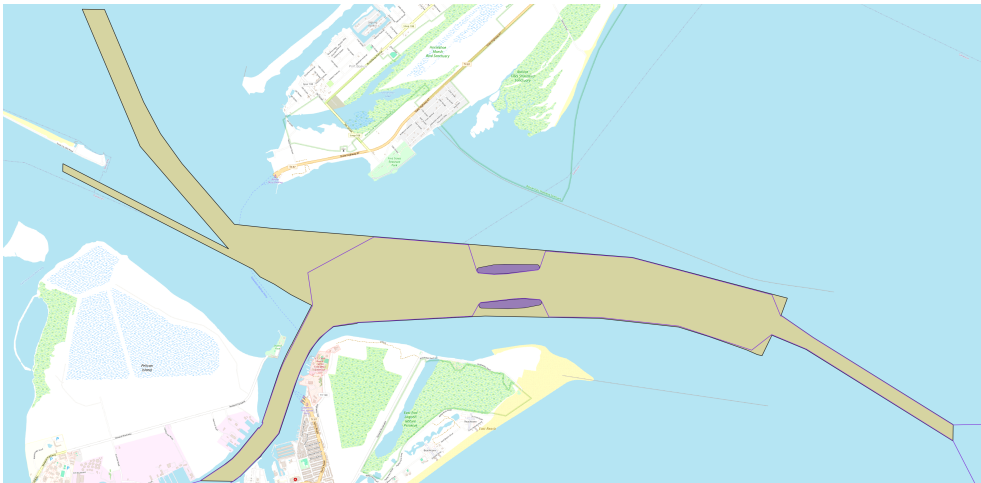


Figure G.11: Bank suction lines: IB/OB-GAL, configuration 2; (from QGIS).

Configuration 3

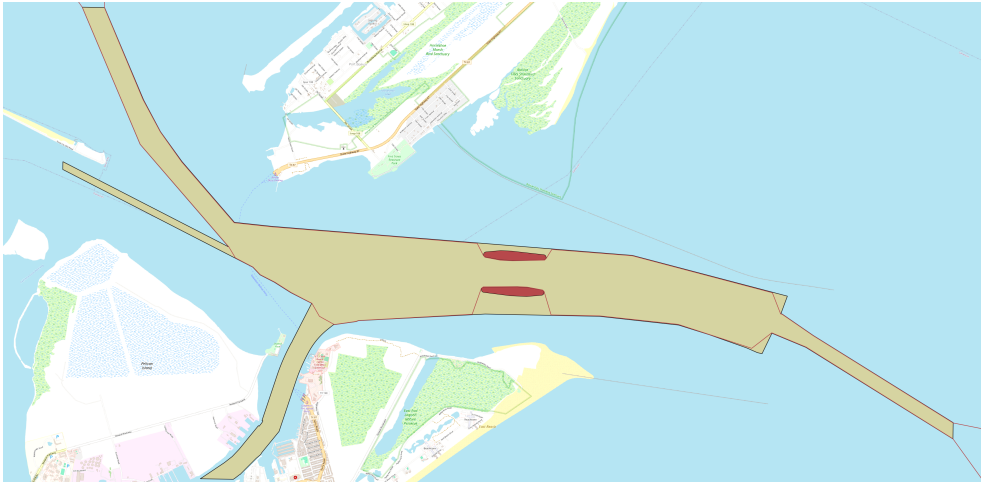


Figure G.12: Bank suction lines: IB/OB-HOU, configuration 3; (from QGIS).

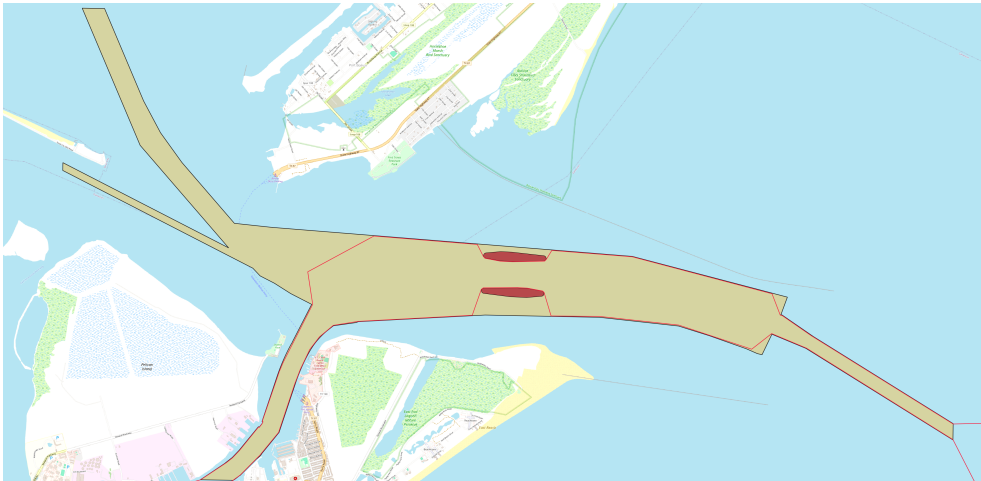


Figure G.13: Bank suction lines: IB/OB-GAL, configuration 3; (from QGIS).

Configuration 4

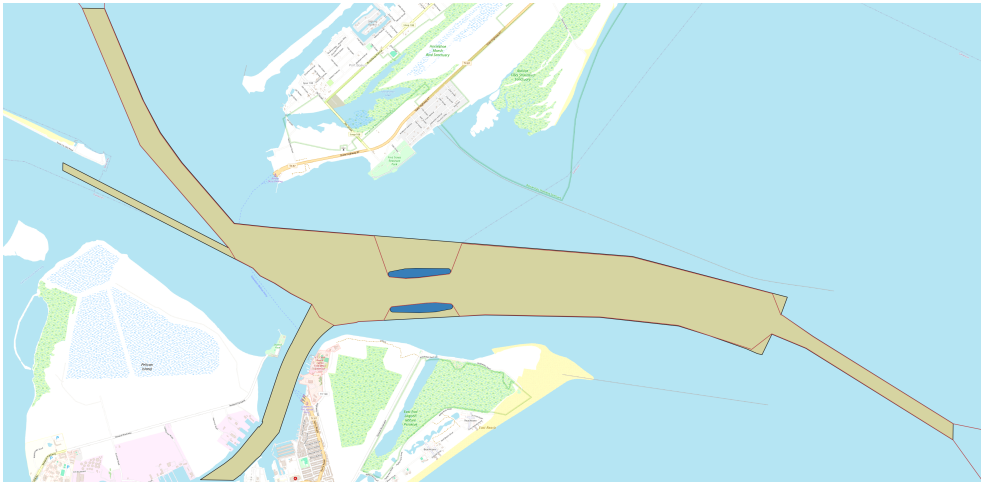


Figure G.14: Bank suction lines: IB/OB-HOU, configuration 4; (from QGIS).

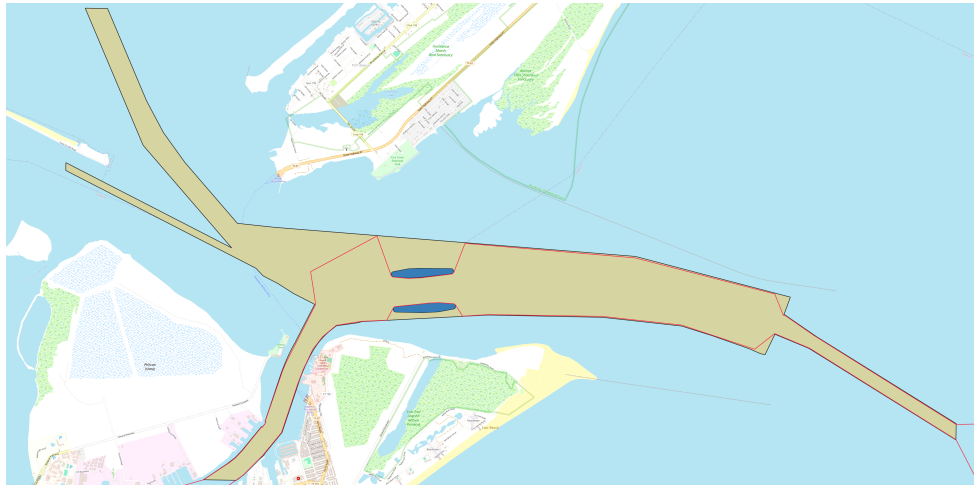


Figure G.15: Bank suction lines: IB/OB-GAL, configuration 4; (from QGIS).

G.3. Desired Tracks

Configuration 1

Table G.1: Desired tracks for barrier *configuration 1*, CRS = EPSG:32615 - WGS84 / UTM zone 15N [m].

Track	X-coordinate* [m]	Y-coordinate** [m]	Radius [m]
IB-HOU	15863.687	4777.653	0
	13634.029	5597.546	1000
	7464.104	5262.455	2000
	5294.433	7793.193	800
	4456.304	9729.056	0
OB-HOU	4344.177	9683.724	0
	5159.911	7762.081	500
	7701.206	4916.978	2200
	13584.619	5245.407	500
	15832.2	4593.574	0
IB-GAL	15863.687	4777.653	0
	13634.029	5597.546	1000
	8306.209	5309.499	1100
	7278.772	2778.39	600
	6601.512	2070.563	0
OB-GAL	6692.925	2053.784	0
	7325.152	2754.026	400
	8210.461	4944.226	1200
	13584.619	5245.407	500
	15832.2	4593.574	0

*= CRS-coordinate - 319898 m
 **= CRS-coordinate - 3242281 m

Configuration 2



Figure G.16: Desired track: IB-HOU, configuration 2; (from AutoCAD).



Figure G.17: Desired track: OB-HOU, configuration 2; (from AutoCAD).



Figure G.18: Desired track: IB-GAL, configuration 2; (from AutoCAD).



Figure G.19: Desired track: OB-GAL, configuration 2; (from AutoCAD).

Table G.2: Desired tracks for barrier *configuration 2*, CRS = EPSG:32615 - WGS84 / UTM zone 15N [m].

Track	X-coordinate* [m]	Y-coordinate** [m]	Radius [m]
IB-HOU	15863.687	4777.653	0
	13634.029	5497.659	1000
	7544.674	5168.477	2200
	5294.433	7793.193	800
	4456.304	9729.056	0
OB-HOU	4344.177	9683.724	0
	5159.911	7762.081	500
	7691.447	4927.83	2500
	13584.619	5256.804	600
	15832.2	4593.574	0
IB-GAL	15863.687	4777.653	0
	13634.029	5497.659	600
	8264.753	5207.371	1100
	7278.772	2778.39	1000
	6601.512	2070.563	0
OB-GAL	6692.925	2053.784	0
	7325.152	2754.026	400
	8215.663	4957.094	1200
	13584.619	5256.804	600
	15832.2	4593.574	0

*= CRS-coordinate - 319898 m

**= CRS-coordinate - 3242281 m

Configuration 3



Figure G.20: Desired track: IB-HOU, configuration 3; (from AutoCAD).



Figure G.21: Desired track: OB-HOU, configuration 3; (from AutoCAD).



Figure G.22: Desired track: IB-GAL, configuration 3; (from AutoCAD).



Figure G.23: Desired track: OB-GAL, configuration 3; (from AutoCAD).

Table G.3: Desired tracks for barrier *configuration 3*, CRS = EPSG:32615 - WGS84 / UTM zone 15N [m].

Track	X-coordinate* [m]	Y-coordinate** [m]	Radius [m]
IB-HOU	15863.687	4777.653	0
	13632.366	5472.993	1000
	7018.158	5781.408	1500
	5294.433	7793.193	800
	4456.304	9729.056	0
OB-HOU	4344.177	9683.724	0
	5159.911	7762.081	800
	7147.631	5536.732	1500
	13583.31	5234.281	700
	15832.2	4593.574	0
IB-GAL	15863.687	4777.653	0
	13632.366	5472.993	800
	8468.865	5712.782	1900
	7278.772	2778.39	600
	6601.512	2070.563	0
OB-GAL	6692.925	2053.784	0
	7325.152	2754.026	700
	8425.3	5476.689	1300
	13583.31	5234.281	1000
	15832.2	4593.574	0

*= CRS-coordinate - 319898 m

**= CRS-coordinate - 3242281 m

Configuration 4



Figure G.24: Desired track: IB-HOU, configuration 4; (from AutoCAD).



Figure G.25: Desired track: OB-HOU, configuration 4; (from AutoCAD).



Figure G.26: Desired track: IB-GAL, configuration 4; (from AutoCAD).



Figure G.27: Desired track: OB-GAL, configuration 4; (from AutoCAD).

Table G.4: Desired tracks for barrier *configuration 4*, CRS = EPSG:32615 - WGS84 / UTM zone 15N [m].

Track	X-coordinate* [m]	Y-coordinate** [m]	Radius [m]
IB-HOU	15863.687	4777.653	0
	13634.029	5497.659	1000
	7544.674	5168.477	2200
	5294.433	7793.193	800
	4456.304	9729.056	0
OB-HOU	4344.177	9683.724	0
	5159.911	7762.081	500
	7691.447	4927.83	2500
	13584.619	5256.804	600
	15832.2	4593.574	0
IB-GAL	15863.687	4777.653	0
	13634.029	5497.659	1000
	8264.753	5207.371	1100
	7278.772	2778.39	600
	6601.512	2070.563	0
OB-GAL	6692.925	2053.784	0
	7325.152	2754.026	400
	8215.663	4957.094	1200
	13584.619	5256.804	600
	15832.2	4593.574	0

*= CRS-coordinate - 319898 m

**= CRS-coordinate - 3242281 m



Assessment Metrics S.C. 1

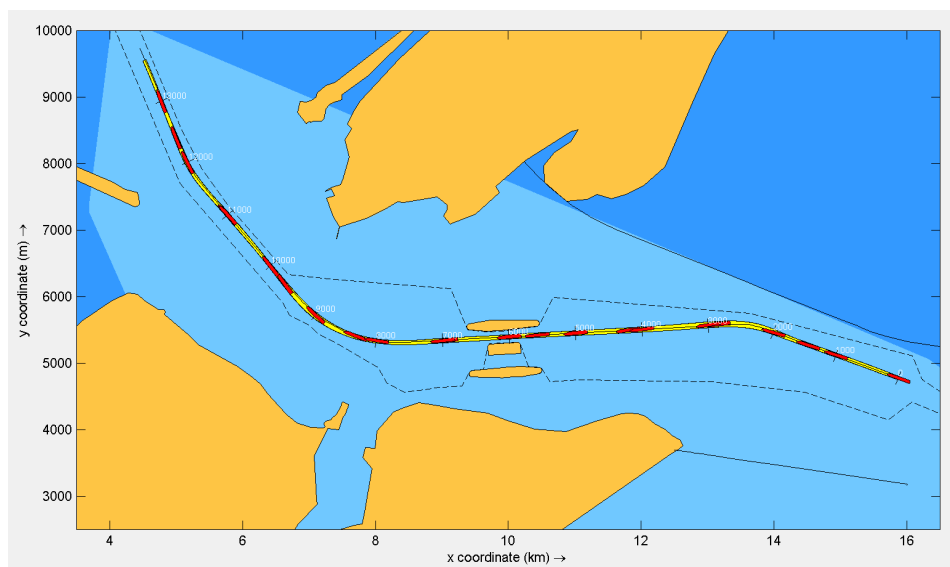


Figure H.1: S.C. 1: spatial overview plot (from SHIPMA). Swept path in yellow.

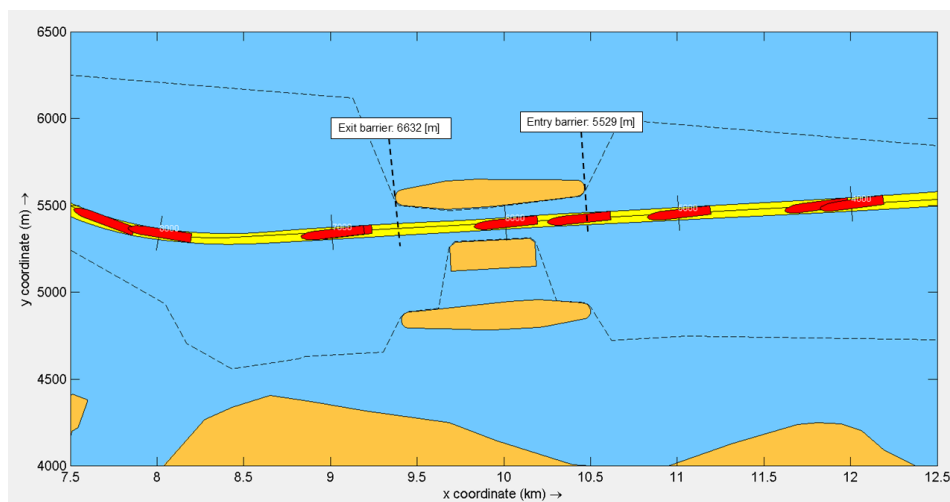


Figure H.2: S.C. 1: points of barrier entry and barrier exit (from SHIPMA).

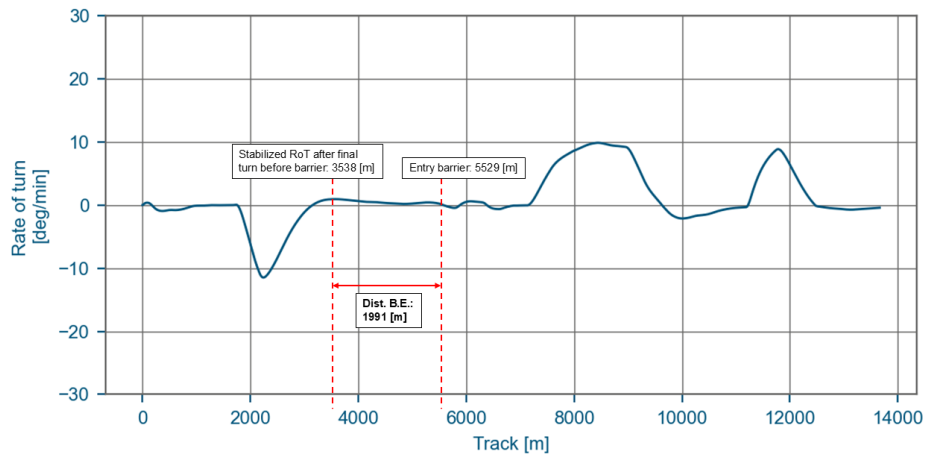


Figure H.3: S.C. 1: Distance Before Entry (from SHIPMA).

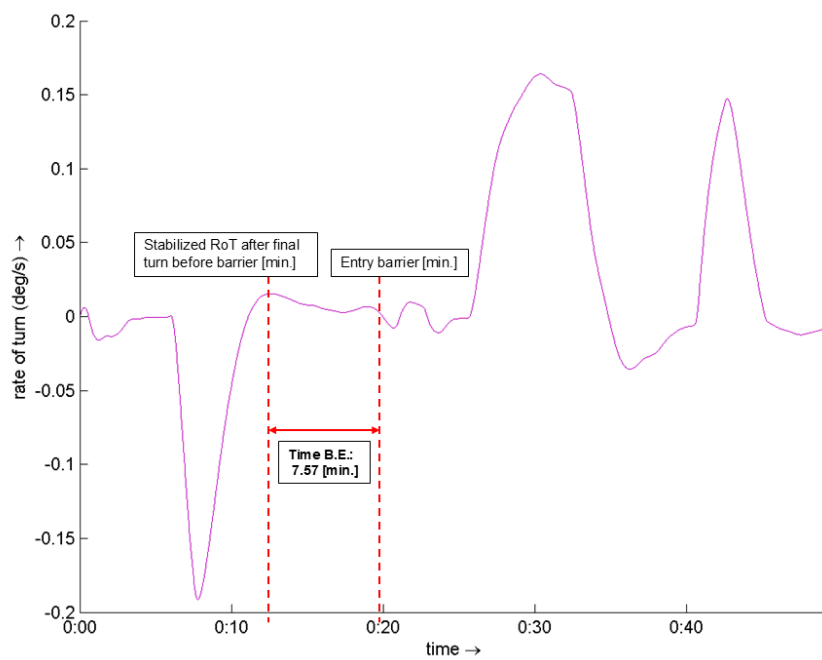


Figure H.4: S.C. 1: Time Before Entry (from SHIPMA).

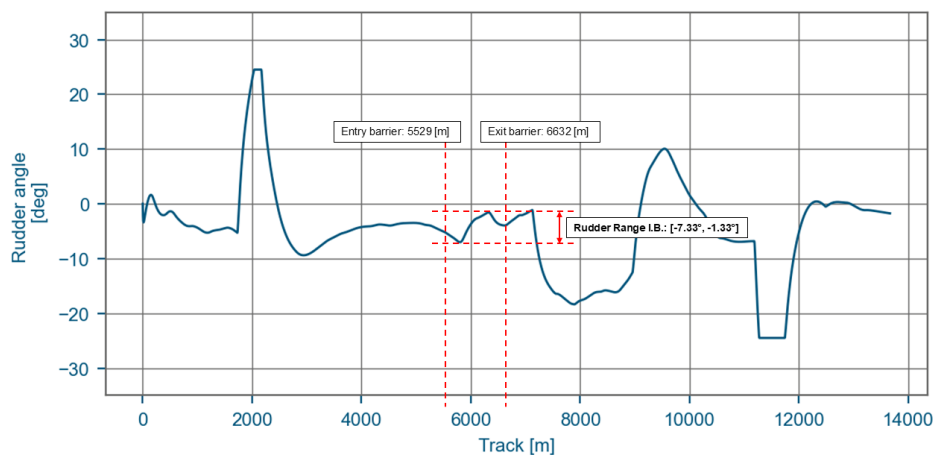


Figure H.5: S.C. 1: Rudder Range In Barrier (from SHIPMA).

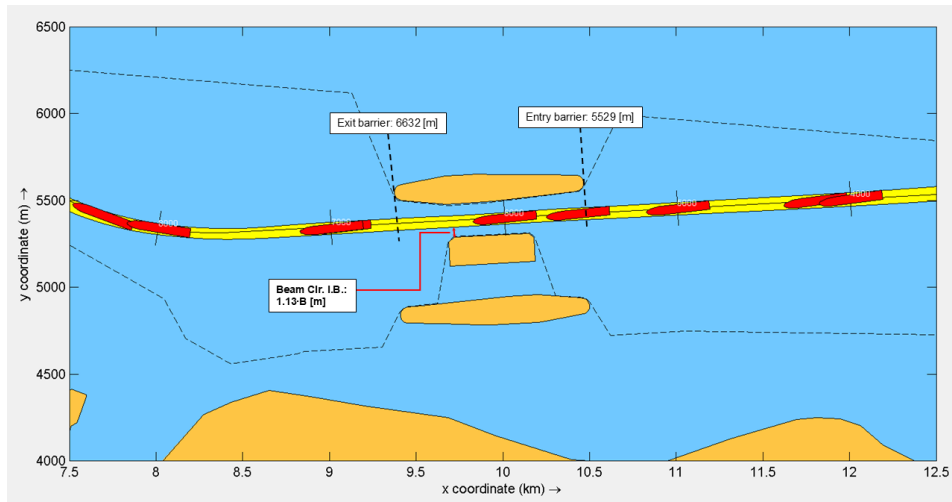


Figure H.6: S.C. 1: *Beam Clearance In Barrier* (from SHIPMA). Swept path in yellow.

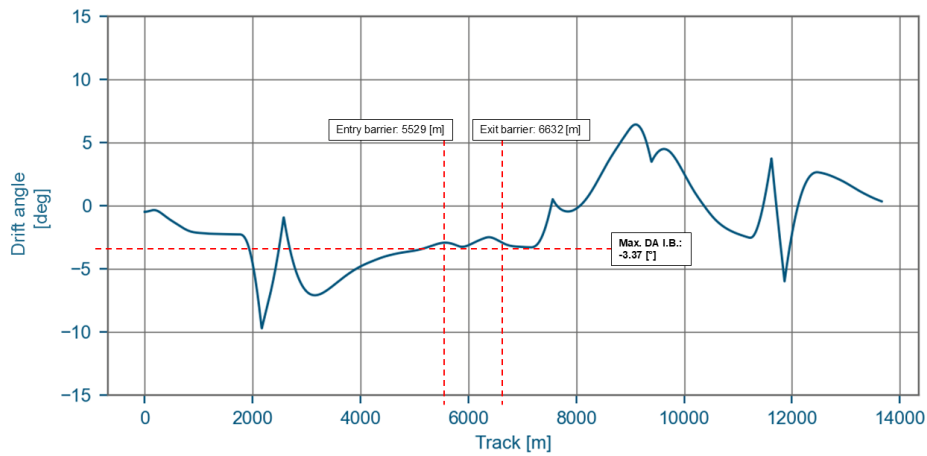


Figure H.7: S.C. 1: *Maximum Drift Angle In Barrier* (from SHIPMA).

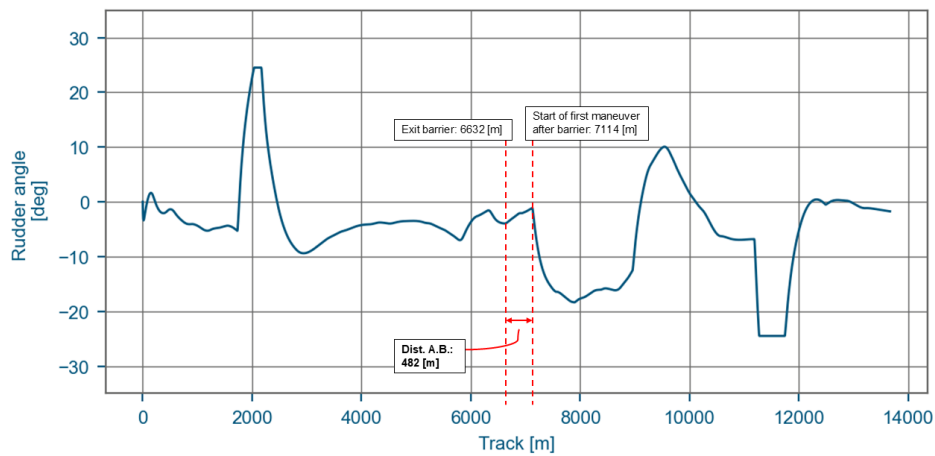


Figure H.8: S.C. 1: *Distance After Barrier* (from SHIPMA).

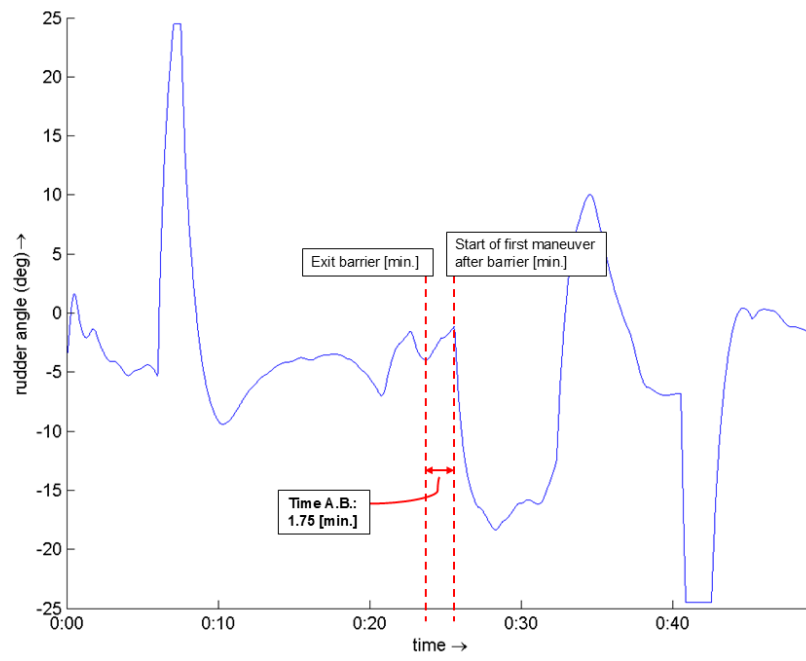


Figure H.9: S.C. 1: *Time After Barrier* (from SHIPMA).

List of Figures

1.1	Numbers that highlight the value of the Texas coast (USACE, 2021c).	4
1.2	Digital rendition of the proposed Bolivar Roads Gate System (USACE, 2021c).	5
1.3	Overview of report structure, indicating where the research questions are addressed and how chapters are related.	7
2.1	Translatory and rotary ship motions (De Winter, 2018).	10
3.1	The three segments of a vessel passage, transit direction indicated by white arrow. . . .	32
3.2	Vessel passage requiring the execution of three turning maneuvers (turns indicated by numbers).	34
3.3	Three turns decomposed into their four parts (corresponding turns shown in Figure 3.2). . . .	34
3.4	Points of barrier entry and barrier exit.	35
3.5	Assessment metric visualization: <i>Distance Before Entry</i>	35
3.6	Assessment metric visualization: <i>Time Before Entry</i>	36
3.7	Assessment metric visualization: <i>Rudder Range In Barrier</i>	37
3.8	Assessment metric visualization: <i>Beam Clearance In Barrier</i> . Swept path in yellow. . . .	37
3.9	Assessment metric visualization: <i>Maximum Drift Angle In Barrier</i>	38
3.10	Assessment metric visualization: <i>Distance After Barrier</i>	39
3.11	Assessment metric visualization: <i>Time After Barrier</i>	39
3.12	Overview of the developed nautical safety assessment method for storm surge barriers. . . .	40
3.13	Map of the Greater Galveston Bay Area, Bolivar Roads marked with red circle (Google, 2025).	41
3.14	Hurricane storm surge (l), coastal erosion (m), and relative SLR (r) on the Texas coast (USACE, 2021c).	42
3.15	Upper Texas coast, Gulf Lines of Defense (USACE, 2021c).	43
3.16	Detailed overview of Bolivar Roads Gate System (USACE, 2021c).	43
4.1	Nautical chart of Bolivar Roads (NOAA, 2025a).	46
4.2	Base map of Bolivar Roads, CRS = EPSG:32615 - WGS84 / UTM zone 15N [m]; (from QGIS).	46
4.3	Baseline and alternative barrier configurations for Bolivar Roads, on existing dredged channel; (from QGIS).	48
4.4	Overview of barrier configurations: 1 (brown), 2 (purple), 3 (red), and 4 (blue); (from QGIS).	49
4.5	Spatial schematization, Bolivar Roads, existing bathymetry (purple) and extension (beige); (from QGIS).	50
4.6	Final spatial schematization, Bolivar Roads; (from QGIS).	50
4.7	Location of current (blue markers) and wind stations (red/yellow markers) at Bolivar Roads (NOAA, 2025b).	51
4.8	Wind rose of measured winds in 2023 (wind direction is the direction from which the wind blows).	52
4.9	Current rose of measured currents in 2023 (current direction is the direction to which the current flows).	53
4.10	Current field: flood current, inbound vessels, configuration 1; (from QGIS).	53
4.11	Current field: ebb current, outbound vessels, configuration 1; (from QGIS).	54
4.12	Vessel traffic patterns at Bolivar Roads in the year 2024. Categorized per COG; (from QGIS).	55
4.13	Bank suction lines: IB-HOU, configuration 1; (from QGIS).	57
4.14	Desired tracks: IB-HOU (pink), OB-HOU (green), configuration 1; (from AutoCAD). . . .	59

4.15	Desired tracks: IB-GAL (light blue), OB-GAL (red), configuration 1; (from AutoCAD).	59
4.16	<i>Dist. B.E.</i> and <i>Time B.E.</i> , per configuration, all simulation cases (from Python).	64
4.17	<i>Rudder Range I.B.</i> , per configuration, all simulation cases (from Python).	64
4.18	<i>Beam Clr. I.B.</i> and <i>Max. DA I.B.</i> , per configuration, all simulation cases (from Python).	64
4.19	<i>Dist. A.B.</i> and <i>Time A.B.</i> , per configuration, all simulation cases (from Python).	65
4.20	S.C. 29: zoom-in of spatial overview plot, crossing segment (from SHIPMA).	65
A.1	Physical maneuvering indicators.	84
C.2	Geometric parameter visualization: alignment. Gate width and siting of the barriers are identical across the figures.	87
C.3	Geometric parameter visualization: siting. Gate width and alignment are identical across the barriers.	88
D.1	Speed and direction of measured winds, January 2023 (NOAA, 2023b).	89
D.2	Speed and direction of measured winds, February 2023 (NOAA, 2023b).	89
D.3	Speed and direction of measured winds, March 2023 (NOAA, 2023b).	90
D.4	Speed and direction of measured winds, April 2023 (NOAA, 2023b).	90
D.5	Speed and direction of measured winds, May 2023 (NOAA, 2023b).	90
D.6	Speed and direction of measured winds, June 2023 (NOAA, 2023b).	91
D.7	Speed and direction of measured winds, July 2023 (NOAA, 2023b).	91
D.8	Speed and direction of measured winds, August 2023 (NOAA, 2023b).	91
D.9	Speed and direction of measured winds, September 2023 (NOAA, 2023b).	92
D.10	Speed and direction of measured winds, October 2023 (NOAA, 2023b).	92
D.11	Speed and direction of measured winds, November 2023 (NOAA, 2023b).	92
D.12	Speed and direction of measured winds, December 2023 (NOAA, 2023b).	93
E.1	Speed and direction of measured currents, January 2023 (NOAA, 2023a).	94
E.2	Speed and direction of measured currents, February 2023 (NOAA, 2023a).	94
E.3	Speed and direction of measured currents, March 2023 (NOAA, 2023a).	95
E.4	Speed and direction of measured currents, April 2023 (NOAA, 2023a).	95
E.5	Speed and direction of measured currents, May 2023 (NOAA, 2023a).	95
E.6	Speed and direction of measured currents, June 2023 (NOAA, 2023a).	96
E.7	Speed and direction of measured currents, July 2023 (NOAA, 2023a).	96
E.8	Speed and direction of measured currents, August 2023 (NOAA, 2023a).	96
E.9	Speed and direction of measured currents, September 2023 (NOAA, 2023a).	97
E.10	Speed and direction of measured currents, October 2023 (NOAA, 2023a).	97
E.11	Speed and direction of measured currents, November 2023 (NOAA, 2023a).	97
E.12	Speed and direction of measured currents, December 2023 (NOAA, 2023a).	98
F.1	Design vessel: Houston, container, MMSI 215196000.	99
F.2	Design vessel: Houston, tanker, MMSI 303294000.	99
F.3	Design vessel: Houston, ro-ro vessel, MMSI 403532001.	100
F.4	Design vessel: Galveston, container, MMSI 209444000.	100
F.5	Design vessel: Galveston, tanker, MMSI 319095200.	101
F.6	Design vessel: Galveston, cruise ship, MMSI 311000396.	101
G.1	Current field: flood current, inbound vessels, configuration 2; (from QGIS).	102
G.2	Current field: ebb current, outbound vessels, configuration 2; (from QGIS).	102
G.3	Current field: flood current, inbound vessels, configuration 3; (from QGIS).	103
G.4	Current field: ebb current, outbound vessels, configuration 3; (from QGIS).	103
G.5	Current field: flood current, inbound vessels, configuration 4; (from QGIS).	103
G.6	Current field: ebb current, outbound vessels, configuration 4; (from QGIS).	104
G.7	Bank suction lines: OB-HOU, configuration 1; (from QGIS).	104
G.8	Bank suction lines: IB-GAL, configuration 1; (from QGIS).	104
G.9	Bank suction lines: OB-GAL, configuration 1; (from QGIS).	105
G.10	Bank suction lines: IB/OB-HOU, configuration 2; (from QGIS).	105

G.11 Bank suction lines: IB/OB-GAL, configuration 2; (from QGIS).	105
G.12 Bank suction lines: IB/OB-HOU, configuration 3; (from QGIS).	106
G.13 Bank suction lines: IB/OB-GAL, configuration 3; (from QGIS).	106
G.14 Bank suction lines: IB/OB-HOU, configuration 4; (from QGIS).	106
G.15 Bank suction lines: IB/OB-GAL, configuration 4; (from QGIS).	107
G.16 Desired track: IB-HOU, configuration 2; (from AutoCAD).	108
G.17 Desired track: OB-HOU, configuration 2; (from AutoCAD).	108
G.18 Desired track: IB-GAL, configuration 2; (from AutoCAD).	108
G.19 Desired track: OB-GAL, configuration 2; (from AutoCAD).	109
G.20 Desired track: IB-HOU, configuration 3; (from AutoCAD).	110
G.21 Desired track: OB-HOU, configuration 3; (from AutoCAD).	110
G.22 Desired track: IB-GAL, configuration 3; (from AutoCAD).	110
G.23 Desired track: OB-GAL, configuration 3; (from AutoCAD).	111
G.24 Desired track: IB-HOU, configuration 4; (from AutoCAD).	112
G.25 Desired track: OB-HOU, configuration 4; (from AutoCAD).	112
G.26 Desired track: IB-GAL, configuration 4; (from AutoCAD).	112
G.27 Desired track: OB-GAL, configuration 4; (from AutoCAD).	113
H.1 S.C. 1: spatial overview plot (from SHIPMA). Swept path in yellow.	114
H.2 S.C. 1: points of barrier entry and barrier exit (from SHIPMA).	114
H.3 S.C. 1: <i>Distance Before Entry</i> (from SHIPMA).	115
H.4 S.C. 1: <i>Time Before Entry</i> (from SHIPMA).	115
H.5 S.C. 1: <i>Rudder Range In Barrier</i> (from SHIPMA).	115
H.6 S.C. 1: <i>Beam Clearance In Barrier</i> (from SHIPMA). Swept path in yellow.	116
H.7 S.C. 1: <i>Maximum Drift Angle In Barrier</i> (from SHIPMA).	116
H.8 S.C. 1: <i>Distance After Barrier</i> (from SHIPMA).	116
H.9 S.C. 1: <i>Time After Barrier</i> (from SHIPMA).	117

List of Tables

3.1	Framework for development of nautical safety assessment metrics.	33
3.2	Facts and figures: ports of Galveston, Houston, and Texas City in 2023.	42
4.1	Specification of geometric parameters of barrier configurations developed for Bolivar Roads.	48
4.2	Worst navigable conditions for Bolivar Roads.	54
4.3	Design vessel characteristics obtained from AIS analysis.	56
4.4	Characteristics of SHIPMA vessel models.	57
4.5	Water level, bottom level and resulting water depth for selected SHIPMA vessel models.	58
4.6	RPM setting, speed and RPM usage per vessel.	60
4.7	SHIPMA simulation case matrix.	61
4.8	Outcomes of quantitative nautical safety assessment metrics, per barrier configuration.	63
G.1	Desired tracks for barrier <i>configuration 1</i> , CRS = EPSG:32615 - WGS84 / UTM zone 15N [m].	107
G.2	Desired tracks for barrier <i>configuration 2</i> , CRS = EPSG:32615 - WGS84 / UTM zone 15N [m].	109
G.3	Desired tracks for barrier <i>configuration 3</i> , CRS = EPSG:32615 - WGS84 / UTM zone 15N [m].	111
G.4	Desired tracks for barrier <i>configuration 4</i> , CRS = EPSG:32615 - WGS84 / UTM zone 15N [m].	113